

The Biogenesis of Photosynthetic Complexes PSII and *b₆f*

DISSERTATION

Presented in Partial Fulfillment of the Requirements for the Degree Doctor of Philosophy
in the Graduate School of The Ohio State University

By

Sara Guenthner Cline

Graduate Program in Plant Cellular and Molecular Biology

The Ohio State University

2012

Dissertation Committee:

Hamel, Patrice, Advisor
Bird, Amanda
Mackey, Dave
Somers, Dave

Copyright by
Sara Guenther Cline
2012

Abstract

Photosynthetic complex assembly within the plastid is a blossoming field as science uncovers additional requirements and levels of regulation in the production of these protein complexes. Using both forward and reverse genetics, our lab has revealed two new players in the assembly of Photosystem II and the *b₆f* complex. The first of these factors is LTO1, identified as the thiol oxidant for the production of a disulfide bond within PsbO, a PSII luminal protein. The second is an OPR protein with a novel role in the attachment of heme to cytochrome *f* of the *b₆f* complex. The presence of these assembly factors opens exciting new doors in the possibilities of plastid b, as demonstrated by our relocation of the nuclear *ARG9* gene into the plastid genome.

Dedicated to my Dad.

Acknowledgments

Here I would like to thank my P.I. for his patience and my lab mates for their help.

Vita

2001.....Trimble County High School
2005.....B.A. Biology, Transylvania University,
2005 to presentGraduate Teaching Associate, Department of
Plant Cellular and Molecular Biology, The
Ohio State University

Publications

Mohamed Karamoko, Sara Cline, Kevin Redding, Natividad Ruiz, and Patrice Hamel. Lumen Thiol Oxidoreductase1, a Disulfide Bond-Forming Catalyst, Is Required for the Assembly of Photosystem II in *Arabidopsis*. **Plant Cell** (2011) 28 (12): 4462-4475.

Claire Remacle, Sara Cline, Layla Boutaffala, Stéphane Gabilly, Véronique Larosa, M. Rosario Barbieri, Nadine Coosemans, and Patrice P. Hamel. The ARG9 Gene Encodes the Plastid-Resident N-Acetyl Ornithine Aminotransferase in the Green Alga *Chlamydomonas reinhardtii*. **Eukaryotic Cell** (2009) 8: 1460-1463

Fields of Study

Major Field: Plant Cellular and Molecular Biology

Table of Contents

Abstract.....	ii
Vita.....	v
List of Tables	xii
List of Figures.....	xiii
Chapter 1: Introduction.....	1
1. Photosynthesis Overview	1
2. PSII Components.....	3
2.1 PSII Assembly.....	5
2.2 D2.....	7
2.2.1 HCF136 - <i>Arabidopsis</i> D2 Assembly Factor	8
2.2.2 YCF48 - <i>Synechocystis</i> ortholog of HCF136.....	10
2.3 D1	11
2.3.1 ALB3 - <i>Arabidopsis</i> Insertase	12
2.3.2 ALB3.2 - <i>Chlamydomonas</i> ortholog of <i>Arabidopsis</i> ALB3	14
2.3.3 LPA1 - <i>Arabidopsis</i> D1 Assembly Factor	17

2.3.4 PAM68 - <i>Arabidopsis</i> PSII Assembly Factor	18
2.3.5 Psb27-H2 - <i>Arabidopsis</i> pD1 Assembly Factor	20
2.3.6 HCF243 - <i>Arabidopsis</i> D1 Assembly Factor	21
2.4 CP43	23
2.4.1 LPA2 and LPA3 - <i>Arabidopsis</i> CP43 Assembly Factors.....	24
2.5 Assembly of the Manganese Cluster.....	27
2.5.1 PrtA - <i>Synechocystis</i> Mn Transporter and D1 Assembly Factor.....	28
2.5.2 Psb27 - <i>Synechocystis</i> Mn Cluster Assembly Factor	30
2.6 PsbO	32
2.6.1 LTO1 - PsbO Assembly Factor.....	32
2.6.2 Is there a PsbO reductase?.....	33
2.7 PsbP.....	35
2.8 PsbP Related Proteins	37
2.8.1 Sll1418 - <i>Synechocystis</i> PsbP-like homologue.....	37
2.9 PsbQ	38
2.9.1 Sll1638 - <i>Synechocystis</i> PsbQ-like homolog.....	39
3. b ₆ f.....	40
3.1 Translation of <i>petA</i>	40
3.2 TCA1 - <i>Chlamydomonas</i> Translation Factor of <i>petA</i>	41

3.3 MCA1 - Post Transcriptional Factor of <i>petA</i>	42
3.4 Heme Attachment.....	48
3.4.1 CCS1 and CcsA - System II Heme Synthetase	48
3.4.2 CcsBA - Bacterial Ortholog of CCS1 and CcsA	49
3.4.3 ResB and ResC - <i>B. subtilis</i> orthologs of CCS1 and CcsA.....	50
3.4.4 What is the function of the b-type heme?	52
3.4.5 System II Variation	55
Chapter 2: CCS2, a novel factor required for cytochrome <i>c</i> assembly in the green alga <i>Chlamydomonas reinhardtii</i>	59
Abstract	59
Introduction	60
RESULTS.....	64
Cloning of CCS2 by functional complementation.	64
CCS2 encodes a 170 kDa protein of the OPR family.	65
Localization.	70
Essential domains are located in C-terminus.	71
Specific effects of the <i>ccs2</i> mutation.....	71
MATERIALS AND METHODS	72
Strains and culture condition.....	72
Complementation.	72

Constructs.....	73
Immunoblots.....	74
Chlorophyll Auto-fluorescence.....	74
GFP Fluorescence.....	75
OPR Protein Domains.....	75
DISCUSSION.....	75
Identification of CCS2 as an OPR protein needed for cytochrome <i>c</i> assembly.....	75
Unique Cytochrome <i>c</i> Assembly Factors.....	78
Implications of Unique Assembly Factors.....	79
Chapter 3: Lumen Thiol Oxido-reductase 1 (LTO1), a disulfide bond-forming catalyst, is required for the assembly of photosystem II.....	81
Abstract.....	82
Introduction.....	82
Results.....	86
LTO1, a VKOR-like protein at the thylakoid membrane, is conserved in photosynthetic eukaryotes.....	86
Topological analysis of LTO1.....	89
LTO1 partially complements for loss of DsbAB in bacteria.....	90
Knock-down of <i>Arabidopsis</i> LTO1 impairs plant growth.....	92
Loss of LTO1 produces a photosynthetic defect:.....	93

Loss of LTO1 impacts PSII accumulation:	97
The thioredoxin-like domain of LTO1 interacts with PsbO1 and PsbO2	98
The soluble domain of LTO1 can catalyze disulfide bond formation in PsbO.....	99
Discussion	101
The plastid VKOR-like protein defines a trans-thylakoid thio-oxidation pathway	101
The redox activity of LTO1 is required for the assembly of PSII.....	103
Are there other relevant targets of LTO1 sulfhydryl oxidizing activity?.....	105
Methods.....	106
Bacterial strains and growth media	106
Heterologous complementation of the <i>dsbAB</i> mutant.....	106
Efficiency of plating assay	107
Topological analysis of LTO1 via PhoA/LacZ α sandwich fusions.....	107
Yeast Two-hybrid Experiments	108
<i>In Vitro</i> Redox Assay	109
Growth of <i>A. thaliana</i>	110
Molecular characterization of the <i>lto1</i> mutant lines.....	111
Plasmids for Plant Transformation.....	112
Protein preparation and analysis	112
Fluorescence induction.....	113

Chapter 4: The <i>ARG9</i> gene encodes the plastid resident N-acetyl ornithine aminotransferase in the green alga <i>Chlamydomonas reinhardtii</i>	118
Abstract:	118
Identification of the <i>ARG9</i> mutation	119
Results	119
Functional Confirmation of ARG9	119
Localization of ARG9	120
Restoration of Nuclear Mutant via Chloroplast Transformation	123
Proof of Concept	126
Conclusion	129
References	132

List of Tables

Table 1 - Interactions demonstrated between assembly factors and PSII reaction center components.	26
Table 2 - Interactions demonstrated between known PSII assembly factors.....	27
Table 3 - Topological analysis of <i>Arabidopsis</i> LTO1 from PhoA and LacZ fusion analysis.....	113
Table 4 - Efficiency of plating on MacConkey agar of dsbAB strains expressing <i>Arabidopsis</i> LTO1.	115
Table 5 - Quantum efficiency, non-photochemical quenching and photoinhibition in wild-type and lto1 lines.	116
Table 6 - Quantum efficiency of wild-type, lto1 and LTO1-complemented lto1 lines. .	117

List of Figures

Figure 1 - Schemata of Photosynthesis from (Remacle, 2012).	2
Figure 2 – Stepwise Assembly of PSII from (Nixon et al., 2010).....	4
Figure 3 - Placement of Known PSII Assembly Factors in <i>Arabidopsis</i>	7
Figure 4 – D1 Assembly Protein Motifs.....	14
Figure 5 – CP43 Assembly Factors and Other Proteins	22
Figure 6 - PsbP Related Proteins	36
Figure 7 - Three Systems for Cytochrome <i>c</i> assembly from (Kranz et al., 2009).....	47
Figure 8 - An OPR Gene Restores Photoautotrophic Growth to the <i>ccs2</i> Alleles.....	65
Figure 9 - Restoration of Cytochrome <i>c</i> and CCS5 Accumulation in Complemented Mutants.	66
Figure 10 - Identification of the <i>CCS2</i> cDNA and Allele Mutations.	67
Figure 11 - Features of the Deduced <i>CCS2</i>	68
Figure 12 - Characterization of <i>CCS2</i> -HA.	69
Figure 13 - Localization of GFP to Chloroplast by <i>CCS2</i> Targeting Sequence.....	70
Figure 14 - Proposed topological arrangement of plastid <i>Arabidopsis</i> LTO1.....	87
Figure 15 - <i>Arabidopsis</i> LTO1 partially complements the <i>E. coli dsbAB</i> mutant for disulfide bond formation.....	88

Figure 16 - Knock-down of <i>LTO1</i> results in a growth defect.	89
Figure 17 - The photosynthetic defect in the <i>lto1</i> mutant is due to a limitation in the electron flow from photosystem II.....	91
Figure 18 - Accumulation of cytochrome <i>b₆f</i> and photosystem I is not affected by loss of LTO1.....	92
Figure 19 - Accumulation of photosystem II subunits is impacted by loss of LTO1.	94
Figure 20 - Complementation of the <i>lto1</i> photosynthetic defect by LTO1 cDNA.	96
Figure 21 - PsbO1 and PsbO2 interact with the thioredoxin-like domain of LTO1 in a yeast two-hybrid assay.....	97
Figure 22 - The thioredoxin-like domain of LTO1 catalyzes disulfide bond formation in PsbO2.	100
Figure 23 - Heterologous functional complementation of the <i>S. cerevisiae arg8</i> mutant by the <i>C. reinhardtii ARG9</i> cDNA encoding NAOAT.....	120
Figure 24 - ARG9 localizes to the plastid in <i>Chlamydomonas</i>	121
Figure 25 - Plastid transformation of the <i>arg9-2</i> strain with the <i>arg9c</i> cassette restores arginine prototrophy.....	122
Figure 26 - Restoration of NAOAT activity in nuclear and plastid transformants.....	125

Chapter 1: Introduction

1. Photosynthesis Overview

The chloroplast is known to contain some of the most crucial proteins for life on Earth as we know it. Assembled in the thylakoid membrane itself are Photosystem II (PSII), the *b₆f* complex, Photosystem I (PSI) and ATP synthase. These complexes, through the process of oxygenic photosynthesis, are necessary for the creation of chemical energy necessary for growth from air and water. Photosystems I and II capture light through chlorophyll and other pigments. PSII then uses this light energy to extract two electrons from water, producing oxygen as an unwanted byproduct. In addition to the hydrogen ions produced from this reaction, both photosystems use these excited electrons to aid in creating an electrochemical gradient and reducing equivalents for the cell to use in the production of ATP or as reducing agents. The *b₆f* complex uses the light energy from PSII to pump protons into the lumen of the chloroplast. The resulting electrochemical gradient is used by ATP synthase to generate ATP for the cell's use, while the excess oxygen is released into the atmosphere, creating the aerobic conditions favored by multicellular life.

This side reaction occurs because the ultimate electron donor in oxygenic

photosynthesis comes from H_2O . This causes the splitting of water into its component elements: H^+ and oxygen. The manganese cluster, found at the center of PSII, extracts these electrons, which then reduce an essential tyrosine found in the D1 subunit of PSII. The tyrosine then passes on the electrons to the core chlorophylls of PSII, termed P680. Upon excitation by energy that ultimately comes from light, the electron is then passed on from quinol A (Q_A) to quinol B (Q_B) within PSII to generate reduced plastoquinol (PQH_2).

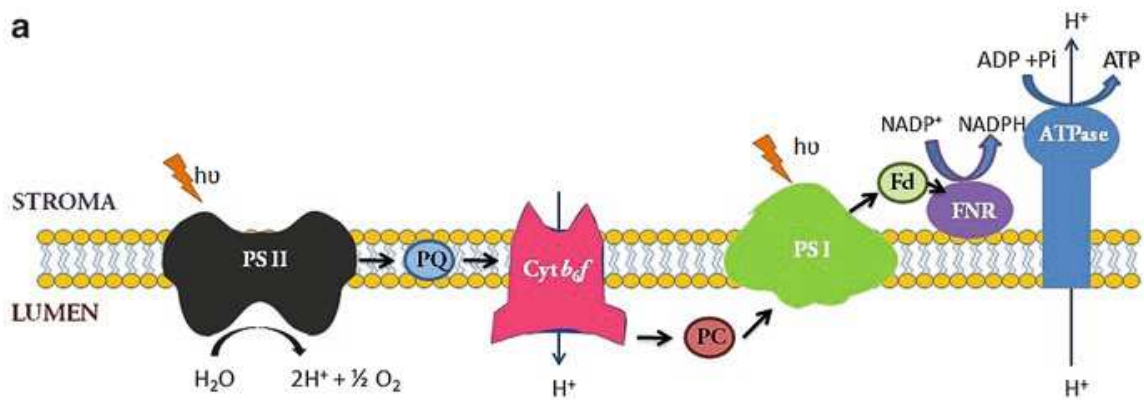


Figure 1 - Schemata of Oxygenic Photosynthesis from (Remacle, 2012).

The membrane soluble molecule, PQ, then transports this excited electron to the *b₆f* complex, which uses the energy of the electron to help pump a variable number of protons into the chloroplast lumen. From there, the spent electron is passed on to the soluble luminal protein plastocyanin (PC). PC then moves to PSI, which, through a series of additional reactions, ultimately reduces $NADP^+$ (See Figure 1).

Assembly and maintenance of these intricate complexes requires the coordination of both nuclear and plastid gene transcription and translation, cofactor production, protein

and co-factor transport, post-translational modifications and assembly of not just monomeric complexes, but hetero-multimeric photosynthetic complexes. This text will focus on the translation and assembly of two crucial proteins: the nuclear encoded PsbO, required for the stable splitting of water as a protector of PSII's Oxygen Evolving Complex (OEC) and the plastid encoded cytochrome *f*, one of three catalytic proteins in the *b₆f* complex characterized by its covalently attached heme moiety. Following the traditional Z scheme of photosynthesis, this text will look first at the core subunits of Photosystem II, following them from translation to assembly. It will then turn to the factors involved in the second complex of the Z scheme: cytochrome *f* translation and assembly. The focus will be on the assembly of these complexes in plants and green algae, with some discussion of the conundrums regarding research in cyanobacteria. Finally, a short conclusion will follow, considering the implications of these processes for the potential use of the chloroplast for bioengineering purposes.

2. PSII Components

Photosystem II is a multisubunit complex that tends to prefer a dimer configuration (Boekema et al., 1995). These subunits are encoded by both nuclear and chloroplastic genes, which are inserted into or transported across the thylakoid membrane by a variety of pathways. These include the signal recognition particle (SRP) pathway, which can work independently or in conjunction with the secretory (Sec) pathway, and the twin-arginine translocase (Tat) pathway (Aldridge et al., 2009). The Sec pathway transports unfolded proteins into the using ATP as the driving force, while the Tat pathway utilizes the proton motive force to transport appropriately folded proteins. Both of these pathways will become important in our discussion of PSII assembly later in this

dissertation.

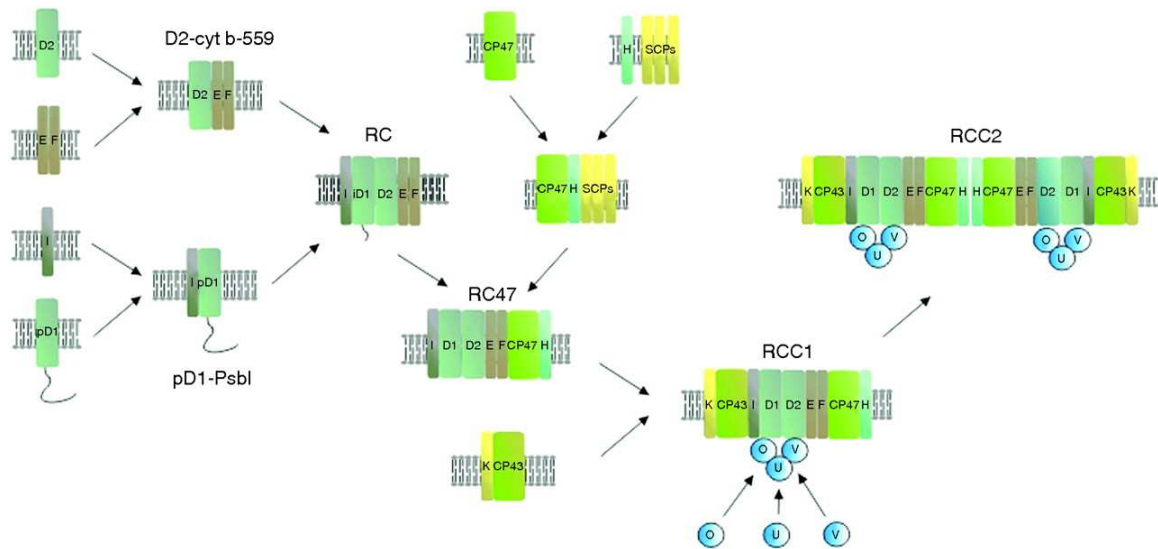


Figure 2 – Stepwise Assembly of PSII from (Nixon et al., 2010) Depiction of the stepwise assembly as it is now known in cyanobacteria. This process has thus far been confirmed in plants, barring the fact that pD1 is processed in one step, SCPs have yet to be identified in plants and PsbU and PsbV are replaced by PsbP and PsbQ, respectively

One monomer of PSII includes the Reaction Center (RC) heterodimer: D2 and D1, encoded by the plastid genes *psbA*, and *psbD*. The proteins D1 and D2 bind the redox active cofactors, including the two critical P700 chlorophylls, two pheophytins and one non-heme iron. CP47 and CP43, encoded respectively by the plastid genes *psbB* and *psbC*, are the core antenna proteins. Flanking D1 and D2, they function in light capture and aid in stabilizing the redox active cofactors. In addition, the plastid encoded cytochrome *b₅₅₉* and PsbI complete the core of a PSII monomer (Nixon et al., 2010). This core is supported by a number of small subunits (PsbE-M, PsbR-T, PsbW-Z, etc.) (Shi et al., 2012). Surrounding this Reaction Center Core (RCC) are the light harvesting

complexes (LHC), which expand the surface area of the complex, increasing light capture.

On the luminal side of the membrane, the nuclear encoded PsbO aids in binding the manganese (Mn) cluster, which is composed of four manganese, one calcium and one chloride ions (Becker et al., 2011). In eukaryotes, PsbO associates with two additional nuclear encoded, soluble luminal proteins: PsbP and PsbQ. Together, these three proteins compose a 'luminal cap' for PSII and the manganese cluster (Bricker and Frankel, 2011; Bricker et al., 2011). Interestingly, the roles of PsbP and PsbQ seem to be filled by the non-orthologous proteins PsbU and PsbV in cyanobacteria (Seidler, 1996). Meanwhile, evidence suggests that cyanobacteria use PsbP-like and PsbQ-like proteins during PSII assembly (Ifuku et al., 2011). This is but one example of many demonstrating the difference between cyanobacterial and eukaryotic PSII, a trend that casts doubt on the appropriateness of using *Synechocystis* and other cyanobacteria as systems for identifying assembly factors that can be correlated to plastids. This dissertation will therefore attempt to keep the two systems separate, focusing on the factors identified or confirmed in plastids and making note of a few exciting bacterial genes whose functional counterparts in eukaryotes have not yet been identified.

2.1 PSII Assembly

One aspect of assembly that appears to be conserved from cyanobacteria to plants is the finding that the RCC is assembled in a stepwise manner (Plucken et al., 2002; Boehm et al., 2011), beginning with the insertion of cyt *b*₅₅₉ and D2 into the membrane. This is followed progressively by attachment of D1, CP47 and finally CP43. The D1 protein is translated with a precursor (pD1) on its c-terminus, which is cleaved by CtpA

(carboxyl-terminal processing protease A) (Anbudurai et al., 1994; Inagaki et al., 1996) as CP47 is added (See Figure 2).

After assembly of the transmembrane components of the RCC, the manganese cluster is assembled. Modeling of crystal structures from *Synechocystis* complexes show that additions of CP47 and CP43 leave an opening in the RCC. Mn ions are added within this opening in a stepwise process. An initial Mn atom is added, and the others follow in a light-dependent succession via a process called photoactivation (Burnap, 2004; Becker et al., 2011). The addition of PsbO then sterically blocks this site, effectively covering the Mn cluster. Further modeling suggests that PsbP and PsbQ (or PsbU and PsbV in cyanobacteria) then assemble adjacent to PsbO (Calderone et al., 2003; Ifuku et al., 2004; Balsera et al., 2005; Nield and Barber, 2006; Barber, 2008; Michoux et al., 2012).

As the location for light capture and water splitting, the PSII complex is particularly sensitive to damage from Reactive Oxygen Species (ROS). The D1 protein takes the brunt of this damage, and so turnover of the D1 protein is higher than the rest of the complex (Aro et al., 1993a; Aro et al., 1993b; Andersson et al., 2004). To avoid rebuilding the entire PSII complex every time the D1 protein is damaged, cyanobacteria, plants and eukaryotic algae can specifically replace this protein within the RCC (Takahashi and Badger, 2010; Komenda et al., 2012). As such, one of the challenges in the study of PSII biogenesis is distinguishing between assembly factors and repair factors. Assembly factors are involved in the *de novo* production and assembly of PSII complexes while repair factors are involved in the removal of damaged proteins and coordinating the insertion of a new D1 protein into an assembled complex. This text will attempt to focus on assembly factors, where the current state of research allows, though

the reader should understand that some of these factors may have dual functions that are inexorably intertwined with both processes. An assembly factor mutant is defined by the slowed production of or incomplete production of wild type complexes while transcription and translation are not. On the other hand, repair factor mutants have completely assembled complexes, but damaged complexes accumulate.

2.2 D2

To produce the PSII center, the first protein that must be produced is cytochrome *b₅₅₉* (composed of two peptides translated from the typically plastid genes *psbE* and *psbF*) and D2 (Rochaix, 2012). While *cyt b₅₅₉* does not appear to be essential for the primary charge separation, its production is nonetheless necessary for PSII accumulation. These two subunits are generally encoded by a *psbE-F-J-I* operon in the chloroplast of plants, while these genes are encoded separately in other organisms, such as the green alga *Chlamydomonas reinhardtii* (Martin et al., 2002; Merchant et al., 2007).

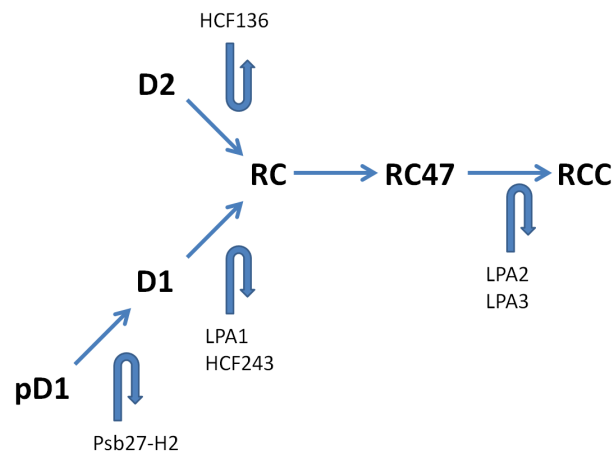


Figure 3 - Placement of Known PSII Assembly Factors in Arabidopsis The placement of various PSII assembly factors via phenotypic and protein-protein interaction data.

2.2.1 HCF136 - *Arabidopsis* D2 Assembly Factor

In this stepwise process, D2 is then produced. One gene implicated in D2 assembly is HCF136 (high chlorophyll fluorescence). The *hcf* mutants are defined by increased chlorophyll autofluorescence as compared to wildtype plants. *Arabidopsis hcf136* mutants pale on exposure to even low light (20-50 $\mu\text{mol}/\text{m}^2/\text{s}$), suggesting photooxidative damage (Meurer et al., 1998). Spectroscopic data indicates that PSII is completely inactive in this mutant and BN-PAGE shows the complete lack of PSII assembly. Furthermore, the thylakoid architecture is strikingly altered, being dominated by tightly packed grana. Comparing the behavior of *hcf136* with three other *hcf* mutants (*hcf173*, *hcf154* and *hcf107*) affected at various levels for PSII accumulation, (Plucken et al., 2002) showed that at 50-70 $\mu\text{mol}/\text{m}^2/\text{s}$ there is a general trend for reduced accumulation of PSI as a secondary effect of these mutations. This down accumulation compared to wild type is less drastic at 2-5 $\mu\text{mol}/\text{m}^2/\text{s}$, but still evident (Plucken et al., 2002). The reader might wish to take note of this phenotype - that of PSI down accumulation - because it is a recurring theme in PSII assembly mutants. The interrupted nuclear gene in the *hcf136* mutant encodes for a protein predicted to be 403 amino acids long. Immunoblot with protein specific antibodies reveals its size to be around 37kDa. A homolog in *Synechocystis*, Slr2034, is encoded just prior to the *psbE-F-J-I* operon, emphasizing the gene's potential role in photosynthesis. Sub-organelle fractionation identified the protein in the stroma thylakoids and as the hydropathy plot predicted, it was easily removed by carbonate extraction, indicating a loose membrane association. Further thermolysin treatment of extracted thylakoids indicate that the protein is protected within the lumen, as predicted by the presence of a bipartite luminal targeting

sequence (Meurer et al., 1998).

The primary defect of *hcf136* appears to be in PSII assembly or stability, since accumulation of all proteins is equally down by immunoblot analysis, but translation is not obviously altered or inhibited by pulse labeling (Meurer et al., 1998). Investigating [35S]methionine incorporation into PSII, (Plucken et al., 2002) found that incorporation of radio-labeled protein into PSII dimers, monomers and PSII assembly sub-complexes was greatly reduced in these mutants, while unassembled CP47, CP43, D2 and D1 accumulated as free protein, indicating the block is a result of slowed assembly. Since this mutant is also missing a PSII assembly sub-complex, composed of *cyt b₅₅₉*, D1 and D2, which is formed in mutants deficient for the transcription of CP47, it indicates that HCF136 acts prior to or during the association of D1 and D2. Furthermore, during pulse-chase in the mutant, free D1 protein was lost, but some radiolabel appeared in a 290kDa of aggregated D1, suggesting D1 stability was not the primary defect. These results place HCF136 in an assembly role between D2 translation and the association of D1 and D2.

Protein-protein interaction experiments confirm this role. Using a HCF136-Protein A construct, (Plucken et al., 2002) identified HCF136 as a free protein, but also in several complexes from 70 to 200 kDa. The sizes of these complexes correspond to PSII dimers, monomers and PSII assembly sub-complexes containing D2. Pull-downs using HCF136-Protein A revealed interactions with D2 and *cyt b₅₅₉* (Plucken et al., 2002) but not D1. This data places HCF136 early in PSII assembly, perhaps in the role of initiating the association of D2 with *cyt b₅₅₉*.

Some final attributes of HCF136 that support its role in PSII assembly include its expression in etiolated seedlings and up regulation upon light exposure. This mimics the

expression behavior of the luminal PSII component, PsbO, indicating that HCF136 is expressed under the same conditions that PSII assembly is occurring (Meurer et al., 1998). In addition, HCF136 was shown to be imported into the chloroplast lumen via the Tat pathway in pea chloroplasts (Hynds et al., 2000). The proposed placement of HCF136 in the stepwise assembly of the RCC can be seen in Figure 3.

2.2.2 YCF48 - *Synechocystis* ortholog of HCF136

Noticeably, there is no twin arginine motif on cyanobacteria orthologs of *HCF136*, so it is likely to be directed to the thylakoid membrane by some other pathway. In fact, *Synechocystis* strains mutant for the ortholog of *HCF136*, YCF48 (encoded by *slr2034*), do not display the same phenotype as *hcf136 Arabidopsis* mutants. YCF48 is not essential for the photosynthetic growth of *Synechocystis*, and therefore must not be absolutely essential for PSII assembly.

Like *hcf136 Arabidopsis* mutants, *ycf48* deletion mutants did not produce PSII at the same levels as wild type. The basis for this down accumulation appears to be the rate of assembly, as all of the PSII reaction center components accumulate as free protein, as indicated by 2D gel analysis. Furthermore, YCF48 is similar enough to HCF136 that antibodies produced against *Arabidopsis* HCF136 recognized the presence of YCF48 in a PSII assembly intermediate. This intermediate complex was composed of cyt *b*₅₅₉, D2 and, unlike what was seen in *Arabidopsis*, D1. Confirmation that YCF48 was part of this assembly sub-complex was obtained by the absence of this complex in a cyt *b*₅₅₉ mutant, which does not produce the RC intermediate, and its continued presence in a CP47 mutant which does (Komenda et al., 2008).

Upon examining the maturation of D1 in these *ycf48* mutants, they found that not

only was pD1 still processed as in wild type, but also that the mutant under accumulated D1 precursors, over accumulated the processed D1 protein and over produced the *psaD* mRNA as compared to the wild type. This indicates that there is a bottleneck just past the point of pD1 processing in the mutants. By Yeast-2-Hybrid, they found that YCF48 interacts with pD1 but not mature D1, D2 or CtpA, the enzyme involved in removing the D1 precursor. This is contrary to evidence in *Arabidopsis*, where HCF136 interacted with D2. Furthermore, the authors found that the absence of YCF48 altered D1 repair in damaged complexes, making YCF48 an example of a protein that is required for both assembly and repair of PSII. These differences suggest that either the role or primary protein associations of HCF136 may have altered slightly during the evolution of the plastid (Komenda et al., 2008).

2.3 D1

The maturation of the D1 protein has been extensively studied in *Synechocystis*. Unfortunately, while the D1 protein itself is conserved in plants and eukaryotic algae, data such as that presented for YCF48 suggests that the maturation pathways were not conserved upon endosymbiosis. The author of this dissertation suggests that this could be a result of the unpredictable nature of gene transfer to the nucleus of the endosymbiotic host. This could lead to evolution favoring factors that were transferred to the nucleus at earlier time points and adaptive radiation of those factors that were nuclear encoded and targeted to the chloroplast, as seen in some factors, such as PsbP, described later in this text.

As mentioned earlier, it does appear that the basic process of D1 maturation is conserved. The D1 protein has been shown to be inserted into the thylakoid membrane of

co-transcriptionally via the chloroplast SecY pathway (Zhang et al., 2001), perhaps targeted or aided during transcription by chloroplast SRP54 (Nilsson and van Wijk, 2002). After insertion into the membrane, the precursor of D1 (pD1) is cleaved by the CtpA protease. This must happen for both *de novo* assembly and during PSII repair (Sakamoto, 2006). Unlike *Synechocystis*, which absolutely requires CtpA for maturation of the D1 protein and addition of the manganese cluster, and so for photosynthetic growth (Roose and Pakrasi, 2004), a T-DNA insertion into the major CtpA ortholog is not greatly detrimental to photosynthetic growth in *Arabidopsis* (Yin et al., 2008). Yin and colleagues note that there are two additional isoforms of CtpA encoded by the nuclear genome of *Arabidopsis* which may have partially overlapping function (Sakamoto, 2006; Kato et al., 2009; Kato and Sakamoto, 2009; Kato et al., 2010).

Currently, five proteins have been implicated in the assembly of the D1 protein in *Arabidopsis*: ALBINO3 (ALB3), Low PSII Accumulation 1 (LPA1), Photosynthesis Affected Mutant 68 (PAM68), High Chlorophyll Fluorescence 243 (HCF243) and PSB27-H2. All of these proteins have been shown to have an interaction with either pD1, D1 or both (See Table 1). Furthermore, ALB3, LPA1 and PAM68 also interact with one another (See Table 2). Of these three, ALB3 is the most investigated, although it perhaps has the most contentious role in PSII assembly.

2.3.1 ALB3 - *Arabidopsis* Insertase

ALB3 is necessary for the co-translational insertion of D1 into the thylakoid membrane (Woolhead et al., 2001). ALB3 is an ortholog of YidC and Oxa1p (Sundberg et al., 1997) and in addition to its potential role in D1 assembly, it has been shown to integrate LHC into the thylakoid membrane (Woolhead et al., 2001; Bellafiore et al.,

2002) and to interact with the chloroplast SECY translocase (Pasch et al., 2005). The YidC/Oxa1p/ALB3 family is involved in the insertion of proteins into redox active membranes. YidC is found in bacteria and acts either separately or in coordination with the bacterial Sec-YEG translocon (Samuelson et al., 2000; Samuelson et al., 2001; Chen et al., 2002) to integrate proteins into the cytoplasmic membrane. Likewise, Oxa1p works to insert proteins into the inner mitochondrial membrane (Bonnefoy et al., 1994; Hell et al., 2001). Confirming its ability to act as an insertase, ALB3 complements a bacterial YidC mutant (Jiang et al., 2002). The motifs in these proteins can be seen in

Figure 4.

Interestingly, ALB3 appears to be specifically essential for integration of the LHC proteins in *Arabidopsis*, as antibodies against ALB3 inhibit LHC integration into the thylakoid while the Sec and Δ pH pathways were unaffected (Moore et al., 2000). Furthermore, ALB3 can apparently integrate LHC3 without the help of SECY (Mori et al., 1999). And yet, ALB3 and SECY proteins have been shown to work together at other times, as (Klostermann et al., 2002) showed that ALB3 and SECY are both found in complexes of approximately 160-200 kDa during gel-filtration analysis and blue native gel electrophoresis. Interestingly, blue native gel analysis identified both of these proteins in at least five additional higher molecular weight complexes up to 700 kDa. These two proteins also co-immunoprecipitate and double immunogold labeling places them side by side at the thylakoid membrane. While nearly all of the SecY was associated with ALB3 in these immunogold experiments, ALB3 could be found separate from SecY. Finally, Klostermann and colleagues confirmed this association using chemical cross-linking. So the question arises: are the protein associations seen with

ALB3 a result of its insertase role, or does it have an additional role in D1 assembly?

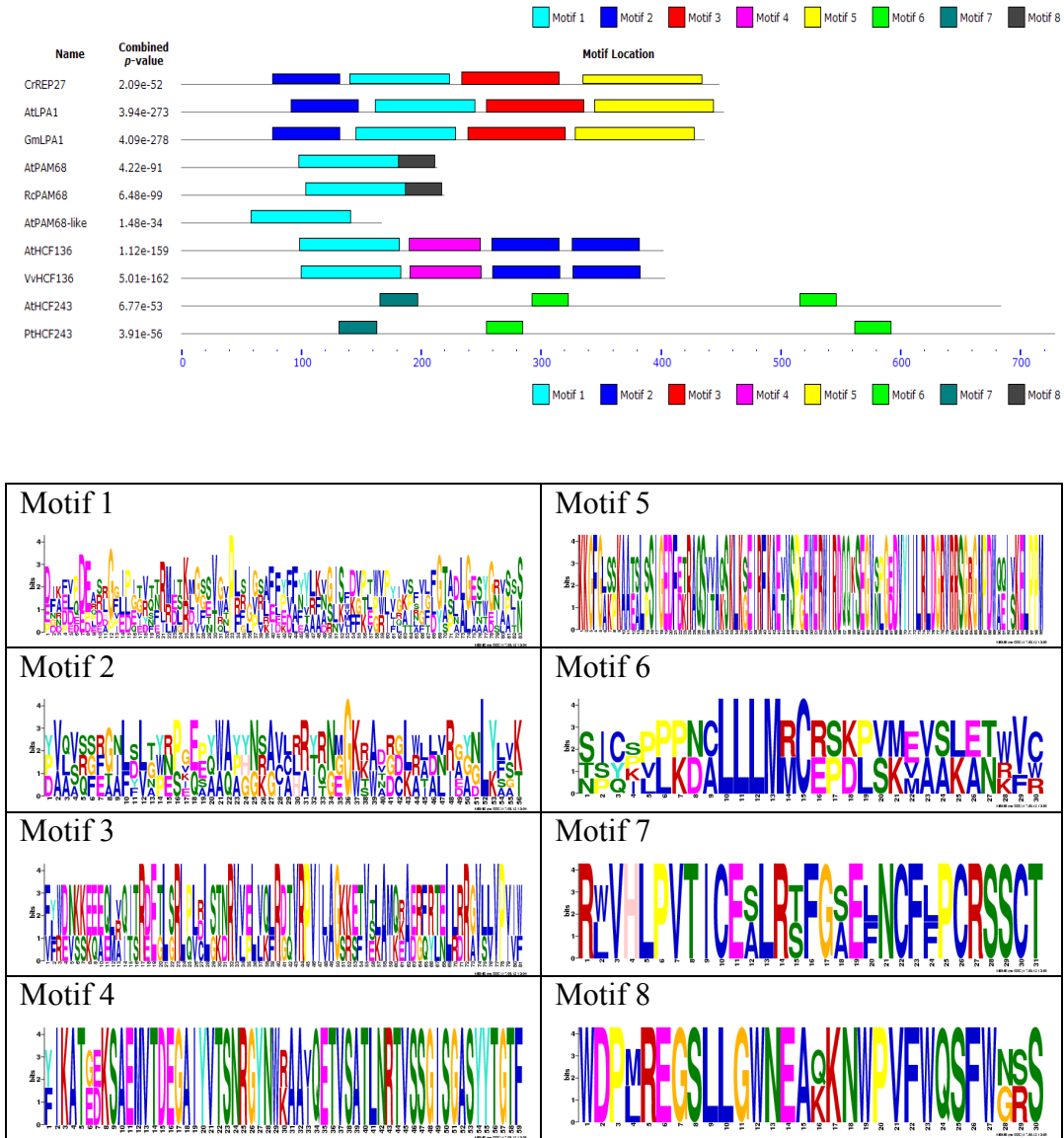


Figure 4 – D1 Assembly Protein Motifs

Arranged by relatedness as predicted by MAFFT. At, *Arabidopsis thaliana*, Gm, *Glycine max*, Pt, *Populus trichocarpa*, Vv, *Vitis vinifera*, Syn, *Synnechocystis* PCC 6803, Rc, *Ricinus communis*

2.3.2 ALB3.2 - Chlamydomonas ortholog of Arabidopsis ALB3

Work in Chlamydomonas would suggest that it could have this additional role.

There are two isoforms of ALB3 in *Chlamydomonas*. ALB3.1 has been implicated in the assembly of the PSII LHC (Ossenbuhl et al., 2004) while ALB3.2 has been shown to interact with D1, among other proteins (Gohre et al., 2006). ALB3.2 is localized to the thylakoid membrane and sucrose density centrifugation identified it in two high molecular weight complexes of 300 and 650kDa. This distribution is very similar to ALB3.1 and blue native gels reveal that these two complexes correspond to the PSII monomers and dimers, as identified by immunoblotting with D2 antibodies and their absence in the PSII-deficient *FuD7* mutant.

To examine the regulation of this protein in relation to photosynthetic complex assembly, the authors looked at ALB3.2 accumulation in a mutant that is deficient for light-independent chlorophyll biosynthesis. Similar to etiolated seedlings, these chlorophyll biosynthetic mutants must be exposed to light for the accumulation of the two photosystems. ALB3.2 expression was not noticeably altered in this mutant, and so its regulation either does not parallel that of photosystem assembly or is uncoupled from the regulation system in these mutants.

To test for ALB3.2 interaction partners within the photosystems, co-immunoprecipitations were performed. These experiments revealed interactions with ALB3.1, D1, D2, PsaA and VIPP1 (vesicle inducing protein in plastids 1). VIPP1 has been identified as a primary player in thylakoid membrane formation and implicated in the assembly of the photosynthetic complexes (Kroll et al., 2001), yet there was no interaction found between ALB3.2 and two partners of VIPP1, HSP70B or CDJ2. This supports a growing body of literature that VIPP1 may be involved in the assembly of the photosystems.

A third ALB3.2 containing complex was also identified via BN-PAGE and most likely corresponds to PSI-LHC, as identified by PsaA immunoblot and the absence of this complex in the PSI-deficient mutant *F15*. Furthermore, a subcomplex is accumulated in the *alb3.2* mutant that corresponds to PSI without LHC association. This indicates an additional role for ALB3.2 in LCH maturation and/or association with the photosynthetic complexes. Finally, it should be noted that neither of the assembly factors SRP54 nor SECY was identified, nor was ALB3.2 found to be associated with polysomes. This indicates that ALB3.2 is not involved in regulating translation via the polysomes or the SECY pathway. This supports the hypothesis that ALB3 may have roles in addition to its interaction with SECY in *Arabidopsis*.

To look more specifically at the interaction with D1 and D2, the authors next produced an RNAi line against ALB3.2. Knockdowns below 50% wild type levels of transcript appeared to be lethal, indicating the essential nature of this transcript. In lines that survived, levels of D1 and D2 were reduced by as much as 75%, while CP43 and PSII-LCH were less affected. The levels of other complexes did not appear to be altered. Interestingly, VIPP1, HSP70 and CDJ2 protein levels were up, indicating an up regulation of this assembly pathway when ALB3.2 levels are decreased.

Unfortunately, ALB3.2 is not the only ortholog of ALB3 involved in *Chlamydomonas* PSII assembly. ALB3.1 has also been identified as being involved in the assembly of the LHC-PSII in *Chlamydomonas* while a second homolog in *Arabidopsis*, ALB4, has been implicated in the assembly of the plastidic ATP synthase (Gerdes et al., 2006; Benz et al., 2009). This makes any direct comparison to *Arabidopsis* PSII assembly unreliable. In contrast to *alb3.2*, *alb3.1* *Chlamydomonas* mutants do not

have altered D1 integration into the thylakoid membrane (Ossenbuhl et al., 2004). It therefore remains to be seen whether or not ALB3 or ALB4 in *Arabidopsis* has a dual role.

2.3.3 LPA1 - *Arabidopsis* D1 Assembly Factor

Shown to interact with both D1 and ALB3, a factor identified specifically as a D1 chaperone in *Arabidopsis* is LPA1 (or At1g02910). This protein was identified by (Peng et al., 2006) through the *lpa1* mutant, which is deficient in PSII accumulation and has reduced growth on soil as compared to the wild type. In this mutant, the translation of D1 and D2 are down as determined by pulse labeling while turnover of D1, D2, CP43 and CP47 is increased as determined by pulse-chase. This results in a decreased accumulation of all four of these RCC proteins in the mutant, especially in the PSII dimer. The mutant also demonstrates the secondary characteristics of plants with PSII defects described earlier: PSI is down and the mutant's chloroplasts are smaller as viewed by electron microscopy (EM). While investigating PAM68, another protein implicated in PSII assembly, the Liester lab noted that a *lpa1* mutant has a decrease in the ratio of PSII supercomplexes to dimer and monomer formations, that the turnover of the dimer is slower than in the wild type, and that D1 and D2 subunits are translated but remain unassembled (Armbruster et al., 2012). Together, this over accumulation of subunits indicates a block at the post-translational level that results in feedback inhibition (or enhancer suppression) of translation as indicated by the reduced translation of the D1 and D2 subunits.

The *LPA1* gene itself encodes a 453 amino acid long protein, calculated to be 50 kDa, that accumulates in the chloroplast (Peng et al., 2006). It has two predicted TPR

(tetra-trico-peptide repeat) motifs, indicating a role in protein-protein interactions, and two predicted two trans-membrane domains. Primary sequence homology searches in 2012 indicate that there are orthologs in green plants and algae. Notably, REP27, a protein involved in D1 repair in *Chlamydomonas* (Park et al., 2007; Dewez et al., 2009), has significant homology and similar domain architecture. Because of this, the role of LPA1 as an assembly factor and/or repair factor must be clarified, although it is likely to be involved in both processes.

2.3.4 PAM68 - *Arabidopsis* PSII Assembly Factor

Evidence that LPA1 interacts specifically with D1 came from the Liester lab as they worked with the *Arabidopsis* protein PAM68, one of two homologs in *Arabidopsis* that have a loose primary sequence similarity to Sll0935 in *Synechocystis* (Armbruster et al., 2012). Like *lpa1* mutants, the *pam68* mutant has decreased chlorophyll fluorescence and decreased levels of the reaction center core subunits. Transcription and polysome association of the D1 transcript appears unaffected, but pD1 and D2 turnover is very high in the mutant, as determined by pulse-chase analysis and the half life of D1 is particularly affected. There is also an increase in the amount of pD1 in relation to mature D1, indicating that the mutant is deficient in pD1 processing. Unlike what is seen in the *lpa1* mutant, while all RC complex subunits are down to at least 20% of wild type by blue native and 2D gel, the proportion of RC complexes in the dimer configuration has increased in the mutants when compared to wild type (Armbruster et al., 2012). Taken together, this data places PAM68 in a pD1 maturation role, perhaps with the additional function of stabilizing PSII monomers, although we will see as this dissertation progresses that its role may be much more complex than this.

PAM68 itself is a thylakoid transmembrane protein with its amino-terminus acidic domain exposed to the stroma. Yeast-2-Hybrid experiments suggest that the amino-terminus of PAM68 interacts with PsbI while trans-membrane I interacts with D2, LPA1 and ALB3. Transmembrane I also interacts with another small subunit of PSII, PsbH, and LPA2, a factor proposed to aid in the assembly of CP43. Furthermore, the full-length protein appears to interact with CP47 and HCF136. With this association data, the authors propose that perhaps PAM68 is working with LPA1 to mature the pD1 protein (Armbruster et al., 2012). The finding that PAM68 interacts with so many proteins associated with PSII places it in a key position during the assembly process and suggests additional roles for this protein. One possibility is that PAM68 facilitates the interaction between the ALB3/Sec pathway and specific PSII proteins and assembly factors, localizing this insertion in the area of incomplete RCCs, although this remains to be tested.

As mentioned earlier, a PAM68-like protein called Sll0935 is present, but poorly conserved from *Synechocystis* to *Arabidopsis*. In particular, the *Synechocystis* ortholog is missing its acidic domain. Accordingly, these *pam68-like* mutants do not have the same phenotype as *Arabidopsis pam68* mutants: photoautotrophic growth, photosynthesis and formation of WT levels of PSII appear to be unaffected when compared to wild type. Strangely, early PSII assembly intermediates are absent in the mutant by 2D/BN-PAGE, suggesting either that they are more labile or that PAM68-like stabilizes these sub-complexes. Further evidence that Sll0935 is part of these early assembly intermediates comes from immunoblot against the PAM68-like protein, which reveals the presence of this protein at the same size as the early complexes in wild type extractions (Armbruster

et al., 2012). Interestingly, the MEME program (Bailey and Elkan, 1994) indicates that the PAM68-like domain of Sll0935 is more similar to a second PAM68 homolog in *Arabidopsis* (Figure 3). It will be enlightening to uncover the role of this second homolog in *Arabidopsis*, as perhaps its phenotype will more closely resemble the *sll0935* *Synechocystis* mutant.

2.3.5 Psb27-H2 - *Arabidopsis* pD1 Assembly Factor

Psb27-H2 was originally identified by Wei as the *Arabidopsis* mutant *lpa19* (Wei et al., 2010). These mutants have reduced growth, especially under high light conditions, and a PSII defect. Identification of the molecular lesion revealed that LPA19 is an ortholog of *Synechocystis* Psb27, which is described later in this dissertation as possibly having a role in assembly of the Mn cluster. This is the second Psb27 ortholog identified in *Arabidopsis*, so to avoid confusion, the authors renamed the previous Psb27 homolog as Psb27-H1 and gave LPA19 the label Psb27-H2. The authors note that Psb27-H1 and Psb27-H2 appear to have distinct roles in *Arabidopsis*, with Psb27-H1 being involved in PSII repair and Psb27-H2 in PSII assembly (Wei et al., 2010).

Contrary to some results in *Synechocystis*, Wei and colleagues found reduced accumulation of the PSII core complex proteins in the *psb27-h2* mutants and delays in the maturation of D1 as identified by pulse labeling. Immunoblot identified Psb27-H2 as part of monomeric PSII complexes and subcellular fractionation identified PSB27-H2 as a thylakoid lumen protein whose association with the membrane could be disrupted by the addition of CaCl₂ but not NaCl. To determine interaction partners, co-immunoprecipitation revealed that PSB27-H2 interacts with pD1 and D1 while Yeast-2-Hybrid results suggest that this interaction is specifically with pD1 and the carboxy-

terminus of mature D1. This data places PSB27-H2 as part of pD1 processing. Although its exact role is still unknown, one possibility based on data from *Synechocystis* (Liu et al., 2011b; Liu et al., 2011a) is that it recruits CtpA to the pD1 processing site. It would therefore be interesting to uncover the phenotype of a *ctpA psb27-h2* double mutant in *Arabidopsis*, as we might expect an epistatic interaction.

2.3.6 HCF243 - *Arabidopsis* D1 Assembly Factor

Recently, a new potential D1 assembly factor, HCF243, has been identified in *Arabidopsis* (Zhang et al., 2011). The Chen lab identified the *hcf243* mutant by its high chlorophyll fluorescence phenotype and found the affected gene to be *At3g15095*. Searches based on primary sequence homology revealed no orthologs in non-vascular plants or cyanobacteria. Even within angiosperms, the primary sequence is highly variable and exhibits no known functional domain. Immunoblot revealed the presence of HCF243 within the thylakoid fraction. This association is only disrupted by the addition of urea, indicating an intrinsic membrane protein.

Further characterization of this mutant via noninvasive fluorometry indicated defects in energy transfer within PSII. Meanwhile, BN page analysis revealed a complete lack of PSII super-complexes and down accumulation of PSII monomers and immunoblot showed reduced accumulation of D2, D1, CP43 and CP47 proteins. The incorporation of proteins into the few PSII complexes that are produced is constant but slowed. While the authors did not specifically look at pD1, their pulse analysis shows no extreme aberration in its processing (Zhang et al., 2011).

reduced. In addition to this down accumulation, pulse-chase indicates an increased degradation rate of these two proteins. The authors do not mention a quantification of this turnover, but suggest that it may not be sufficient to explain the extent of the down accumulation (Zhang et al., 2011).

As D1 was more strongly affected than D2, the authors examined the association between the two using BiFC. These experiments indicated an association of the amino-terminus of HCF243 with D1 within the chloroplast of *N. benthamiana*. This interaction was supported via pull-down assays, showing that HCF243 could pull-down the D1 protein but not CP47 (Zhang et al., 2011). Further characterization of this protein must be completed before its function is determined, but its identifiable presence in vascular plants, its stretches of amino acid repeats, and its lack of identifiable functional domains suggest a role in protein-protein interactions.

2.4 CP43

The addition of CP47 must occur before CP43 completes the large transmembrane components of the RCC. As pD1 is processed, CP47 is added to the complex. Assembly factors involved in the specific assembly of CP47 are also as yet few, although an interaction has been demonstrated with PAM68 and a distinct sub-complex including *cyt b₅₅₉*, D2, PsbI, D1 and CP47 (often referred to as RC47) can be identified in cyanobacteria and plants (Boehm et al., 2011). Small chlorophyll binding proteins (SCPs) have also been identified as interacting with CP47 in *Synechocystis*, but no primary sequence has been identified in plants (Promnares et al., 2006). It has been suggested that early light induced proteins (ELIPs) may be full-filling this role, but experimental evidence for this is largely absent from the literature (Mulo et al., 2008).

After CP47 is added, the assembly of CP43 is coordinated by several proteins. Following the trend seen with HCF243, these assembly factors do not display primary sequence conservation when compared to *Synechocystis*. The arrangement of the motifs found in these assembly factors can be seen in Figure 5.

2.4.1 LPA2 and LPA3 - *Arabidopsis* CP43 Assembly Factors

LPA2 (At5g51545) and LPA3 (At1g73060) are involved in CP43 post-translational stabilization, but both seem to be absent from *Chlamydomonas* and cyanobacteria as determined by primary sequence homology (Rochaix, 2012). These proteins have also been shown to interact with ALB3, mentioned previously as a factor involved in LHC and D1 assembly. This text will look first at LPA2, which appears to be a key component of CP43 assembly, and then the related LPA3 which may have a more regulatory function.

The Zhang Lab showed that the *lpa2* mutant has a defect in PSII assembly and that all PSII core proteins are down, especially D1 and CP43. While transcription and polysome association of the CP43 and D1 transcripts is unaffected, the translation of CP43 is inhibited and the turnover of all the core proteins is increased. In particular, the turnover of D1 is markedly rapid in pulse chase experiments as compared to wild type. This could suggest incomplete assembly or increased susceptibility to oxidative damage (Ma et al., 2007).

As the name suggests, the *lpa3* mutant once again has reduced accumulation of PSII RC proteins and reduced growth. Like *lpa2*, transcript accumulation and polysome association is unaffected in this mutant but CP43 translation is down by pulse labeling and D1 turnover is increased as revealed by pulse-chase analysis. Notably, LPA3 is down

in the *lpa2* mutant, but not *vice versa* (Cai et al., 2012). Cai and colleagues also examined a double *lpa2 lpa3* mutant and found it to have an exaggerated phenotype, with severely reduced growth, a yellow phenotype and the near absence of PSII RCC proteins as seen by pulse labeling. This indicates that both proteins are functional and have either partially redundant or distinct roles in the assembly of CP43.

The LPA2 protein itself is 185 amino acids long and is predicted to have two transmembrane domains (Ma et al., 2007). It is tightly associated with the thylakoid membrane fraction, as it is not removed by NaCl, CaCl₂ or urea. This supports the prediction that it is an integral membrane protein (Ma et al., 2007). LPA3 has some domain homology to LPA2, based on primary sequence, and is found in both the stroma and thylakoid membrane associated fractions. This membrane association is unperturbed by NaCl, loosened with CaCl₂ and completely abolished only upon addition of urea. The differences between LPA2 and LPA3 thylakoid association suggests distinct, rather than duplicate, functions (Cai et al., 2012). This hypothesis is supported by the finding that the association of LPA3 with the thylakoid seems to be mildly light dependent. Under high light conditions, the protein tends to be more associated with the thylakoid membrane whereas in low light conditions, it has a looser association and a larger population of the protein can be found in the stroma – a variation of approximately 20% as quantified by multiple replicates (Cai et al., 2012). Because of these results, the authors suggest that LPA3 might be performing a regulatory function, either regulating assembly of PSII itself or acting as part of a signaling cascade effecting another process.

When run on a sucrose gradient, LPA2, CP43 and ALB3 are enriched in the same fractions of ~67-140 kDa and Yeast-2-Hybrid experiments suggest that LPA2 interacts

with CP43 and ALB3 but not D1, D2 or LPA1. They do not test the association with pD1 (Ma et al., 2007). Later experiments by the Zhang lab showed that LPA3 also interacted with LPA2, CP43 and ALB3 by Yeast-2-Hybrid, but not D1, D2, LPA1 or CP47 (Cai et al., 2012). Together, this data, combined with earlier work on PAM68, suggests that a complex composed of LPA2, LPA3, CP43, ALB3 and PAM68 *may* be found at one point during the assembly of PSII in *Arabidopsis*. Known interactions between PSII assembly factors and the four primary RCC components described here within can be seen in **Table 1** and **Table 2**.

		PSII Components				
		<i>D2</i>	<i>D1</i>	<i>pD1</i>	<i>CP47</i>	<i>CP43</i>
PSII Assembly Components	<i>LPA1</i>	N/D	√	N/D	N/D	N/D
	<i>LPA2</i>	X	X	--	N/D	√
	<i>LPA3</i>	X	X	--	X	√
	<i>HCF243</i>	N/D	√	√	X	N/D
	<i>HCF136</i>	√	X	X	X	X
	<i>PSB27-H2</i>	N/D	√	√	N/D	N/D
	<i>PAM68</i>	√	√	√	√	√

Table 1 - Interactions demonstrated between assembly factors and PSII reaction center components. √ indicates interaction has been demonstrated experimentally, X indicates an interaction was tested and not observed, N/D indicates no published data regarding this interaction. -- indicates that, while such an interaction has not been tested, the likelihood is low, as a result of lack of interaction with the D1 protein.

The questions that follow this possibility are: (1) is there such a complex (2) are there multiple complexes at different stages of PSII assembly or (3) are the association results with ALB3 simply an artifact of these proteins being targeted to the thylakoid membrane? Regarding to the last possibility, it must be explained why LPA3, a non-integral membrane protein, would show an association with ALB3. In addition, the role

of PAM68 in PSII assembly is particularly intriguing, considering its association with so many proteins. A possible explanation that remains to be tested is that the various assembly factors use PAM68 as a 'docking station', perhaps in coordination with ALB3, as they sequentially incorporate their RCC components. One way to approach this question might be deletion analysis in order to determine the domains of interaction. If all domains of the proteins it is associated with interact with a single domain of PAM68 or ALB3, it would support the sequential interaction model.

	<i>ALB3</i>	<i>LPA1</i>	<i>HCF136</i>	<i>PAM68</i>	<i>LPA2</i>	<i>LPA3</i>
<i>ALB3</i>	--	√	N/D	√	√	√
<i>LPA1</i>	√	--	N/D	√	X	X
<i>HCF136</i>	N/D	N/D	--	√	N/D	N/D
<i>PAM68</i>	√	√	√	--	√	√
<i>LPA2</i>	√	X	N/D	√	--	√
<i>LPA3</i>	√	X	N/D	√	√	--

Table 2 - Interactions demonstrated between known PSII assembly factors. √ indicates interaction has been demonstrated experimentally, X indicates an interaction was tested and not observed, N/D indicates no published data regarding this interaction.

2.5 Assembly of the Manganese Cluster

Once the membrane proteins have been assembled, the Mn cluster must be assembled and the nuclear encoded luminal proteins attached. Factors involved in this process in *Arabidopsis* have been elusive, because once again, there seems to be little conservation from cyanobacteria to eukaryotes. Because of the extensive studies done in *Synechocystis* and other cyanobacteria, this text will take a moment to explore some of the exciting new proteins being revealed in these organisms, including PrtA and Psb27.

The first of these has been proposed to present manganese to D1 while the second has been implicated in ‘protecting’ the unassembled OEC binding site. Since primary homology has not identified orthologs for these proteins in plants, we can anticipate the discovery of functional homologs, or perhaps even novel processes, as plastids complete these requirements for PSII assembly.

2.5.1 Prata - *Synechocystis* Mn Transporter and D1 Assembly Factor

In cyanobacteria, evidence suggests that the pD1 protein is associated with a protein called Prata (processing associated TPR) in the cellular membrane. Prata is an interesting protein, but no ortholog has been identified either by primary sequence or function in *Arabidopsis*. In a *prata* mutant, Klinkert et al. found reduced PSII accumulation, reduced PSII efficiency and altered pD1 processing (Klinkert et al., 2004). While the D1 and PsbO proteins are down in the mutant, they find that the transcripts of *psbO*, *psbB* and *psbD* are up. Since synthesis rates are the same as seen in the wild type, the decreased protein amounts must be a result of reduced stability or increased degradation.

Prata binds both pD1 and D1 via both Yeast-2-Hybrid and pulldown (Klinkert et al., 2004; Schottkowski et al., 2009). Using PepSpots and Yeast-2-Hybrid, Klinkert et al determined that the pD1 and D1 bind to amino acids 314-328, which are predicted to form an alpha-helix near the c-terminus of Prata. The protein itself is membrane associated and can be removed with Na₂CO₃ but not NaCl, indicating a non-ionic interaction. In accordance with their data that Prata and D1 associate, they find that Prata is in a high molecular weight complex, probably associated with pD1, as one of the complexes that pD1 is identified in is shifted in a *prata* mutant.

It was Stengel et al. that introduced the idea of a PratA Defined Membrane (PDM), which the authors report as being small regions of the membrane where PratA clusters (Stengel et al., 2012). The isolated supernatant of the periplasmic space was green for the wild type, but yellow for the *pratA* mutant, suggesting the absence of a cofactor from the mutants. They found that the amount of manganese in the mutant was reduced by about 35% of wild type levels.

The PratA protein itself contains 9 internal helix-turn-helix TPR motifs and its mRNA is expressed in the periplasm (Klinkert et al., 2004). Stengel et al. used circular dichroism to determine that PratA can bind as many as eight Mn atoms, with one high affinity site and seven low affinity (Stengel et al., 2012). It does not bind iron, magnesium or calcium. Using immunogold labeling, they showed that PratA tended to localize to membrane ‘buds’ that they called PDMs. Excitingly, they find a similar pattern when labeling pD1. Furthermore, these PDMs were absent in the *pratA* mutant. They suggest that these vesicular buds are biogenesis centers for some of the RC preassembly complexes.

While no obvious homologue for PratA has been identified in *Arabidopsis*, its presence in cyanobacteria emphasizes the point that a similar process for transporting manganese has yet to be found in *Arabidopsis*. VIPP1, mentioned earlier as interacting with the *Chlamydomonas* protein ALB3.2, is proposed to be involved in thylakoid formation via vesicle transport in *Arabidopsis* and *Chlamydomonas* (Kroll et al., 2001; Vothknecht et al., 2011). This role for VIPP1 must be tested, but there is indication that VIPP1 interacts with the Tat pathway in *Arabidopsis* (Lo and Theg, 2012) and may aid photosynthetic apparatus organization in *Chlamydomonas* (Nordhues et al., 2012).

2.5.2 Psb27 - *Synechocystis* Mn Cluster Assembly Factor

The *Synechocystis* protein Psb27 is another interesting player in OEC assembly. A stromal protein lipoated with three fatty acid residues, HPLC pure complexes in a $\Delta psb27$ mutant contain CP47, CP43, D1 and D2 as well as the characteristic small subunits, but these sub-complexes do not have the lumen proteins PsbO, PsbU or PsbV. Cell fractionation experiments show that Psb27 is tightly attached to the membrane fraction via a strong hydrophobic interaction, probably aided by the fatty acid residues, based on $MgCl_2$ washes (Nowaczyk et al., 2006). Further characterization of photosynthetic defects in a $\Delta psb27$ *Synechocystis* mutant shows no Mn oxidation and impaired electron transfer from the Qa site (Mamedov et al., 2007) and it seems that *Synechocystis* Psb27 aids in the recovery of the Mn cluster under high light conditions (Roose and Pakrasi, 2008). Roose and Pakrasi suggest that Psb27 acts by excluding PsbO, preventing PsbO from prematurely photoactivating the Mn cluster as it is being replaced. While the growth phenotype of the $\Delta psb27$ mutant is mild, the authors showed that wild type easily out-competes the mutant under high light conditions.

Crystallization of *Synechocystis* Psb27 revealed that the protein is composed of a right-handed, four helix bundle with an up-down-up-down topology. Furthermore, the helices are amphipathic, creating a hydrophobic side to the protein. Two crystallization studies using *Synechocystis* were published sequentially in 2009 (Cormann et al., 2009; Mabbitt et al., 2009) arguing that Psb27 fits perfectly into the PsbO binding site. Although it must be noted that later work using *T. elongatus* caused (Michoux et al., 2012) to argue that Psb27 may instead dock at PsbV, which would suggest a different function for this protein.

Michoux and colleagues made their argument based on data from the Pakrasi lab, who propose that Psb27 is NOT blocking the PsbO binding site (Liu et al., 2011b). When His-tagged Psb27 pre-assembly complexes are isolated from a *Synechocystis ΔctpA* mutant, they identify pD1 as an association partner of Psb27. The *ΔctpA* mutant does not process the carboxy-terminus of D1, which leads to an abundance of pD1. Meanwhile, in the His-tagged Psb27 wild type, they identify PsbO as an association partner. This challenges the idea that Psb27 blocks the manganese cluster. Using HPLC as an alternative purification process, (Grasse et al., 2011) deny this association in wild type cells. Using this method, the authors identified Psb27 in both a monomer and a dimer fraction with O₂ splitting activity. In these fractions, there was no PsbO.

Synechocystis Psb27 has also been shown to bind CP43 using chemical cross-linking (Liu et al., 2011b) and pulldowns (Komenda et al 2012). This second method also suggests an interaction with CP47. Furthermore, (Komenda et al 2012) show that the *Δpsb27* mutant has increased degradation of CP43 and 2D gel electrophoresis shows that Psb27 is in a pre-assembly complex with CP43 but not CP47. Interestingly, Psb27 does not accumulate in a *ΔpsbC* mutant, but does accumulate in a *ΔpsbB* mutant, suggesting that a block post-addition of CP43 to the RCC increased the expression or stabilization of Psb27. Fluorescence measurements indicate that the protein helps PSII accumulation in high light (Komenda et al 2012).

Adding to the mystery, mutants of Psb27 orthologs in *Arabidopsis* do not display the same phenotypes. These two homologs have distinct roles in *Arabidopsis*, with Psb27-H1 (encoded by At1g03600) involved in recovery after high light stress, based on data from PSII recovery kinetics and immunoblots (Chen et al., 2006) and Psb27-H2

being involved in D1 assembly, as discussed earlier (Wei et al., 2010). It could be that Psb27 is fulfilling two roles in *Synechocystis*: regulation of D1 processing, as suggested by (Liu et al., 2011a) and repair of the OEC complex, as indicated by (Roose and Pakrasi, 2008). These two functions could have then become separated in *Arabidopsis*, the first role being completed by Psb27-H1 and the second by Psb27-H2. If so, a dual role of Psb27 in *Synechocystis* might be revealed via mutational analysis.

2.6 PsbO

The *Arabidopsis* nuclear genome encodes for two, nearly identical, isoforms of PsbO, PsbO-1 and PsbO-2. While PsbO-1 is the dominant iso-form, based on expression levels, mutant analysis suggests that their roles are not completely overlapping. In a detailed review of the function of PsbO, Bricker and Frankel explore the current literature on potential roles and functions of the two PsbO homologs and seem to champion the idea that expression of PsbO-2 is increased under cold stress, indicating a role for this protein in improving PSII function under these conditions (Bricker and Frankel, 2011). PsbO is imported into the lumen via the bacterially conserved Sec pathway (Robinson and Mant, 1997) and once transported across the membrane, must be folded, a process which includes the formation of a disulfide bond.

2.6.1 LTO1 - PsbO Assembly Factor

The oxidant in this process, LTO1 (Lumen Thiol Oxidoreductase 1) was identified via homology search for a VKOR (for vitamin K epoxide reductase) like proteins in the green lineage. Our research has shown that this thylakoid resident protein is involved in the formation of the disulfide bond in PsbO. (See Chapter 3 for more details.)

2.6.2 Is there a PsbO reductase?

This leaves open the question of disulfide reductase in the lumen and whether or not such a protein may be associated with LTO1. The disulfide bond relay system in *E. coli* has been exhaustively studied. In this system, DsbA oxidizes sulfhydryls, forming intra-molecular disulfide bridges as they cross into the periplasmic space. The electron from reduced DsbA is then passed on to DsbB and finally to ubiquinone (Kadokura and Beckwith, 2010; Depuydt et al., 2011). These initial disulfide bonds are often not the bridges needed for correct folding of the mature protein, and so a number of additional factors are required for reducing or rearranging these disulfide bonds. These include enzymes such as DsbC, a disulfide bond isomerase that functions in rearranging these bonds (Missiakas et al., 1994; Shevchik et al., 1994), and CcmG, a disulfide bond reductase involved in processes such as heme attachment to *c*-type cytochromes (Page and Ferguson, 1997; Li et al., 2001; Reid et al., 2001). In *E. coli*, DsbD provides the reducing equivalents to these proteins from thioredoxins, which ultimately get electrons from NADPH (Ito and Inaba, 2008; Inaba, 2009).

In addition to LTO1, a number of proteins have been identified as redox proteins within the lumen of the chloroplast via primary sequence homology (Page et al., 2004; Motohashi and Hisabori, 2010). Among these include orthologs of CcdA from bacterial systems that do not encode DsbD. CcdA and DsbD share some primary sequence homology, although CcdA is a smaller protein missing the carboxy- and amino-terminus domains which encode for a thioredoxin-like and immunoglobulin-like domain respectively in DsbD (Katzen and Beckwith, 2002). CcdA and DsbD are implicated in the reduction of a number of proteins, including a class of proteins called cytochromes *c*,

which are characterized by the covalent attachment of heme to a CxxCH motif. CcdA works with orthologs of ResA, a thioredoxin-like protein identified in *Bacillus subtilis* (Sun et al., 1996). ResA interacts specifically with these apo-cytochromes. The homolog of ResA is HCF164 in *Arabidopsis* (Lennartz et al., 2001) and CCS5 in *Chlamydomonas* (Gabilly et al., 2010). This protein, along with a poorly conserved, small protein in plastids called HCF153 in *Arabidopsis* (Lennartz et al., 2006) and CCS4 in *Chlamydomonas* (Gabilly et al., 2011), appears to be essential for the reduction of apo-cytochromes *c* in the lumen. In this system, it is proposed that CcdA acts as DsbD, providing reductant from stromal thioredoxin via ferredoxin. This thioredoxin then interacts specifically with the apo-cytochrome *c*, reducing it in preparation for the covalent attachment of heme. It is currently unknown what function HCF153 or CCS4 play in this process.

The reader may have noted a balance within the bacterial system: oxidation roles being played by DsbA and DsbB while reduction roles are played by DsbD and thioredoxins. However, the components that balance this process in the lumen of the chloroplast have not yet been found. The identification of a thiol-oxidant for PsbO implies that the cysteines within the unfolded PsbO are reduced. Current literature supports the idea that these sulfhydryls are maintained reduced throughout the transportation process. If this is so, the method by which these sulfhydryls are maintained has yet to be uncovered. Likewise, the presence of thioredoxins involved in cytochrome *c* biogenesis implies an oxidant for apo-cytochromes *c*. While it is possible that LTO1 is performing this function, immunoblot analysis did not reveal notable defects in cytochrome *f* accumulation within the lumen. These discoveries, therefore, open wide

the doors to uncovering the answers behind these “missing” assembly factors.

2.7 PsbP

After the association of PsbO, the nuclear-encoded luminal proteins PsbP and PsbQ must be associated. Unlike PsbO, both PsbP and PsbQ use the Tat pathway in *Arabidopsis* (Settles and Martienssen, 1998; Dalbey and Robinson, 1999). Like PsbO, PsbP has two isoforms in *Arabidopsis*, PsbP1 and PsbP2 (Yi et al., 2007; Yi et al., 2009). Using RNAi against Tobacco PsbP, Ifuku et al. showed that mutant plants had reduced growth, pale green leaves and thermoluminescence showed a defect in Mn cluster stability (Ifuku et al., 2005). Repeating the experiment in *Arabidopsis*, Yi et al. showed that reduced PsbP resulted in decreased quantum yield of photosynthesis (Yi et al., 2007), showing that PsbP functions in the stabilization of PSII. In these mutants, PsbQ is completely absent from isolated RCC, while CP47 and D2 show reduced accumulation. Interestingly, D1, PsbO and CP43 are less affected, suggesting that PsbP is specifically involved in the stabilization of CP47 and D2 (Yi et al., 2007). The PsbP protein itself is mainly composed of beta-sheets, as revealed from the crystal structure of tobacco PsbP. (Ifuku et al., 2004). Ifuku and his colleagues found that while PsbP was not similar to any of the known luminal components of the cyanobacterial RCC, it did have an electrostatic surface potential similar to PsbV, the cyanobacterial protein that PsbP physically replaces in plants.

to less than 1% of the wild type and they display only a faintly yellow phenotype, but cannot be grown except on sucrose media. On the other hand, their thylakoid structure is extremely deviated from wild type. In an attempt to explain this phenotype, the authors suggest that PsbP might be involved in PSII partitioning or organization within the grana (Yi et al., 2009).

2.8 PsbP Related Proteins

In addition to PsbP1 and PsbP2, *Arabidopsis* has two PPL (PsbP-like) proteins and six PPD (PsbP Domain) proteins, defined on the basis of sequence homology. The Chlamydomonadaceae appear to have PsbP homologues, but not all have obvious PPL orthologs (See Figure 6). For instance, no PPL orthologs have been identified in *C. reinhardtii*, but *C. incerta* is predicted to have at least one. Both of the PPL genes in *Arabidopsis* have been implicated in assembly and/or maintenance of plastid complexes: PPL1 is required for efficient repair of PSII and PPL2 is co-expressed with NDH (NADH dehydrogenase) subunits (Ishihara et al., 2007).

Furthermore, there are six PsbP Domain (PPD) proteins with unknown function in *Arabidopsis*. This supports the trend in *Arabidopsis* (and land plants) for regular gene duplication, seen mainly with the nuclear encoded, extrinsic proteins (PsbO, -P, -Q). Meanwhile the intrinsic proteins remain encoded by the chloroplast genome (Sato, 2010). The question becomes, do these PsbP related protein also have roles in the assembly of the photosynthetic complexes? And if so, do they have divergent or duplicate functions? Further investigations must be made to determine this.

2.8.1 Sll1418 - *Synechocystis* PsbP-like homologue

Identified by loose primary sequence homology, a PPL (Sll1418) in *Synechocystis*

is found to be tightly bound to the thylakoid membrane and is non-stoichiometrically associated with PSII - less than 10% of the PSII complexes are associated with Sll1418 (Thornton et al., 2004). Although the phenotype of the *sll1418* mutant is mild (Ishikawa et al., 2005), it does have slightly reduced growth in calcium and chlorine depleted medias, based on liquid culture growth curves (Thornton et al., 2004; Summerfield et al., 2005a). Notably, CP47 still accumulates in these mutants, unlike in the *psbP Arabidopsis* mutant. Oxygen evolution is very inhibited at higher light intensities (Thornton et al., 2004), which is probably a result of decreased stability of the Mn cluster (Sveshnikov et al., 2007). When the RCC is extracted, a lower oxygen evolution is observed in the *psbP-like* mutants (Sveshnikov et al., 2007). From the striking differences in phenotype and primary sequence between *ppl* cyanobacteria mutants and *psbP Arabidopsis* mutants combined with the functional radiation of PsbP in eukaryotes, any extrapolation of function must be carefully tested. This difference emphasizes the caution that should be extended to bioinformatic analysis, especially in regard to assembly and regulatory factors.

2.9 PsbQ

The importance of PsbQ in higher plants has been even more elusive. Once again, there are two PsbQ homologs in *Arabidopsis* – PsbQ-1 (At4g21280) and PsbQ-2 (At4g05180) (Yi et al., 2009). RNAi against tobacco PsbQ revealed no phenotype under normal to high light (Ifuku et al., 2005). However, a low light phenotype was identified performing the same experiment in *Arabidopsis* (Yi et al., 2007). In the *Arabidopsis* RNAi plants, Yi and his colleagues showed that under normal light conditions, there was little effect of reduced PsbQ on growth, O₂ evolution, chlorophyll fluorescence or loss of

other PSII components. However, low light conditions resulted in a slow death of the lines. The authors found reduced PSII, including CP47 and D2, in these yellowing plants and that the PSII complexes were very unstable (Yi et al., 2007). EM data revealed that there was no change in the thylakoid structure, even when PsbQ was reduced to less than 5% of the wild type (Yi et al., 2007).

2.9.1 Sll1638 - *Synechocystis* PsbQ-like homolog

A *PsbQ-like* (*Sll1638*) gene was also found in *Synechocystis* and mutant characterization revealed that its phenotype paralleled that of the *psbP-like* mutant described above, with poor growth in calcium and chloride depleted media (Thornton et al., 2004). In particular, the oxygen evolution was more inhibited than the *psbP-like* mutant at higher light intensities, especially in the *psbQ-like* mutants (Thornton et al., 2004). Sll1638 also seems to be involved with the stabilization of the Mn cluster, perhaps interacting with PsbU and PsbV in *Synechocystis*, as double mutants are especially stressed when grown on Ca²⁺, Cl⁻, and iron-depleted media (Summerfield et al., 2005b). Since both the PsbP-like and PsbQ-like cyanobacteria orthologs are targeted to the luminal side of PSII, it raises an interesting conundrum: if they are performing a necessary function in cyanobacteria, what is performing this function in *Arabidopsis*? Have PsbP and PsbQ taken up the roles of both of these PsbP-like and PsbQ-like proteins as well as their functional counterparts, PsbV and PsbU, or is another protein performing these stabilization roles? Alternatively, the need for these stabilizing factors might be lessened in plastids for some unknown reasons.

Assembly factors for PsbP and PsbQ themselves have not been identified and may not be needed. In fact, the radiation of PsbP proteins indicates that these proteins have

been conscripted for assembly functions themselves.

3. *b₆f*

The assembly of the cytochrome *b₆f* complex is nearly as intricate as that of PSII, with similar variation in post-transcriptional factors between organisms. This text will focus primarily on cytochrome *f*, a *c*-type cytochrome with a heme moiety covalently attached to a characteristic CXXCH motif (Thony-Meyer, 1997; Ferguson et al., 2008; Bonnard et al., 2010).

The translation of cyt *f* is regulated in a manner comparable to the RCC components. That is, its translation is dependent upon the stable accumulation of the gene product of *petD*, subunit IV of the *b₆f* complex (Choquet et al., 1998). At least two factors have been identified as specifically involved in the translation of the *petA* mRNA: MCA1 and TCA1.

3.1 Translation of *petA*

Before entering a discussion as to the components involved in *petA* translation, it must first be noted that the *petA* gene product regulates its own translation. The Wollman lab describes some of the first evidence that cytochrome *f* translation is regulated through the 5'UTR of the *petA* transcript in *Chlamydomonas reinhardtii* (Choquet et al., 1998). Furthermore, it is the c-terminus of the unassembled cyt *f* protein that down-regulates this translation. As a basis for their later experiments, the authors note that cytochrome *f* is down in a Δ *petD* (Subunit IV, SUIV) mutant (Choquet et al., 1998). This is expected, as SUIV must accumulate before the *b₆f* complex is assembled, an example of what the authors call “control by epistasy of synthesis” (CES). However, a cytochrome *f* translational product that is degraded more quickly than the wild type does not induce

this negative regulation of its own transcript, even in a $\Delta petD$ mutant. (In this case, the authors used the mutant F52L-55V, which is mutant for the two essential heme binding cysteines at the CXXCH motif.)

To identify the region of the transcript that was causing the translational down-regulation, the authors swapped the 5'UTR of *petA* with the 5'UTR of another chloroplast gene, *atpA*, which encodes for the alpha subunit of plastidic ATPase. Moving this construct into a mutant deficient in *petD* accumulation, *mcd1*-F16, restores cytochrome *f* accumulation, but not *b₆f* assembly. This demonstrated that the 5'UTR of *petA* is essential for this regulation. Furthermore, this region is sufficient for directing the down-regulation onto another transcript, as exemplified by the down regulation of a reporter constructed of the 5'UTR of *petA* fused to the *aadA* spectinomycin resistance cassette transformed into strains that express varying levels of mature cytochrome *f*. Furthermore, (Choquet et al., 2003) identified five residues in the c-terminus of cytochrome *f* that constitute a “translation repressor motif” resulting in repression of *petA* translation. Deletion of this motif results in lack of photoautotrophic growth and point mutation therein result in various levels of increased cytochrome *f* translation.

3.2 TCA1 - Chlamydomonas Translation Factor of *petA*

The Wollman lab later identified two potential proteins involved in this *petA* translation regulation in the form of two nuclear loci, *TCA1* and *MCA1*. Chlamydomonas mutants at these loci do not produce cytochrome *f*. Wostrikoff et al. focused on characterizing the *tca1* mutants and found that they could suppress the *tca1* cytochrome *f* accumulation phenotype by transformation of the 5'UTR-*atpA/petA* gene fusion described above (Wostrikoff et al., 2001). The *tca1* mutants themselves are recessive,

deficient in photosynthetic growth, *b₆f* fluorescence and cytochrome *f* accumulation by pulse labeling, though the *petA* transcript still accumulates (although not to wild type levels). Since the mutation is recessive and the transcript still accumulates, the authors note that this suggests that TCA1 works as an activator of translation, not a repressor.

In addition to restoring cytochrome *f* accumulation by transformation of the *tca1-1* mutant with the 5'UTR-*atpA/petA* gene fusion, moving the 5'UTR-*petA/aadA* reporter construct described above into this background did not confer spectinomycin resistance, showing that a strain deficient in TCA1 cannot produce the reporter protein. A chloroplast *tca1* suppressor mutation also maps to the 5'UTR of *petA* and partially restores *petA* transcript accumulation in *tca1-1* and *tca1-2* mutants.

To determine whether or not the *tca1-1* mutation could suppress the CES phenotype of a Δ *petD* mutant, wherein *cyt f* translation is repressed, they crossed the two mutants. They found that *cyt f* translation in the Δ *petD tca1-1* mutant is more repressed than in either mutant alone. This indicates that TCA1, while recognizing the 5'UTR of and necessary for the translation of *petA*, is not necessary for CES repression. To investigate the possibility that TCA1, while not necessary, may be a player in the CES process, a second cross was made, creating a *tca1-1* strain with a modified cytochrome *f* having the last 14 residues of the c-terminus deleted in which the CES process is lost. In this experiment, the up-regulation of cytochrome *f* translation was dependent upon the presence of TCA1, suggesting that TCA1 is a rate-limiting step in *cyt f* translation occurring upstream of the CES control mechanism.

3.3 MCA1 - Post Transcriptional Factor of *petA*

Meanwhile, the *mca1* mutant does not accumulate the *petA* transcript, and so does

not produce mature cytochrome *f* protein (Loiselay et al., 2008). MCA1 and TCA1 are found in the chloroplast fraction based on chloroplast isolation experiments using HA and FLAG tagged versions of the genes (Raynaud et al., 2007) and can both be found in the soluble fraction using these same constructs (Boulouis et al., 2011). Using transformants that express various levels of MCA1-HA and TCA1-FLAG, (Raynaud et al., 2007) then show that *petA* transcript accumulation (and therefore *cyt f* accumulation) is dependent upon the amount of MCA1 and *cyt f* protein accumulation (but not *petA* transcript RNA) is dependent upon the amount of TCA1.

Cyclohexamide treatment of the tagged strains revealed that MCA1-HA turnover is very rapid - nearly absent after only four hours - while *cyt f* and TCA1-FLAG have longer half lives. This turnover of MCA1-HA is concurrent with the turnover of the *petA* mRNA. They also find that MCA1, TCA1 and the *petA* transcript are much more abundant in early and late log phases of growth than at steady state growth when *b₆f* assembly is less necessary. This down regulation is also seen with nitrogen deprivation, commiserate with growth retardation.

The MCA1 protein itself is a PPR protein 1,068 amino acids long and containing ~ 14 PPR motifs (Loiselay et al., 2008). In addition, it has short stretches of poly A, S, P and Q residues, a characteristic of other nucleus encoded chloroplastic factors found in *Chlamydomonas*. Only one closely related ortholog was identified by primary sequence homology in *V. carteri*.

The dosage-dependent data (Raynaud et al., 2007) suggested that MCA1 acts as a dimer and Yeast-2-Hybrid confirmed this data, indicating that the two proteins probably associate as dimers in a tetramer, with TCA1 associating with its own c-terminus, MCA1

associating with its own n-terminus and the c terminus of MCA1 associating with the n-terminus of TCA1 (Boulouis et al., 2011). There are two distinct regions of PPR repeats in MCA1, and this association could mean that one of the regions aids in homodimer formation while the second region would aid in heterodimer formation (Boulouis et al., 2011).

Loiselay and her colleagues found that, like TCA1, the function of MCA1 is dependent upon the 5'UTR of *petA* (Loiselay et al., 2008). Transforming the *mca1-2* mutant with the *5'UTRpsbB/petA* construct similar to the one described above resulted in restored accumulation of the *petA* mRNA. In addition, transforming the inverse construct, *5'UTRpetA/psbB*, results in lack of *psbB* transcript accumulation. This indicates that *petA* transcript accumulation is dependent upon MCA1.

Using RNA ligase mediated (RLM)-RACE with and without tobacco acid pyrophosphatase, they demonstrate that the *mca1* mutant still accurately attaches the 5'cap to the *petA* mRNA, as they can amplify a product from the mutant in both instances. This means MCA1 must be conferring stability to the *petA* transcript in some other manner. They investigated the possibility that MCA1 is protecting the 5'UTR of *petA* from 5'→3' degradation by transforming the *mca1-1*, *mca1-2* and wild type strains with a *petA* construct that had been modified by the addition of a poly-guanine tract at the beginning of the 5'UTR which protects from this type of degradation (Drager et al., 1998; Nickelsen, 1999; Vaistij et al., 2000). This construct increased the accumulation of *petA* transcript in all three strains (although there is no quantification of the accumulation in the wild type), suggesting that MCA1 is facilitating the protection of this transcript from degradation.

They further narrowed down the stabilization element to a 40 nucleotide region surrounding the *petA* transcriptional start site by swapping this region with the same region from *petD* that had previously been shown to function in *petD* RNA stability. Both this and a reciprocal construct (*petD* with the stabilization element from *petA*) were transformed into *mca1-1*, *mca1-2* and *mcd1-1*. This last strain is mutant for a protein identified as being involved in stabilization of the *petD* transcript through the stabilization element. In this way, they were able to swap the stability of the *petA* and *petD* transcripts from their respective dependence on MCA1 and MCD1 from one protein to the other. The *petD* stabilization element/*petA* construct was also moved into a *tca1-8* mutant. This resulted in increased translation of *petA*, suggesting that TCA1 hampers the production of the chimeric transcript, and so TCA1 may have a dual role of translational activation and transcriptional suppression. They did not produce the *tca mca* double mutant with this construct.

Further dissecting the roles of these proteins, the stabilized poly-(G) *petA* construct described above was placed into the *tca1-2* mutant and, while the *petA* transcript was still stabilized, translation of cytochrome *f* did not occur. This was expected, given the deduced role of TCA1. However, a discrepancy in the amount of *petA* transcript as compared to *cyt f* accumulation when using the poly-(G) *petA* construct in the *mca1-1* and *mca1-2* backgrounds leads the authors to suggest that MCA1 might also have a dual role. MCA1 might not only be stabilizing the transcript, but also enhancing translation, perhaps in conjunction with TCA1. To explore this, nucleotides 22-63 after the translational start site were removed (following the first 20 nucleotides of the *petA* stabilization element) and the resulting construct was transformed into a *mca1*

mutant. While this transcript is produced, the resultant protein is not, indicating that these nucleotides are required for translation, perhaps through TCA1 via its interaction with MCA1.

Co-IP experiments confirm the Yeast-2-Hybrid results described above, and furthermore, these co-IPs show association with or without the presence of the *petA* transcript (Boulouis et al., 2011). Size exclusion chromatography reveals that MCA1 and TCA1 run in the same fraction around 670 kDa. The proteins run in lower fractions in *mca1-6*, *tca1-8*, and Δ *petA* mutants as well as in samples treated with RNase. This demonstrates that both proteins are associated in a large complex with the *petA* RNA.

While investigating the regulation of TCA1 and MCA1 themselves, it was found that both proteins over-accumulate in a Δ *petA* strain. In strains wherein the holo-cytochrome *f* is not formed (*ccs1*) or the c-terminus of *cyt f* is deleted or modified, MCA1 also accumulates. However, in a strain where the 5'UTR of *petA* has been replaced with that of *atpA*, levels of MCA1 are normal. Finally, in a Δ *petD* strain where *petA* transcription is repressed, the authors find a shortened half life of the MCA1 protein. This demonstrates that the lifespan of MCA1 correlates not only with *cyt f* protein accumulation, but also with enhanced accumulation of the *petA* transcript. These experiments further indicate that MCA1 and TCA1 are increased in strains where holo-cytochrome *f* is absent and that MCA1 is modulating the CES effect of *petD* on the *petA* transcript.

In summary, MCA1 is required for the stable accumulation of *petA* while TCA1 is required for the translation of *petA*. These proteins are limiting for the processes for which they are involved, particularly MCA1, being a short-lived protein, and through the

c-terminus of mature cytochrome *f* regulate the production of this protein.

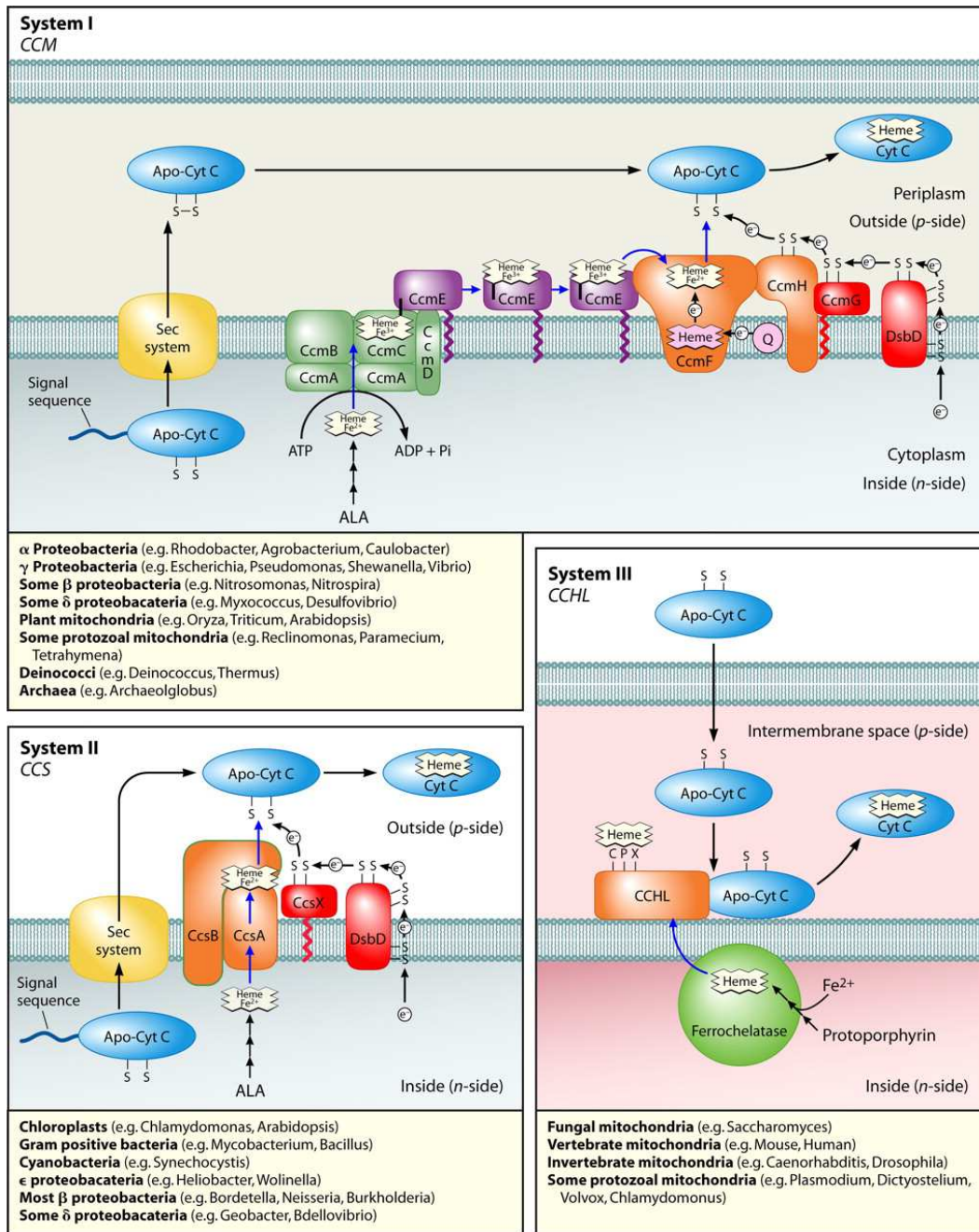


Figure 7 - Three Systems for Cytochrome c assembly from (Kranz et al., 2009).

3.4 Heme Attachment

The post-translational assembly of the cytochrome *f* protein requires the covalent attachment of a heme to a characteristic *c*-type cytochrome -CxxCH- motif. There are a diversity of Systems (I, I*, II, III, IV, V) that complete *c*-type cytochrome assembly depending not only on the organism, but also on the organelle. The chloroplasts of *Chlamydomonas* and *Arabidopsis* have been shown to use a variant of System II that was originally identified in *Chlamydomonas* (Howe and Merchant, 1992). This dissertation will therefore focus specifically on how System II attaches heme to cytochrome *f* and how this system varies from organism to organism. For an overview of this and the other two systems, please reference Figure 7.

3.4.1 CCS1 and CcsA - System II Heme Synthetase

System II is typically defined by the presence of one protein, CcsA (also called ResC in *Bacillus*), a protein with six to fifteen trans-membrane helices depending on the organism, several conserved histidine, aspartic acids and a characteristic WWD motif (Hamel et al., 2003). CcsA appears to be in a complex with another protein with four to six trans-membrane spanning domains, which also has several conserved histidines plus a large C-terminal domain protruding into the lumen, called Ccs1 (also CcsB in *Helicobacter* and ResB in *Bacillus* – this text will use the names given to the chloroplast biogenesis System except when discussing specific proteins) (Dreyfuss et al., 2003). *C. reinhardtii* *ccs* mutants do not produce holo-cytochrome and as a result of the loss of holo-cytochrome *f*, the mutants do not assemble the *b₆f* complex and so cannot grow photoautotrophically (Xie et al., 1998).

CcsA is well conserved in plants, algae and cyanobacteria, especially in the *c*-

terminus, where the three invariant histidines and a WWD motif can be found. It was demonstrated, using *phoA/lacZ* fusion constructs in *E.coli*, that the WWD domain and two histidines face the lumen/periplasmic space (Hamel et al., 2003). (These two compartments are functionally analogous in regard to electrochemical gradient production.) Meanwhile, one of the histidines is to be found nearer the stromal/cytoplasmic side, nestled within a transmembrane domain. They also show that at least four tryptophans, three aspartic acids and three of the histidines are necessary for cytochrome *f* assembly (Hamel et al., 2003). Using the same procedure, Dreyfuss et al. revealed that *Chlamydomonas* CCS1 has three trans-membranes and an extended luminal domain (Dreyfuss et al., 2003). Mutation of the conserved histidine in the third trans-membrane loop results in lack of complementation of the *ccsI-1* mutant, but mutations in a conserved cysteine and aspartic acid did not appear to affect cytochrome *c* biogenesis. (Dreyfuss et al., 2003)

3.4.2 CcsBA - Bacterial Ortholog of CCS1 and CcsA

Underlining the fact that these two proteins work together, CCS1 and CcsA orthologs are found to be encoded as one large protein called CcsBA in organisms such as *Helicobacter pylori* or *Wolinella succinogenes*, the latter of which encodes three homologs, CcsA1, CcsA2 and Nrt1. Excepting the reduction of the cysteines on the apo-protein, these multi-domain proteins appear to be all that is necessary for heme attachment in some systems. This was shown by the production of a cytochrome *c*₄ reporter from a “delta System I” ($\Delta ccmABCDEFGH$) *E. coli* mutant expressing the CcsBA protein from *Helicobacter pylori* (Feissner et al., 2006). At this point, the reader should note that *E. coli* in its native environment only produces *c*-type cytochromes under

anaerobic conditions. However, if proteins requiring the covalent attachment of heme are placed under non-native promoters, *E. coli* will effectively mature these proteins under aerobic conditions. Hence the use of a cytochrome *c*₄ reporter.

Feissner and colleagues could not increase the expression of their reporter cytochrome *c* by co-transforming with CcsX from *H. pylori*, a System II component ortholog of CcdA which was discussed earlier as being implicated in the reduction of the apo-protein. Nor could they increase expression by adding exogenous DTT to the media in an attempt to increase the level of reduced apoprotein. This suggests that CcsBA, in conjunction with the native *E. coli* disulfide bond reducing pathway (DsbD), is sufficient to reduce the -CXXCH- motifs at optimal levels. The inability to increase expression also suggests either that there is no direct interaction between the heme attachment and the apo-protein reduction proteins, or that such an interaction is unnecessary.

Frawley and Kranz (2009) further investigated the function of this fused System II, testing CcsBA proteins from *Bordetella pertussis*, *H. pylori*, *Bacteroides thetaiotaomicron* and *Helicobacter hepaticus* for their ability to complement a System I *E. coli* mutant (Frawley and Kranz, 2009). The last of these most robustly produced their reporter *c*-type cytochrome. Astoundingly, they found that Hh-CcsBA itself binds heme. Boiling removes this heme from the CcsA-like portion of the protein, suggesting that the heme is non-covalently bound. Using UV-visible absorption, the authors demonstrate that the full length protein binds reduced [Fe²⁺] heme in a *b*-type coordination, i.e. non-covalently.

3.4.3 ResB and ResC - *B. subtilis* orthologs of CCS1 and CcsA

The finding that CcsBA from *H. hepaticus* contains a *b*-type heme and can still

complement a System I mutant is intriguing, because previous attempts to complement a System I (*ccmABCDEFGH*) *E. coli* mutant with the ResABC operon from *B. subtilis* were unsuccessful (Ahuja et al., 2009). (This would be similar to attempting to complement with CCS5, CCS1 and CcsA from *Chlamydomonas* (Le Brun et al., 2000).) However, Ahuja and colleagues did identify a protein with a covalently attached heme in the membrane fraction of these ResABC *E. coli*.

Mass spectrophotometry revealed that this protein corresponded to the CCS1 ortholog while pyridine hemeochromogen spectrum and HPLC revealed that the extracted heme group was protoheme IX. Treatments such as boiling indicated that the heme is attached covalently and mutation of a conserved cysteine identified by the Merchant Lab at position 138 resulted in loss of covalent heme binding activity (Dreyfuss et al., 2003). Furthermore, attachment of this heme did not appear to be dependent upon the CcsA or CCS5 orthologs, as operon constructs with the start codons of these genes mutated into stop codons still produced a CCS1 ortholog with covalently bound heme.

With this discovery, the group reanalyzed *B. subtilis* to identify the heme binding protein using multiple copies of the ResABC operon under the native promoter. Using this construct, they identified two proteins at ~62 and 27 kDa. Mass spectrophotometry revealed that the higher band held the Ccs1 ortholog and the lower band held the CcsA ortholog, which must be truncated to run at this size on an SDS-Page, as MS identified this protein at its predicted size as well. The authors note that this could, of course, be an artifact of expression. Despite this, the Cys138Ala mutation described above does not affect *c*-type cytochrome production in a wild type grown under normal conditions, suggesting either that this cysteine is binding a nearby heme as a result of the artificial

system or the covalent attachment of heme is not necessary for the CCS1/CcsA orthologs to produce cytochromes *c*. They did not confirm that heme was attached covalently in cells with the native ResABC promoter, so it is still possible this heme attachment is an artifact of over-expression (Ahuja et al., 2009). This is still an interesting question with the discovery that CcsBA from *H. hepaticus* contains a *b*-type heme, as members of the *Bacillus* species tend to encode an additional cysteine containing motif at the very N-terminus of the CCS1 ortholog (prior to the cysteine mentioned above), exemplified by the -CxC-N10-CxxC- found in *B. subtilis* (Le Brun et al., 2000).

3.4.4 What is the function of the b-type heme?

Frawley and Kranz (2009) investigated the *b*-type heme binding by mutating the previously identified histidines flanking the WWD motif of *H. hepaticus* CcsBA (those facing the periplasmic space in the CcsA ortholog) or the WWD residues themselves (in the sequence -WGWD-) and found that all of these resulted in loss of *c*-type cytochrome formation in their artificial system. Interestingly, the *WWD* mutant still retains reduced heme in a typical *b*-type conformation, whereas in the histidine mutants, the heme is found in the oxidized state. This indicates that these two histidines are instrumental for the reduction of heme for later attachment to the apo-cytochrome *c* but are not the *b*-type heme ligands themselves.

Mutation of two additional histidines that would be analogous to the conserved histidine in CCS1 and the histidine closer to the stromal side of CcsA, also results in an inability to produce cytochrome *cs*. Interestingly, the loss of these residues results in a significant decrease in CcsBA *b*-type heme binding, indicating they are the ligands for the *b*-type heme. Furthermore, addition of imidazole to the media of these histidine mutants

suppresses the *c*-type cytochrome phenotype under both aerobic and anaerobic conditions, probably by functional replacement of the imidazole groups on the histidine residues. (Interestingly, this treatment does not suppress mutations in the second and fourth histidines.) The authors suggest that this domain acts as a channel to transport heme across the membrane (Frawley and Kranz, 2009).

It must be mentioned, however, that within a month of this publication, (Richard-Fogal et al., 2009) demonstrated that the cytochrome synthetase of System I, a protein called CcmF, also required a *b*-type heme in addition to a reduced heme and that the reduction of this heme can be achieved in vitro by the addition of quinols to the solution. CcmF is evolutionarily related to CcsA and the amino-terminus of CCS1. Using a His-tagged CcmF, a complex containing another System I component, CcmH, was purified. They note that the interaction between the two proteins is salt sensitive, suggesting a weak ionic binding between the proteins and that the purified complex is reddish brown in color, suggesting the presence of iron. Low-temperature absorption spectra of purified CcmF indicate that this heme is bound in a *b*-type conformation and quantification showed an approximately 1:1 molar ratio of heme:CcmF.

This *b*-type heme does not come from a proposed heme holdase in System I called CcmE, because deletion of *ccmE* does not result in the loss of the *b*-type heme. In addition, they used *phoA/lacZ* constructs to modify an earlier model of CcmF topology, resulting in a realignment that results in a topology nearly identical to that of CcsBA from *H. hepaticus*, barring the additional soluble domain orthologous to that of Ccs1. One of the two histidines oriented on the side of the cytoplasm (functionally analogous to the stroma of the chloroplast), H261, results in significant *b*-type cytochrome loss when

mutated while another, H173, does not. The authors proposed that this *b*-type heme reduces the oxidized heme attached to CcmE before it is attached to apo-cytochrome *c*. If so, they reasoned, then the *b*-type heme in CcmF must itself be reduced. Indeed, the authors found that both ubiquinol and dimethylquinone could reduce this heme *in vitro* and identify a potential quinol binding site by primary sequence homology, suggesting that a similar reductant is used *in vivo*.

The evolutionary conservation of CcsBA and CcmF makes it tempting to propose a similar mechanism, however, a number of questions must be answered before such an assumption can be confirmed: (1) in both Systems, the path by which heme is transported across the membrane must be further elucidated, (2) if CcmF is truly reducing heme prior to its synthetase function, the reduction of a second heme (ideally from CcmE) through this *b*-type heme must be demonstrated and (3) such experiments must be repeated with the CcsBA protein.

While it is tempting to support the idea that CcsBA is both transporting and attaching heme to the reduced apo-cytochrome, this hypothesis is based solely on the ability of CcsBA to complement a “System I mutant”. This hypothesis assumes that one or more of the proteins encoded by the *ccmABCDEFGH* operon in *E.coli* is transporting heme for use of the formation of *c*-type cytochromes. Several facts cast doubt on this possibility. First, CcmF is probably not the (sole) heme transporter, as evidenced by the presence of heme in a CcmCDE complex in a *ccmF* mutant. Second, the proteins encoded by CcmCDE are smaller proteins proposed to have a holdase function as opposed to a transport function. Third, deletion of the *ccmAB* genes does not prevent loading of heme onto CcmCDE complex. Finally, System I mutants in *Rhodobacter*

capsulatus secrete copious amounts of coproporphyrin and protoporphyrin, heme precursors, into the media (Deshmukh et al., 2000). All of these facts suggest that there is at least one additional pathway that can excrete heme or heme precursors.

The excretion of heme precursors in *R. capsulatus* makes it tempting to suggest that heme is being assembled on the positive side of the membrane. However, a mutant for ferrochelatase, the enzyme required for the insertion of iron into protoporphyrin, does not produce cytochrome *cs* in the System II containing *Bacillus subtilis* but these mutants can be rescued by the addition of exogenous heme. This indicates that there is not an alternative heme producing pathway specific for cytochrome *c* production in *B. subtilis* (Schiott et al., 1997a; Schiott et al., 1997b). This means there must be transport of heme by some mechanism *or* heretofore undetected levels of ferrochelatase are transported in conjunction with heme-precursors and heme is assembled *in compartento*.

3.4.5 System II Variation

The cytochrome *c* biogenesis question becomes even more complex when we ask the question: Why are there so many variations? System II varies widely in the number of components required for heme attachment -- from one to as many as five candidates in *Chlamydomonas*. (This count excludes the proteins implicated in apo-protein reduction, which increase the number by two to three, depending on the organism.) One possibility for this diversity is presented by *W. succinogenes* encoding for three different CcsBA-type proteins, CcsA1, CcsA2 and NrfI. Each of these proteins appears to be essential for the production of different *c*-type cytochromes. Of the three, a deletion of CcsA2 produces the most drastic phenotype - without this gene, *W. succinogenes* will not grow. Furthermore, it is this gene that will complement the “*E. coli* System I mutant” described

above. Meanwhile, the CcsA1 mutant will not produce MccA, a protein with multiple *c*-type hemes attached. Finally, NrfI is responsible for the attachment of heme to the atypical -CXXCK- motif found in cytochrome *c* nitrate reductase (Pisa et al., 2002). These findings support the idea that different substrates require slightly different assembly factors. The presence of multiple CcsBA proteins is understandable in this instance, as not all organisms encode proteins with multiple -CXXCH- motifs or the -CXXCK- motif.

This trend is also seen in some organisms that use System III. *Saccharomyces cerevisiae*, for instance, encodes for two cytochrome *c* heme lyases (CCHL), one for each of the respiratory *c*-type cytochromes: cytochrome *c* and cytochrome *c*₁ (Bernard et al., 2003). Appropriately, the biochemical behavior of these proteins is variable. Kern et al. mutated the four conserved histidines in CcsA1, CcsA2 and NrfI (Kern et al., 2010b; Kern et al., 2010a). Their results for the *nrfI* mutants paralleled those seen by Frawley (Frawley and Kranz, 2009) with *H. hepaticus* CcsBA, except they also saw mild rescue of the second and fourth histidine mutants when they added imidazole to the media. Likewise was there some rescue with imidazole for all of the mutations in CcsA1 and in addition, there was a low level production of holo-MccA without imidazole when the cytoplasm-facing histidines are mutated. Notably, mutation of the WWD motif (changing the sequence -WGWD- to -AGAA-) resulted in lack of holo-MccA production but this mutant was not rescued by imidazole. Finally, CcsA2 was tested in the heterologous *ccmABCDEFGH E. coli* mutant, as CcsA2 is essential for the growth of *W. succinogenes*. The production of cytochrome *cs* and phenotype suppression with imidazole in these four histidine mutants was most similar to that seen by Frawley and Kranz, however, Kern and

colleagues saw imidazole suppression with the two cytoplasm-facing histidine mutants only under anaerobic conditions (Kern et al., 2010b; Kern et al., 2010a).

Interestingly, research presented in this dissertation suggests that a new plastid system, System II*, may have to be introduced to the line-up, as twice the number of components is required for this process as compared to bacterial systems. These additional components have, until recently, only been characterized genetically in *Chlamydomonas reinhardtii*. However, new information is revealing the increased complexity of this system in both green alga and plant. In addition to a new protein implicated in the apo-protein reduction, a number of these factors may be related to an enhanced need for regulation in these eukaryotes. This is implicated by the increased expression of CCS1 under highlight in *Chlamydomonas*, but this regulation appears to be unaffected by the absence of *cyt f* or by the presence or absence of copper. The reader may like to know that the impact of copper availability is interesting to those studying *Chlamydomonas*, because in this organism, the absence of copper results in the specific expression of a *c*-type cytochrome, cytochrome *c*₆, which replaces the copper containing plastocyanin.

This data on CCS1 indicates that, while there is light-dependent regulation, there is no feedback regulation from downstream products. However, the CCS1 protein accumulates less in the chloroplast mutant *ccsA-B6* and the nuclear mutants *ccs2*, *ccs3* and *ccs4* while the *CCS1* transcript is expressed at wild type levels. (Dreyfuss et al., 2003) Likewise, *ccsA* transcript accumulation appears to be unaffected in the nuclear mutants *ccs1* through *ccs4* (Xie and Merchant, 1996). This suggests that the CCS1 protein is either unstable without the presence of these additional CCS components, or

perhaps it is regulated at the translational level.

Following the theme of photosynthetic complex assembly, Chapter 2 is a contribution to continuing investigations of System II* in the chloroplast of *Chlamydomonas reinhardtii*. This highlights CCS2, a new factor controlling heme attachment to apo-cytochrome *cs* in the plastid. Next, Chapter 3 illustrates the importance of disulfide bond formation for the assembly of PSII. As mentioned previously, an *lto1 Arabidopsis* mutant is characterized in this chapter, the first thiol-oxidase to be described as functioning in the lumen. Finally, Chapter 4 underscores the potential of plastid engineering through the complementation of a nuclear mutant in the arginine biosynthetic pathway via transformation of the chloroplast. This technical achievement opens the doors to future possibilities for plastid genome manipulation through the design of a new marker for organelle transformation.

Chapter 2: CCS2, a novel factor required for cytochrome *c* assembly in the green alga *Chlamydomonas reinhardtii*

Sara G. Cline^{*,§}, Isaac A. Laughbaum^{*} and Patrice P. Hamel^{*,§}

^{*}Department of Molecular Genetics and Department of Molecular and Cellular Biochemistry, The Ohio State University, Columbus, Ohio, USA

[§]Plant Cellular and Molecular Biology Graduate Program, The Ohio State University, Columbus, Ohio, USA

Running title: plastid cytochrome *c* assembly

Key words: plastid/photosynthesis/cytochrome *c*/heme/redox

Address correspondence: Patrice Hamel, 500 Aronoff Laboratory, 318 W. 12th Avenue, 43210 Columbus, Ohio, [Tel.: 614-292-3817](tel:614-292-3817), Fax: 614-292-6345, E-mail: hamel.16@osu.edu

AUTHOR CONTRIBUTIONS: P.H. and S.C. designed the experiments, analyzed the data, and wrote the article. S.C. performed the bulk of the experiments, aided in the cyt *c*₆ expression by I.L.

Abstract

In bacteria and organelles, cytochromes *c* are universal electron carriers with a heme cofactor covalently linked to the sulfhydryls of a CXXCH motif in the apoprotein. Despite the ubiquitous nature of cytochromes *c*, recent advances show their assembly pathways are incredibly divergent. In the green alga *Chlamydomonas reinhardtii*, the CCS2 locus was defined through the isolation of the *ccs2-1* to *ccs2-5* photosynthetic

deficient mutants. The *ccs* mutants display a dual deficiency in production of the holoforms of cytochrome *f* and *c₆*, the two plastid cytochromes *c* in the thylakoid lumen. Here we show that the complementing *CCS2* gene encodes a predicted 170 kDa protein and identify the molecular lesions in the *ccs2* alleles. *CCS2* displays a new variant of the OPR motif and does not appear to be conserved in the green lineage with the exception of *Volvox*. A plastid site of action is inferred from the finding that GFP fused to the first 100 amino-acids of *CCS2* localizes to the chloroplast in tobacco. We discuss the possible roles of *CCS2* in the biogenesis of plastid cytochromes *c*.

Introduction

Energy-transducing membranes are specialized membranes in bacteria, mitochondria and chloroplasts relying on electron carriers to generate the proton gradient necessary for ATP synthesis. The *c*-type cytochromes, also generically referred to as cytochromes *c*, are a class of structurally diverse metalloproteins participating in electron transfer reactions in all energy-transducing membranes (Thony-Meyer, 1997; Bonnard et al., 2010). Cytochromes *c* are defined by the covalent attachment of a ferroporphyrin IX moiety to the cysteine sulfhydryls in a characteristic *CXXCH* motif in the apocytochrome, also referred to as heme-binding site (Ferguson et al., 2008). Extensive investigations in bacterial and eukaryotic model systems and *in vitro* reconstitution of holocytochrome *c* assembly led to a definition of the minimal biochemical requirements for the heme attachment reaction. These requirements include:

(1) the separate transport of both heme and apocytochrome to the positive side¹ of the membrane, (2) the reduction and maintenance of both ferroheme and cysteines at the heme binding site and (3) the stereospecific covalent attachment of the heme vinyl groups to sulfhydryls via a thioether linkage.

To date, four systems (I to IV) required for the covalent attachment of heme to the apoforms of cytochromes have been identified. The prototypical assembly proteins, CcmE (System I), Ccs1 (System II) and CCHL (System III) are the hallmark of each maturation pathway (Ferguson et al., 2008; Hamel et al., 2009; Kranz et al., 2009). In the first three Systems (I, II, III), covalent attachment of the heme moiety occurs on the positive side of energy-transducing membranes (*i.e.* bacterial periplasm, mitochondrial intermembrane space, thylakoid lumen) (Ferguson et al., 2008; Giege et al., 2008; Hamel et al., 2009; Kranz et al., 2009). System IV is a maturation pathway required for the covalent attachment of heme C_i to cytochrome b_6 , in the b_6f complex of cyanobacteria and photosynthetic eukaryotes (Kuras et al., 1997; Kuras et al., 2007; Lyska et al., 2007). This system differs from Systems I, II and III because attachment of heme C_i occurs on the negative side of the membrane at a single cysteine that does not lie within a motif.

Common to Systems I and II is the operation of components dedicated to heme handling, the reduction of the heme co-factor and attachment of heme to the apocytochrome targets. System II, the system under study in this paper, is found in β -, δ - and ϵ -proteobacteria as well as cyanobacteria and bikont chloroplasts (Kranz et al., 2009).

¹ Energy transducing membranes characteristically produce a space where protons are concentrated, the positive side, and a space where they are not, the negative side.

Here, we will use the protein terminology introduced for System II in *Chlamydomonas*, unless otherwise stated, as it is currently the most consistent nomenclature for cytochrome *c* assembly factors in eukaryotes.

In *Chlamydomonas*, *ccs* (cytochrome *c* synthesis) mutants are defined by a dual deficiency in the holoforms of both cytochrome *f* and cytochrome *c*₆ (Howe and Merchant, 1992; Inoue et al., 1997; Dreyfuss, 1998; Xie et al., 1998; Page et al., 2004). Mutants display a photosynthetic defect because blocking production of cytochrome *f* reduces accumulation of the *b₆f* photosynthetic complex. An additional advantage of *C. reinhardtii* is the fact that it has a nuclear encoded, facultative *c*-type cytochrome termed cytochrome *c*₆ that will replace the copper containing protein plastocyanin in copper deficiency. All *ccs* mutants exhibit a block at a post-translational step which is common to the biogenesis of both molecules. Indeed, the application of pulse-chase experiments revealed that both plastid apocytochromes *c* are synthesized, imported in the plastid and processed by lumen-resident signal peptidase but not converted to their respective holoforms (Howe and Merchant, 1993, 1994; Xie et al., 1998; Balczun et al., 2005). Based on these experiments, it was concluded that the *ccs* mutants exhibit a defect at the level of the heme attachment step, which occurs in the thylakoid lumen (Howe and Merchant, 1993, 1994; Xie et al., 1998). This defect is specific to plastid *c*-type cytochromes because other lumen-resident proteins such as plastocyanin (a copper containing protein) are assembled normally in the *ccs* mutants (Howe and Merchant, 1993, 1994; Xie et al., 1998). This allows efficient screening for mutants defective in the production of both cytochromes *c*.

The heme handling and delivery component of this system is proposed to partially

be fulfilled by CCS1, an integral membrane protein with a large luminal domain (Dreyfuss et al., 2003). The nuclear encoded CCS1 of *Chlamydomonas* is found in the thylakoid membrane as a complex with the proposed synthetase, CcsA (Hamel et al., 2003). CcsA is a multiple transmembrane domain protein, encoded by the plastid genome of *Chlamydomonas* (Allen et al., 2007). Its function in a complex with CCS1 is emphasized by the fact that in some organisms, such as *Helicobacter pylori*, these two proteins are fused (Frawley and Kranz, 2009; Kern et al., 2010b). This fusion protein, CcsBA, is sufficient to complement the cytochrome *c* synthetase function of an *E. coli* mutant with the entire System I operon *ccmABCDEFGH* deleted (Frawley and Kranz, 2009). If the binding domain of CcsBA is extrapolated to *Chlamydomonas*, it can be assumed that two conserved histidines on the stromal side of the membrane, one in CCS1 and the other in CcsA, form a noncovalent *b*-type cytochrome binding pocket (Frawley and Kranz, 2009). Interestingly, some organisms, such as *Wolinella succinogenes*, encode as many as three homologs of CcsBA, apparently because of the need for specific factors for heme attachment to apoproteins with multiple -CXXC- motifs or the uncharacteristic -CXXCK- motif (Kern et al., 2010b).

In addition to heme attachment, two factors are necessary for the reduction of the apocytochrome prior to heme attachment in organisms using System II. The first of these is CcdA, a transmembrane spanning protein with some homology to the bacterial thiol-disulfide transporter, DsbD (Katzen and Beckwith, 2002; Katzen et al., 2002). Using the reducing power of stromal localized thioredoxin, CcdA passes electrons to a lumen-facing thioredoxin-like protein called CCS5 (Gabilly et al., 2010), which reduces a disulfide in the CXXCH motif in apocytochromes *c*. In bacteria, it seems that the

CcsA/Ccs1 proteins for heme delivery and attachment and the operation of a thioreducing pathway are all that is required for heme attachment. (Kranz et al., 1998; Beckett et al., 2000). However, mutant screening of *Chlamydomonas reinhardtii* has revealed four additional nuclear *ccs* mutants (*ccs2*, *ccs3*, *ccs4* and *ccs6*) (Howe and Merchant, 1992; Inoue et al., 1997; Xie et al., 1998; Page et al., 2004) indicating that additional factors are needed for assembly of cytochromes *c* in the plastid.

In this article, we report the molecular identification of the CCS2 locus by functional complementation. The CCS2 gene encodes a 170 kDa protein that is targeted to the chloroplast. The CCS2 protein was previously identified by bioinformatics to be a member of the octatricopeptide repeat (OPR) family (Eberhard et al., 2011).

RESULTS

Cloning of CCS2 by functional complementation.

Using the amenable photosynthetic deficient phenotype of the *ccs* mutants, we designed to clone the *CCS2* gene via transformation of a *ccs2-2 arg7-8* mutant with an indexed cosmid library (Purton and Rochaix, 1994). Since the phenotype of the *ccs2-2* allele is extremely light sensitive, we were able to co-select for complementing transformants on minimal media supplemented with 1% acetate. This allowed selection to occur in seven days instead of the standard ten.

Two of the transformed pools restored photosynthetic growth to the *ccs2-2* mutant. After isolation of the complementing cosmids G6 and D9 from pools 8 and 5 respectively, sequence results identified the cosmid G6 insert as containing a 30.2kb region from chromosome 19. By sequencing data, the second cosmid appeared to have rearranged. Therefore, all further work was done with cosmid G6.

Restriction digest analysis of cosmid G6 reduced the complementing fragment to 8.2kb. A smaller, 6.9kb fragment produced by digesting with *ApoI* also complemented, but less robustly. Determination of the *CCS2* cDNA sequence showed that *ApoI* cuts 135 bp upstream of the ATG, suggesting the promoter is interrupted in this fragment. Cosmid G6 and the cloned 8.2kb fragment complemented alleles *ccs2-1* through *ccs2-5*, restoring photosynthetic growth (Figure 8A), wildtype fluorescence rise and decay kinetics (Figure 8B and not shown) and both holo-cytochrome *f* and cytochrome *c*₆ accumulation (Figure 9A and B).

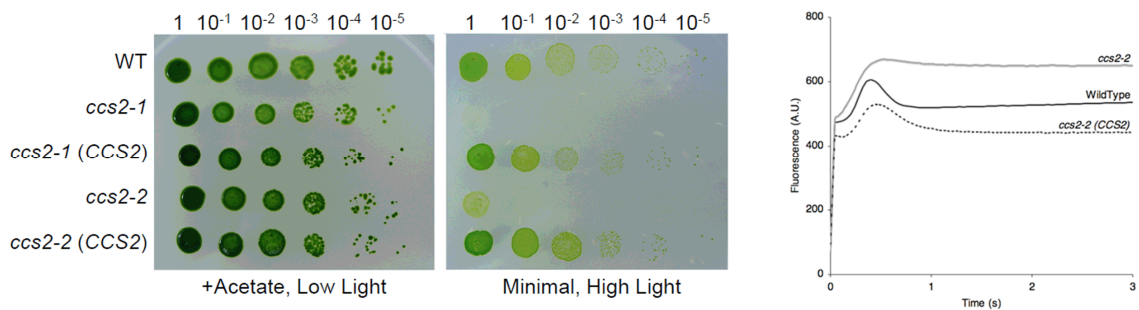


Figure 8 - An OPR Gene Restores Photoautotrophic Growth to the *ccs2* Alleles. For A and B, complemented mutants have been transformed with the 8.2 kb genomic fragment. A, 10-fold dilution series of representative *ccs2* and complemented strains under respiratory, low light (.6 μ E) and phototrophic, high light (50 μ E) conditions for 1 week at 22°C. B, Representative fluorescence kinetics of *ccs2-2* indicates restoration of cytochrome *b₆f* in the complemented mutant. A.U., Arbitrary Units.

CCS2 encodes a 170 kDa protein of the OPR family.

Because of the large size, low abundance and high (80%) GC content of the *CCS2* mRNA, the full-length cDNA proved difficult to amplify. This trouble is common when working with assembly factors in *Chlamydomonas* (Balczun et al., 2005). Instead, the sequence of the transcript was amplified in overlapping, 2 kb sections. The complete

cDNA was then extrapolated by aligning these pieces along the genomic sequence. The deduced intron/exon boundaries can be seen in **Figure 10A** and extended the 5' end of the annotated sequence. *Chlamydomonas* transcriptome 454 reads corroborate this transcript sequence (<http://genomes.mcdb.ucla.edu/Cre454/>). All complementation and expression work was henceforth accomplished with the genomic sequence.

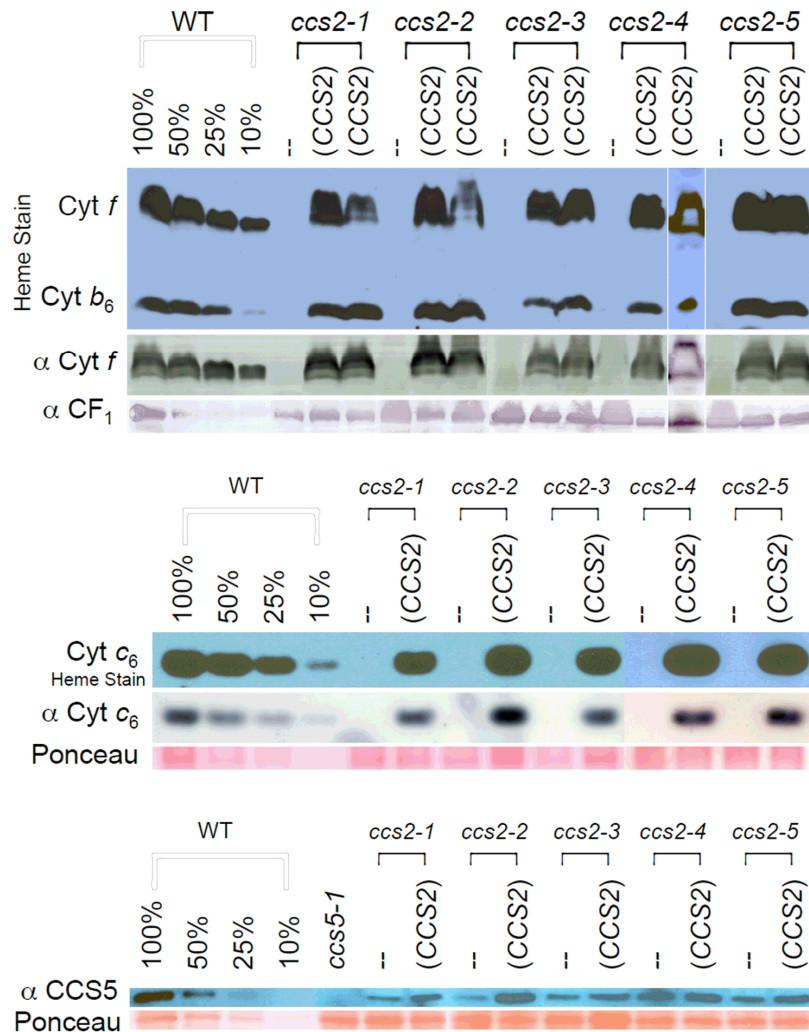


Figure 9 - Restoration of Cytochrome *c* and CCS5 Accumulation in Complemented Mutants. For A, B and C, *ccs2* alleles have been complemented with 8.2 kb genomic fragment. A, Wild Type (*cc124*), the *ccs2* alleles and two independent transformants

were analyzed for cytochrome *f* accumulation via heme stain and anti-cyt *f* immunoblot. Anti-*CF1* of the ATPase is shown as a loading control while dilutions of the wild type sample indicates degree of restoration. *B*, Same as in *A*, except only one transformant is shown, immunoblot corresponds to anti-cytochrome *c6* and Ponceau staining is shown as a loading control. *C*. Same as in *B*, except immunoblot is anti-*CCS5*.

The deduced protein sequence can be seen in **Figure 11A**. The OPR motifs are highlighted and a consensus OPR sequence from all OPR containing genes functionally identified to date can be seen in **Figure 11C**. The OPR family is further characterized by the presence of low complexity regions, often of alanine, glycine or glutamine repeats. The relative locations of the motifs in the proteins used to deduce **Figure 11C** can be seen in **Figure 11B**, as well as the locations of the glutamine rich regions in these proteins. MCA1 is included as an example of a *Chlamydomonas* PPR proteins.

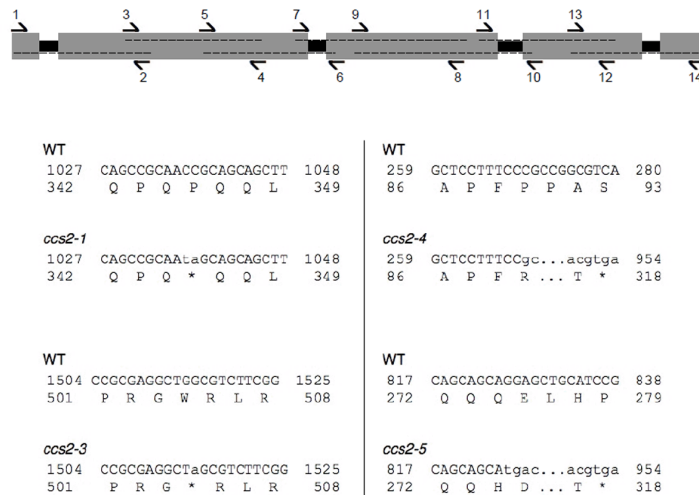


Figure 10 - Identification of the CCS2 cDNA and Allele Mutations. A, Schemata of CCS2 cDNA and its extraction. Introns are shown in gray, exons in black, cDNA products as dashed lines and primers indicated as arrows. Primers are numbered as *ccs2*.#, where # is the given primer name, as listed in Supplementary Materials. B, Identified mutations in *ccs2* alleles. Top line indicates the mutation position within the cDNA,

lower line indicates the change within the protein.

```

MLAPHSATLP PRCTCHSHGL AQLQTSVLRP STGYGAQQAV ARFRPDASMQ ASAEPGDSAN ATDPQLDHTQ 70
HLRRRSTAAV PPRRAWAPFP PASQQGSDKS PAPAPOPAPA SAPAPAPTAT LPPADSSCTA PGRRRHSGYG 140
ASVPVSVSVF ATPVAVGPAP AAPEPGTVQD QSSGALLLPL PATHPAAATA TAASRRRSRR GGRRAAAAH 210
QQQQLGRCSSG DGEGESAAEG DAGEPEAGEE PGVVLVPVWE GQFWQQPRRH GAAQYSEQR HRQQQLHPV 280
AAFAPAAADA TVAVGTARPE QLGPWTGAAA AAAAEADVIR VAVPADASRL ASAVPRPRLQ QPQPQPQQLE 350
LDLVYSRRRA GDLSEAGVAE QGLCGVAPAR EAAAAAAVA AVAAGRVCSS AAGGGPTATG HAERPPLGPR 420
RSMPTGTPAG AAAGVGRGGR PGAHTATAA TATAVAPMVE TAGNCTQVEE RAESREPGGT GYATAGDTGG 490
RAWGSGSSD GPRGWRLRDE PGGAAPAALS FRVVGKGRAA AGAAEAAAAR QLMRQLMACR DWRELYEVIS 560
PCLGGTTARA AAAAATEGAV AEAGATATAM PTTANALHIT AALNQLASMQ LPPPQGTAAA TAAAGQGAVA 630
VAGAGAAATA AAEVQELLVR LEAAYRAHLM AAWAPAGISH TGRGGSSSSS SSSSSGSSNAV PFARPGPSAH 700
AAAAASSPSL AAAGSGSGSG MGTGAEPRLG PRQLATCLGA LARLRARGWH VASERRLLHL SVATAARWRL 770
SAFPPQELTT LLHALATLGH RPSGDWMAAA AGAVAAAAAG GSMSPRQLST TMWALAVLRQ RPSRALMAAW 840
ALASLQTMH ASAYDVSQSL WAVAKLHRDA VMDAAAAEA GGGGGGAGGA DGDGGGEAAA LWPVVDPV 910
AAAEGLPAGG WRCGVFVAVL AAAMERCCAV MRPAAPVPEA AGRAGDVSTAT WTARRGSSNA GSSNSHSGGG 980
SSCKAQDVCN ALWAVAQLGL RPPRAWVLAV AAGALSSLPH EHPAPVLPFA GALPSPSPGP ASTIHHHQ 1050
QQQHYREQQP LQQPHHNGLA GPRRDGPHRG AASLPALSPP PLTPAPPTFP AAVATAAATA AAATGAATA 1120
APPAPGAQRW RAGDVAGMMW ALAKLRVRPP PQQMLRLCRA AAGAAARGEL GEQHCANVLV ALAVLRYRPP 1190
PDVLRALGAR AAQLATRAAA GAAAARAGAG AGVAAAAGQG AARGVGEQEW TEHDVAGAGP QLVSTALWCC 1260
LRLGLPPGRG LLLPLLRAAA AAAAATCSAA TAATPGSSGG GAGAPAAAAT AAATAAGRRM CPQSAALLY 1330
CLARMRHIGW LDRLLLLQPP PQQPPQQLAA APVALAVAPL AAGAKGAAA EESTATTGRL HLPVVPAPGG 1400
AAGSGGVTES AAERAAACCG GSCGDTTALL LAAAGLDIRA VLEAALRSVE EVEEDTSDCH GSSNSRSGSS 1470
SGSSNDAGSK SAMLGGNAS SSTSTSSSTP SHSGRRINAA GGAATGPAT APAAAAGGAR SSFPPRSLPV 1540
LLWSLSRLGC RPEECMRRL LVHSVESLPL LSPHEATLA SALVALRYAP PPLWLDREVE LLLRRRAAAA 1610
AVAAARLAEQ LEQEEELAEA REEEGRWEEG QEEVECEAGA TGDWGRQARP TARVLLSNRA PSYVDVRQR 1680
RRAAAALRHV ASALARLRRS LAALRAAAA RQQAQQQQRQ 1722

```

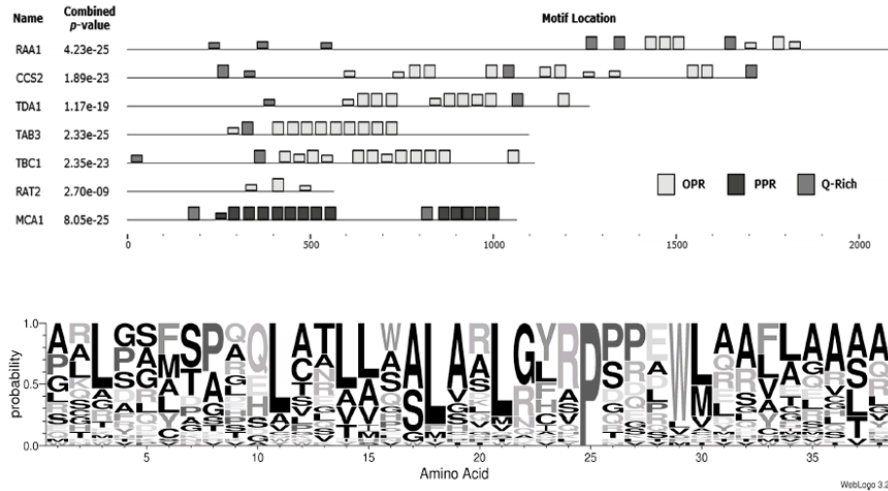


Figure 11 - Features of the Deduced CCS2. A, Full-length protein sequence. Light gray text indicates the peptide used for GFP targeting, light gray highlighting indicates OPRs, the underlined portion contains the most conserved region. B, Schemata generated by MEME show the locations of OPR motifs and Q-repeats within the identified OPR proteins. MCA1 is included as an example of a PPR protein. Heights of blocks indicate relative proportion of the p -value $1e^{-10}$. C, WebLogo Consensus sequence of the OPRs identified by the MEME program. Height indicates the probability of a particular amino acid at the given position.

In order to further characterize the CCS2 protein, a series of carboxy-terminus HA tagged proteins were constructed using the 8.2kb fragment. These were either left under the control of their own promoter or over-expressed by replacing the 880 bp upstream of the ATG with that of *psaD*. Immunoblot analysis against whole cell extracts from these transformants over-expressing the CCS2 protein tagged at the carboxy-terminus revealed that CCS2 runs at the predicted size (Figure 12B). Unexpectedly, a second band also appeared at ~200 kDa. A similar pattern was seen for the control protein, MCA1, suggesting this higher band may be a result of poor solubilization because of the extraction methods needed to visualize the protein (See Materials and Methods).

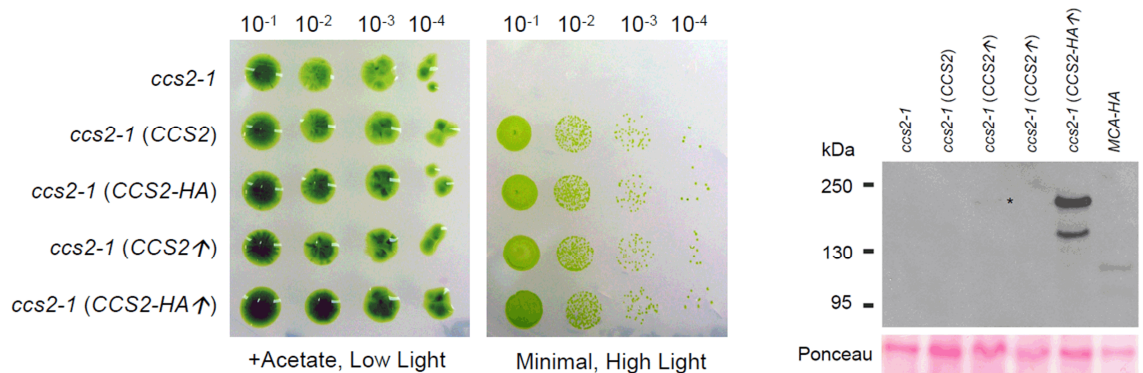


Figure 12 - Characterization of CCS2-HA. For A and B, a cell wall minus *ccs2-1* strain was transformed with, in sequence: 8.2 kb genomic fragment, HA tagged CCS2, CCS2 under the *PsaB* promoter and HA tagged CCS2 under the *PsaD* promoter. A, 10-fold dilution series of strains described under respiratory, low light (.6 μ E) and phototrophic, high light (50 μ E) conditions for 1 week at 22°C. B, Anti-HA blot against these same strains and HA tagged MCA as a control. The (*) indicates the CCS2-HA under native promoter. Ponceau staining serves as a loading control.

Localization.

ChloroP (Emanuelsson et al., 1999) and WoLF PSORT (Horton et al., 2007) both predict a chloroplast targeting sequence. Extraction methods necessary for visualization of the CCS2-HA tagged protein precluded subcellular fractionation, so to test this prediction *in vivo*, we constructed a CCS2/GFP fusion gene composed of the first one hundred codons of CCS2, optimized for expression in *A. thaliana*, fused to the amino-terminus of GFP. This construct, pGWB5/cc2target, was transformed into *Nicotiana benthamiana*. Fluorescence microscopy shows clear overlay of GFP fluorescence and chlorophyll auto-fluorescence (**Figure 13**). This supports the predictions for chloroplast localization.

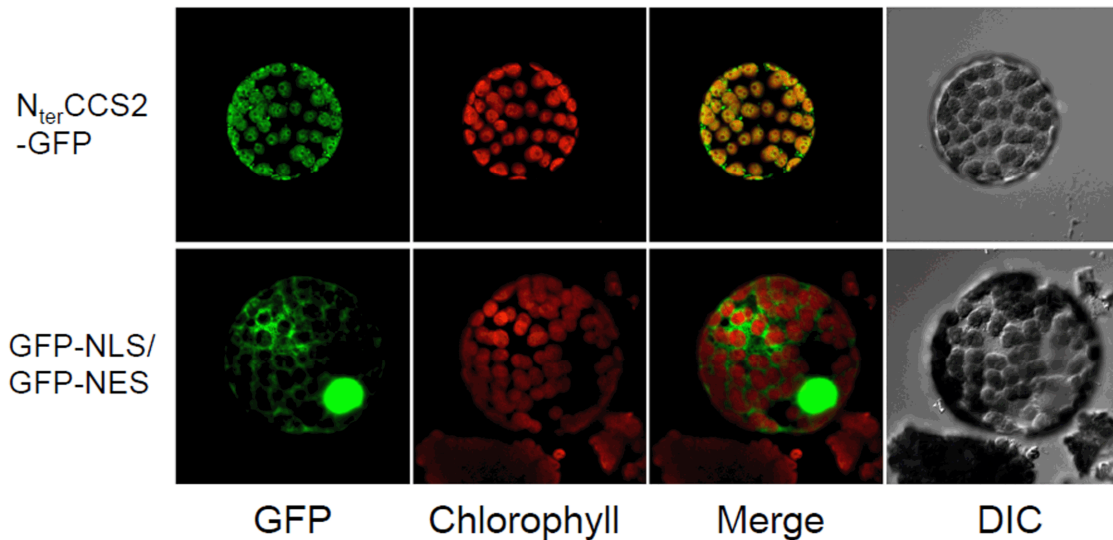


Figure 13 - Localization of GFP to Chloroplast by CCS2 Targeting Sequence. The top row shows *N. benthamiana* protoplasts transformed with CCS2 targeting sequence fused to GFP. The bottom row shows negative control, GFP targeted to nucleus and cytoplasm.

Essential domains are located in C-terminus.

Sequencing of the *ccs2* alleles showed that all mutations introduced nonsense or frameshift mutations which were translated into changes near the amino-terminus of the protein, except for the *ccs2-2* allele (**Figure 10B**). The mutation in this allele appears to have occurred at an intron/exon boundary in the fourth intron, implicating that the carboxy-terminus of the protein is essential for function (**Figure 10**). In addition, introduction of an internal HA tag at a unique BspEI disrupts complementation while a similar tag at BsiWI still complements, these correspond to sites near the amino- and carboxy-termini respectively.

Specific effects of the *ccs2* mutation.

To explore the effects of the *ccs2* mutations on additional System II components, the accumulation of CCS5 was revealed by immunoblot. As seen in Figure 9C, levels of CCS5 are reduced in the *ccs2* mutants. This is unlike CCS5 levels in *ccs* mutants *ccs4-1* (Gabilly et al., 2011) and a *ccsA* mutant, *B6* (not shown) which are unaffected. The reduced accumulation of CCS5 suggests that CCS2 may be involved the thio-reduction pathway for cytochrome *c* assembly. Therefore, we explored the hypothesis that one of the five *ccs2* strains could be rescued by the addition of oxidizing cysteines or reducing DTT or MesNa reagent to the media, but no suppression of the cytochrome *c* deficient growth phenotype was observed (not shown). While not ruling out the possibility, this argues against CCS2 having a direct role in reduction of the cysteine thiols. We also saw no suppression of the photosynthetic deficient phenotype via nuclear transformation of known System II components CCS1, CCDA or CCS5 genomic DNA (not shown).

MATERIALS AND METHODS

Strains and culture condition.

The mutant strains *ccs2-1* through *ccs2-5* were used in complementation experiments. Mutants *ccs2-1* and *ccs2-2* were crossed to wildtype strain cc124 (*arg7-8*) to generate the *ccs2-1 arg7-8* and *ccs2-2 arg7-8* strains. The *ccs2-1 arg7-8* mutant was then crossed with wildtype strain CC425 (*arg7-8 cw15*) to generate the *ccs2-1 arg7-8 cw15* mutant used for tagged complementation. Proving to be the most amenable to manipulation, *ccs2-2 arg7-8* strain #24 was used for transformation. Strains were maintained at 22°C on TAP supplemented with 400 mg/mL arginine at .6 μE. For protein work, wildtype and complemented strains were grown in liquid TAP supplemented with arginine under 50 μE while *ccs* mutants were grown under .6 μE light. Cell wall mutants were cultured in liquid and on solid medias supplemented with 50 mM sorbitol. Copper-free media was prepared as described previously (Howe and Merchant, 1992; Quinn and Merchant, 1998).

Complementation.

An index cosmid library was transformed as described by (Purton and Rochaix, 1994) with the following exceptions: The vector backbone was pCB412 and the transformation required a 30 minute incubation in autolysin followed by electroporation of 5 μg of DNA per pool on a Biorad Micropulser at 1300 V. Transformants were selected under 50 μE light on minimal media supplemented with 1 mL Tris-Acetate. All subsequent transformations were performed in the same manner.

Constructs.

Plasmid pMOL+8.2kb was generated by cloning the 8.2kb genomic fragment (cut *Bam*HI/*Hind*III), isolated from cosmid pool #8, row G column 6, into *Bam*HI/*Hind*III cut pMOLUC (Cha et al., 2002). This plasmid served as the basis for promoter and tagging experiments. Internal HA tags were created by cutting pMOL+8.2kb by *Bsi*WI or *Bsp*EI and inserting the HA tag via infusion. The HA-tag insert was generated by PCR based fill-in of primers CCS2-HA_*Bsi*W1-F and CCS2-HA_*Bsi*W1-R or CCS2-HA_*Bsp*EI-F and CCS2-HA_*Bsp*EI-R. All sequencing was performed by Agencourt, Quicklane Express. All primer sequences can be found in Supplemental Table 1.

Carboxy-terminus 3xHA tags were generated by initial restriction digest of pMOL+8.2kb by *Bsi*WI and *Psh*A1 and insertion of a 200 bp fragment synthesized by Genscript (in plasmid pUC57+ccs2bits) that changed the stop codon into an alanine and added the restriction sites *Xba*I, *Swa*I and *Spe*I just 3' of the gene. This fragment was amplified by primers CCS2-*Bsi*WI-F and CCS2-*Psh*AI-R and cloned using In-Fusion® (CloneTech) to create plasmid p8-noS. This plasmid was this digested by *Xba*I and *Spe*I and a 3xHA tag, created through PCR fill-in of primers 8.3xHA-f and 8.3xHA-r, was inserted via in-fusion cloning. This created vector p8-3xHA. The *psaD* promoter and no-promoter constructs were generated in a similar manner. A 300 bp fragment was amplified from pUC57+ccs2bits using primers CCS2-*Xcm*I.R and CCS2-*Xcm*I.F and inserted via in-fusion cloning after digestion of pMOL+8.2kb and p8-3xHA by *Xcm*I. This created plasmids p8-noP and p8-3xHAnoP. These constructs were then used to generate plasmids p8-PROM and p8-3xHA+P. To create these vectors, the *psaD* promoter was amplified from plasmid pSL18 using primers 8.PROM-f and 8.PROM-r

and inserted via In-Fusion® cloning at the introduced restriction sites *Bgl*III and *Xho*I.

pGWB5/ccs2target was constructed from pUC57+ccs2targeting, which contains the first 300 bp from CCS2, synthesized and codon optimized for expression in *A. thaliana* by GenScript. Using primers CCS2.t1 and CCS2.t2, the targeting sequence was amplified and then inserted in frame with the GFP reporter in the expression vector pGWB5 using entry vector pENTR/SD/TOPO via TOPO cloning.

cDNA extraction: cDNA was retrieved from RNA extracted as described in (Barbieri et al., 2011). Reverse transcription was performed using a bacterial reverse transcriptase from the Roche Transcriptor High Fidelity cDNA Synthesis Kit (05081955001) and gene specific primers ccs2.30 and ccs2.66stp. Fragments were amplified with the following primer pairs: ccs2.69 and ccs2.66stp, ccs2.19 and ccs2.54, ccs2.21 and ccs2.18, ccs2.79 and ccs2.02, ccs2.27 and ccs2.28, ccs2.51 and ccs2.26, and finally ccs2.81atg and ccs2.70. using DV Ready Mix (Sigma). Positive bands were gel isolated, re-amplified and AT-cloned into pGEM-T Easy for sequencing.

Immunoblots.

Immunoblots and heme stains of cytochrome *f* and *c*₆ were performed as in Howe and Merchant 1992. CCS5 blots were performed as in (Gabilly et al., 2010). HA blots were performed on cells prepped as follows: Cells were grown at low light to low log phase and then moved into high light for 5 hours. Cells were then pelleted and washed in 1 mL NaPO₄ buffer.

Chlorophyll Auto-fluorescence.

Measurements were taken as described in (Gabilly et al., 2010) except that strains were inoculated in 3 mL TARG and grown O/N at 22°C and .6 μE with shaking.

Readings were taken on 20 μ L drops of culture placed over a white background.

GFP Fluorescence.

N. benthamiana was transformed with *Agrobacterium* via infiltration after a one hour incubation in Induction Medium (10 mM MgCl₂, 10 mM MES, 100 μ M Acetosyringone). After three days, protoplasts were extracted by a 30 minute incubation in Digestion Buffer (1.5% cellulose, 0.4% macerozyme, 0.4 M mannitol, 20 mM KCl, 20 mM MES-KOH pH 5.5, 10 mM CaCl₂, 0.1% BSA) and concentrated with a 1 second spin at 100 RPM. Supernatant was removed and protoplasts were re-suspended in 100 μ L Digestion Buffer. GFP measurements were taken at 515 nm and chlorophyll auto-fluorescence at 650 nm on a Nikon C2 confocal microscope (Eclipse C90i) using a medium aperture and NIS-Elements software.

OPR Protein Domains

Information for image was generated by MEME (Bailey and Elkan, 1994). Individual protein sequences were entered into the program and base settings were altered to look for any number of motifs per protein that were at least 28 amino acids long. The OPR motifs identified by the MEME program were feed into Weblogo 3.2 (Crooks et al., 2004). Sequences used for these images can be found in supplemental data.

DISCUSSION

Identification of CCS2 as an OPR protein needed for cytochrome *c* assembly

Here we have identified CCS2, a chloroplast localized cytochrome *c* assembly factor that, based on primary sequence homology, appears to be unique to specific branches of the green algal lineage. This protein has been identified as a member of the

recently designated OPR family (Eberhard et al., 2011). Like tetratricopeptide repeat (TPR) and pentatricopeptide repeat (PPR) proteins, these OPRs are defined by loosely conserved repeats, either of 38 (OPR), 34 (TPR) or 35 (PPR) amino acids. TPRs tend to be involved in protein-protein interactions (reviewed in (D'Andrea and Regan, 2003), while PPRs are an expanded family in plants (Lurin et al., 2004) and are known for their interactions with RNA (reviewed in (Schmitz-Linneweber and Small, 2008). Crystallization has shown that both TPRs and PPRs are organized as a series of anti-parallel α -helices and protein predictions using I-TASSER (Zhang, 2008; Roy et al., 2010) suggest that the OPR proteins are organized in a similar manner (not shown).

Similar to the PPR expansion seen in plants, certain branches of the green algal, such as Volvocales and Mamielles, seem to have an expansion in the number of these OPR domain containing proteins (Eberhard et al., 2011). All OPR factors that have been assigned a function to date are displayed in **Figure IIB**. These proteins, barring CCS2, were all identified genetically as being involved in RNA maturation or translational regulation of transcripts in the chloroplast of *Chlamydomonas*. For instance, TBC2 (translation factor for chloroplast *psbC* mRNA) and TDA1 are two factors involved in the translation of the *psbC* and *atpA* transcripts respectively (Auchincloss et al., 2002; Eberhard et al., 2011) while RAA1 (RNA maturation of *psaA*) and RAT2 (RNA maturation of *psaA tscA* RNA) have been identified as being involved in RNA maturation (Balczun et al., 2005; Merendino et al., 2006).

These and other OPR proteins identified by bioinformatics are characteristically around 100 kDa with two to twelve of these leucine rich repeats – the count per protein can fluctuate depending on how stringently one defines a single OPR. These repeats are

not highly conserved. For instance, while CCS2 repeats are characterized by a LWALAR motif, TBC2 and TDA1 repeats are most readily identified by a PPPEW repeat (Auchincloss et al., 2002; Eberhard et al., 2011). The repeats are generally 38 amino acids long and, while they are sometimes repeated one after another, at other times they can be separated by gaps, often by stretches of innocuous amino acids such as alanine (**Figure 11B**). These repeats are found primarily inside the protein while the carboxyl- and amino-termini are characterized by stretches of single amino acid repeats. Interestingly, there is often a poly-glutamine region upstream of the OPR region (**Figure 11B**), which could be involved in the function of the proteins.

Considering its inclusion in the OPR family, it is possible that CCS2 is involved in the maturation or stabilization of the chloroplast encoded CcsA transcript (Xie and Merchant, 1996). However, levels of CcsA transcript in the *ccs2* mutants were previously shown to be unaltered (Xie et al., 1998), indicating that this is not the case. Furthermore, addition of RNase to protein samples did not shift the size of CCS2 seen in **Figure 12B**, so the higher band is not a RNase susceptible complex (not shown). That leaves the hypothesis that CCS2 is involved in the translation of CcsA still viable. However, if CCS2 is involved in the translation of CcsA, the reduction of CCS5 accumulation in the *ccs2* mutants must be explained, as CCS5 still accumulates to wild type levels in the *ccs4-1* truncation mutants (Gabilly et al., 2011). These phenotypes may be explained if CCS5 levels are down in the *ccs1* or *delta-cytf* mutants, which would implicate CCS5 accumulation is dependent upon cytochrome *f* transcription or translation, as the cytochrome c minus phenotypes of both the *ccs4-1* and the *ccsA B6* mutants are leaky. These experiments are in progress.

Another possibility is that CCS2 is a new class of OPR and functions more like a TPR containing protein, stabilizing the System II factors via protein-protein interactions. While a complex has been identified containing CCS1, the observed complex migrated at approximately 200 kDa (Hamel et al., 2003). It is unlikely that both CCS1 (60 kDa) and CCS2 (170 kDa) are the solitary constituents in this complex, as it dissipates in a *ccsA* mutant (Hamel et al., 2003). This tells us that if CCS2 is a stabilizing factor, it is probably not a part of this particular complex, but it does not rule out the presence of CCS2 in a second complex.

Unique Cytochrome c Assembly Factors

While it is unusual to find proteins without widespread orthologs involved in the production of cytochrome *cs*, these unique factors seem more common in plastid biogenesis systems. For instance, the *Arabidopsis* genome encodes for a PORR (plant organellar RNA recognition) protein involved in removing group 2 introns from the mitochondrial *ccmF_c* transcript (Francs-Small et al., 2011). CcmF, the proposed System I heme synthetase, is encoded by three genes in *Arabidopsis*: CcmF_{N1}, CcmF_{N2} and CcmF_C (Rayapuram et al., 2008). The inability of the *wtf9* mutant to mature this transcript results in a cytochrome *f* minus phenotype (Francs-Small et al., 2011). Meanwhile, a PPR protein, PpPPR-71, has been identified as being involved in the editing of the CcmF_c transcript in *P. patens* (Tasaki and Sugita, 2010) which results in the same phenotype. In addition, our own research has revealed a new factor involved in cytochrome *c* assembly, CCS4, as a component of the disulfide reducing pathway. Although bioinformatic searches using the 93-amino acid sequence of CCS4 revealed few orthologs and no known motifs (Gabilly et al., 2011), a protein with a loosely similar structure, HCF153

was identified separately as being involved in cytochrome *c* assembly in *Arabidopsis* by mutagenesis (Lennartz et al., 2006). As a result of the increasing number of factors emerging in the plastid, such as CCS2 and CCS4, that do not seem to be necessary for bacterial assembly of cytochromes *c*, we propose that an additional qualification be made for System II*: defined as System II in the plastid of eukaryotic organisms.

Implications of Unique Assembly Factors

The uniqueness of *Chlamydomonas* proteins does not argue against its use as a model system. In fact, it shows us how necessary it is to ensure that the diversity of model systems is expanded. Research on unique *Chlamydomonas* proteins such as the atypical stator-stalk of the ATP synthase (Vazquez-Acevedo et al., 2006) or the iron scavenging protein FEA1 (Allen et al., 2007) has provided possibilities for solutions to medical problems and plant bioengineering to improve iron uptake. As an example, the protein FEA1 is currently being investigated as a possible method for improving crop production in nutrient poor soils (Leyva-Guerrero et al., 2012). Similarly, it is possible to suggest the introduction of the facultative Cyt *c*₆ into land plants for growth in low iron or high copper soils. However, introduction of this protein will require a greater understanding of its assembly for efficient expression – for instance, we may find that effective expression of this protein requires co-transformation with a specific assembly factor such as CCS2.

In addition, this finding emphasizes the continued role forward genetics must continue to play in our scientific inquiry into the world. The inability of current bioinformatic techniques to identify similarities between CCS4 and HCF153 reveals how inefficient these programs may still be at identifying functional homologs. While on the

other hand, it is becoming more apparent that primary sequence homology does not necessarily indicate functional homology. Findings such as these do not discredit bioinformatics. Instead, they push us to continue basic research in the hopes of improving search algorithms and functional predictions. Such improvements will allow us to stream-line the scientific process, saving time and money by improving the accuracy rate of hypothesis generation.

**Chapter 3: Lumen Thiol Oxido-reductase 1 (LTO1), a
disulfide bond-forming catalyst, is required for the assembly of
photosystem II**

Mohamed Karamoko¹, Sara Cline^{1,2},
Kevin Redding³, Natividad Ruiz⁴, and Patrice Hamel^{1,2}
The Plant Cell December 2011 vol. 23 no. 12 4462-4475

¹Department of Molecular Genetics and Department of Molecular and Cellular Biochemistry, The Ohio State University, Columbus, Ohio, USA

²Plant Cellular and Molecular Biology Graduate Program, The Ohio State University, Columbus, Ohio, USA

³Department of Chemistry & Biochemistry, Arizona State University, Tempe, Arizona, USA

⁴Department of Microbiology, The Ohio State University, Columbus, Ohio, USA

Address correspondence: Patrice Hamel, 500 Aronoff Laboratory, 318 W. 12th Avenue, 43210 Columbus, Ohio, [Tel.: 614-292-3817](tel:614-292-3817), Fax: 614-292-6345, E-mail: hamel.16@osu.edu

The author responsible for distribution of materials integral to the findings presented in this article in accordance with the policy described in the Instructions for Authors (www.plantcell.org) is: Patrice Hamel (hamel.16@osu.edu)

AUTHOR CONTRIBUTIONS: P.H., K.R. and N.R. designed the experiments, analyzed the data, and wrote the article. S.C. performed the topology and cross-species complementation experiments. M.K. characterized the Arabidopsis mutant, with the exception of the *in vivo* spectroscopic measurements, which were performed by K.R. and performed the *in vitro* LTO1 functional analysis.

Abstract

Here we identify *Arabidopsis thaliana* LTO1 (Lumen Thiol Oxido-reductase 1) as a disulfide bond-forming enzyme in the thylakoid lumen. Using topological reporters in bacteria, we deduced a luminal location for the redox active domains of the protein. LTO1 can partially substitute for the proteins catalyzing disulfide bond formation in the bacterial periplasm, which is topologically equivalent to the plastid lumen. An insertional mutation within the *LTO1* promoter is associated with a severe photoautotrophic growth defect. Measurements of the photosynthetic activity indicate that the *lto1* mutant displays a limitation in the electron flow from photosystem II (PSII). In accord with these measurements, we noted a severe depletion of the structural subunits of PSII but no change in the accumulation of the cytochrome *b₆f* complex or photosystem I. In a yeast two-hybrid assay, the thioredoxin-like domain of LTO1 interacts with PsbO, a luminal PSII subunit known to be disulfide bonded, and a recombinant form of the molecule can introduce a disulfide bond in PsbO *in vitro*. The documentation of a sulfhydryl oxidizing activity in the thylakoid lumen further underscores the importance of catalyzed thiol-disulfide chemistry for the biogenesis of the thylakoid compartment.

Introduction

Thiol-disulfide chemistry is an essential process for the biogenesis of the bacterial periplasm, the mitochondrial intermembrane space (IMS) and the thylakoid lumen. Strikingly, each compartment appears to have unique redox enzymes that oxidize sulfhydryls (thio-oxidation) and reduce disulfide bonds (thio-reduction) in target proteins (Herrmann et al., 2009; Depuydt et al., 2011; Kadokura and Beckwith, 2011).

In the periplasmic spaces of most proteobacteria, the thio-oxidizing pathway

consists of a disulfide bond catalyzing system defined by soluble DsbA and membrane-bound DsbB (Dsb for disulfide bond) (Heras et al., 2009; Depuydt et al., 2011; Kadokura and Beckwith, 2011). DsbA catalyzes disulfide bridge formation on cysteine containing substrates that are translocated across the membrane into the periplasmic space. DsbB operates by recycling reduced DsbA to its oxidized form with transfer of the electrons to quinones, which are membrane-soluble redox carriers in the respiratory chain. A central component of the thio-reducing pathway is the thiol-disulfide transporter DsbD/CcdA (Ccd for cytochrome c deficiency). This protein conveys reducing power from the cytosol to several periplasmic protein targets whose activity requires reduced thiols. DsbD/CcdA maintains the reduction state of oxido-reductases that shuffle disulfide bonds that are incorrectly formed and protect proteins containing a single cysteine from hyperoxidation (Depuydt et al., 2011; Kadokura and Beckwith, 2011). DsbD/CcdA is also needed to reduce the active site of a disulfide reductase involved in the assembly of cytochromes *c*, a class of metalloproteins with a heme covalently attached to a CXXCH motif. The accepted view is that the CXXCH motif is first oxidized by the Dsb machinery and then reduced by the disulfide reductase in order to provide free sulfhydryls for the heme attachment (Bonnard et al., 2010; Sanders et al., 2010).

While the presence of thiol-metabolizing pathways is well established in bacteria, there was little support for the operation of thiol-based chemistry in the mitochondrial IMS and the thylakoid lumen, which are topologically equivalent to the bacterial periplasm. Recent discoveries in both organelles have now changed this perception. In mitochondria, Mia40p/Erv1p (Mia for Mitochondrial intermembrane space import and assembly, Erv for Essential for respiration and viability) proteins were found to be key

enzymes of a disulfide relay system driving the import of cysteine-rich proteins into the IMS (Depuydt et al., 2011; Riemer et al., 2011; Sideris and Tokatlidis, 2011). Although unrelated in sequence, Mia40p/Erv1p are functionally equivalent to bacterial DsbA/DsbB. Mia40p introduces disulfide bonds into protein targets and is recycled back to its oxidized form by the flavoprotein Erv1p, which transfers the electrons to cytochrome *c*, a soluble redox shuttle in the IMS. By analogy to the bacterial pathways, the participation of thio-reducing factors in the IMS is expected. The flavoprotein Cyc2p (Cyc for cytochrome c) and CcmH (Ccm for cytochrome c maturation), an oxidoreductase implicated in cytochrome *c* maturation, were proposed to act as a disulfide reductase, but this still awaits experimental validation (Bernard et al., 2005; Meyer et al., 2005; Corvest et al., 2010).

In the thylakoid lumen, the involvement of a thio-reducing pathway was established through classical and reverse genetics approaches. Components of this pathway include a thiol/disulfide membrane transporter of the CcdA/DsbD family and CCS5/HCF164 (cytochrome c synthesis /high chlorophyll fluorescence), a membrane-anchored, lumen facing, thioredoxin-like protein. These proteins define a trans-thylakoid pathway for the delivery of reductants from stroma to lumen (Lennartz et al., 2001; Page et al., 2004; Motohashi and Hisabori, 2006; Gabilly et al., 2010; Motohashi and Hisabori, 2010; Gabilly et al., 2011). Operation of the trans-thylakoid pathway is needed to reduce disulfides in target proteins, a process essential for photosynthesis (Lennartz et al., 2001; Page et al., 2004; Gabilly et al., 2010; Gabilly et al., 2011).

The identities of the thio-oxidizing catalysts in the lumen are currently unknown and no DsbA- or DsbB-like enzymes can be detected in the genomes of cyanobacteria,

which are the presumed ancestors of chloroplasts. However, disulfide bonded proteins are present in this compartment and include not only known structural components such as PsbO, a subunit of photosystem II (Burnap et al., 1994; Betts et al., 1996; Wyman and Yocum, 2005), and Rieske, a subunit of the cytochrome *b₆f* complex (Carrell et al., 1997), but also molecules participating in the assembly/regulation of the photosynthetic chain (Gupta et al., 2002; Gopalan et al., 2004). The operation of one or more disulfide bond forming catalysts in the thylakoid lumen is supported by the finding that bacterial alkaline phosphatase (PhoA), an enzyme requiring two disulfide bonds for activity, is active when targeted to this compartment in tobacco (Sone et al., 1997; Bally et al., 2008).

Recently, a novel class of disulfide bond forming enzymes has been proposed to control disulfide bond formation. This class has similarity to VKOR (vitamin K epoxide reductase) and was recognized in cyanobacteria (Singh et al., 2008; Li et al., 2010), some bacterial phyla lacking the typical DsbAB components (Dutton et al., 2008; Dutton et al., 2010; Wang et al., 2011) and the green lineage (Grossman et al., 2011). The VKOR-like proteins were defined based on the presence of a redox domain containing two cysteine pairs. This domain is related to the one present in VKOR, an integral membrane protein of the endoplasmic reticulum (ER) (Goodstadt and Ponting, 2004; Dutton et al., 2008; Furt et al., 2010). VKOR is well studied for its involvement in the reduction of vitamin K, a phylloquinone required as a co-factor for the γ -carboxylation of clotting factors in blood (Tie and Stafford, 2008). The recent identification of TMX (TMX for Transmembrane oxidoreductase), a membrane anchored thioredoxin-like protein, as a redox partner of VKOR suggests that the enzymatic activity of VKOR is also linked to

oxidative folding of proteins in the ER lumen (Schulman et al., 2011). One current view is that TMX (and possibly other disulfide bond forming proteins such as PDI, the ER resident protein disulfide isomerase) catalyzes disulfide bond formation in protein targets and is recycled to its oxidized form via thiol-disulfide relay within the VKOR domain, the final electron acceptor being vitamin K epoxide in the membrane (Rishavy et al., 2011; Schulman et al., 2011).

In the plant *A. thaliana*, a VKOR-like protein localizes to the plastid (Furt et al., 2010) and is detected at the thylakoid membrane by proteomic analysis (Zybailov et al., 2008). However, its function in plastid biogenesis has so far remained elusive (Furt et al., 2010). In this manuscript, we have investigated the function of plastid LTO1 (Lumen Thiol Oxido-reductase 1), the *Arabidopsis* VKOR-like protein. Genetic and biochemical studies indicate that LTO1 is required for the assembly of PSII through the formation of a disulfide bond in PsbO, a subunit of the PSII oxygen evolving complex (OEC) that resides in the lumen.

Results

LTO1, a VKOR-like protein at the thylakoid membrane, is conserved in photosynthetic eukaryotes

A protein displaying a membrane domain with similarity to VKOR (Vitamin K epoxide reductase) and fused to a thioredoxin-like domain was identified in all sequenced genomes of photosynthetic eukaryotes (Tie and Stafford, 2008). We name this protein LTO1 (for Lumen Thiol Oxido-reductase 1). LTO1-like proteins are predicted to be polytopic membrane polypeptides with five to six transmembrane domains and contain seven strictly conserved cysteines (with the exception of the Volvox and Chlorella

proteins) (Supplemental Figure 1 online). Four of the cysteines are arranged in two motifs: *CXXC* and *WCXXC*. The *WCXXC* motif is part of a thioredoxin-like domain that is absent from VKOR and some bacterial VKOR-like proteins (Goodstadt and Ponting, 2004).

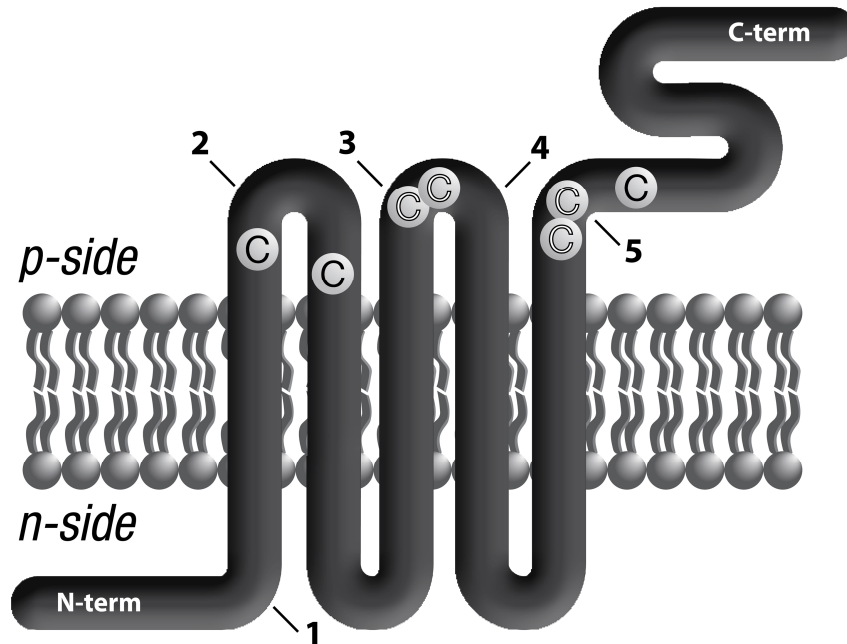


Figure 14 - Proposed topological arrangement of plastid *Arabidopsis* LTO1. The proposed topological arrangement of *Arabidopsis* LTO1 in the thylakoid membrane was deduced from the analysis of PhoA/LacZ α sandwich fusions expressed in bacteria (**Table 3 - Topological analysis of *Arabidopsis* LTO1 from PhoA and LacZ fusion analysis.** Measurements of alkaline phosphatase (PhoA) and β -galactosidase (LacZ) activities of sandwich fusions at the indicated positions within LTO1. Measurements were taken on at least two separate bacterial clones and correspond to an average of three representative measurements. The \pm S.D. is indicated for those measurements. Fusion numbers correspond to those indicated in **Figure 14**. Values are expressed in arbitrary units for LacZ and Miller units for PhoA. The *p*-side corresponds to the bacterial periplasm and the lumen of the chloroplast, while the *n*-side corresponds to the bacterial cytoplasm and the stroma of the chloroplast.). The *p*-side corresponds to the lumen of the thylakoid and the *n*-side corresponds to the stroma of the chloroplast. LTO1 is represented as a thick thread with its transmembrane domains in the lipid bi-layer and extra-membraneous regions. The LTO1 N-terminal end faces the stroma while the C-terminal domain, corresponding to the thioredoxin-like domain, is exposed to the

thylakoid lumen. The arrows indicate the positions of in-frame sandwich fusions with the Pho-Lac mini-reporter, which corresponds to alkaline phosphatase fused to the α fragment of β -galactosidase. Fusions at positions 74 (1), 113 (2), 191 (3), 195 (4) and 573 (5) are indicated on the drawing by arrows. Strictly conserved cysteines are marked (C). Conserved cysteines within CXXC motifs are highlighted in white.

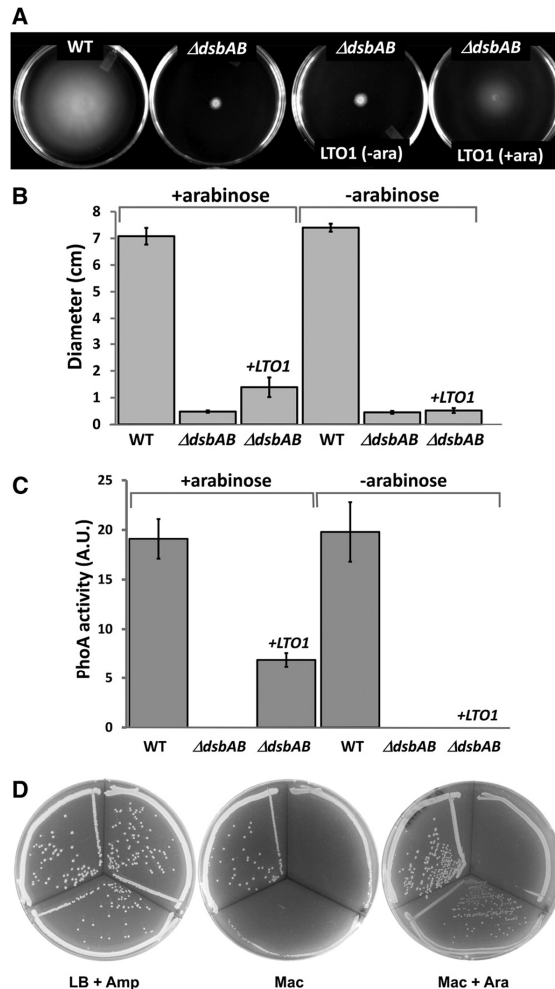


Figure 15 - *Arabidopsis* LTO1 partially complements the *E. coli* *dsbAB* mutant for disulfide bond formation. Strains are wild-type HK295 (pBAD24), $\Delta dsbAB$ HK329 (pBAD24) and $\Delta dsbAB$ HK329 (pLTO200). *A*, Complementation of the motility phenotype in *dsbAB* mutants by *Arabidopsis* LTO1. Representative motility phenotype of wild-type (WT), $\Delta dsbAB$, and $\Delta dsbAB$ bacterial strains expressing LTO1 under an arabinose-inducible promoter (+/-ara) on M9 solid media. *B*, Quantification of motility phenotype represented in *A*. Each bar represents the standard deviation from 10 independent plate measurements. *C*, Complementation of the *phoA*-deficient phenotype in *dsbAB* mutants by LTO1. Each bar represents the standard deviation from three

separate measurements of PhoA activity. *D*, *Complementation of the growth phenotype in dsbAB mutants by LTO1*. In all plates in panel D, the top left sector was inoculated with HK295 (pBAD24), the top right sector was inoculated with HK329 (pBAD24), and the bottom sector was inoculated with HK329 (pLTO200).

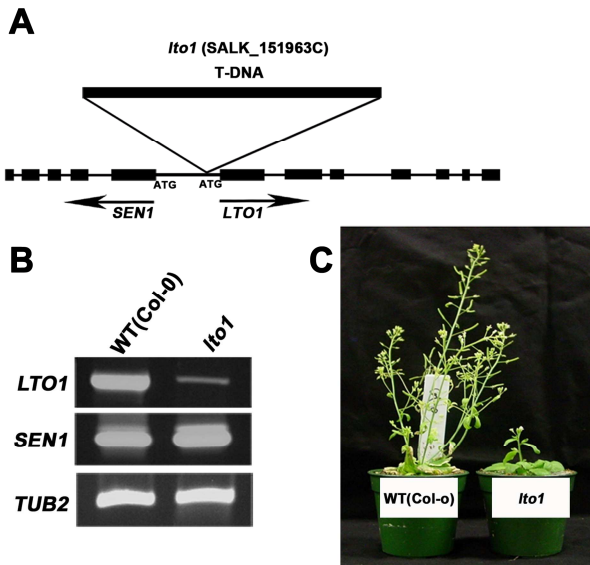


Figure 16 - Knock-down of LTO1 results in a growth defect. *A*, Structure of *LTO1* and *SEN1*. Black boxes represent exons and thin lines correspond to introns in *SEN1* and *LTO1*. The initiation codons (ATG) of *SEN1* and *LTO1* are indicated. The position of the T-DNA insertion in the SALK_15193C line is indicated. *B*, Expression of *LTO1*. Transcripts corresponding to *LTO1* and *SEN1* were analyzed by semi-quantitative RT-PCR in homozygous *lto1* and wild-type (*Col-0*) plants. *TUB2* was used as a control for constitutive expression. *C*, The *lto1* mutant displays a growth defect. Wild-type (*Col-0*) and *lto1* homozygous plants are shown six weeks after seed germination on soil.

Topological analysis of LTO1

To generate a topological model of plastid LTO1, we employed PhoA and LacZ reporters in *Escherichia coli* (Manoil, 1991). We have already demonstrated the reliability of this approach in establishing the topological arrangement of three proteins in the thylakoid membrane, which is analogous in a bioenergetic sense to the bacterial

plasma membrane (Dreyfuss et al., 2003; Hamel et al., 2003; Page et al., 2004). We opted to engineer PhoA-LacZ α sandwich fusions at positions predicted to be at extra-membrane locations (Supplemental Figure 1 online). High PhoA activities indicate a *p*-side location for the insertion site of the fusion, since PhoA is active only in the periplasm. Reciprocally, fusions with high LacZ activity confirm association of the α and ω fragments of β -galactosidase in the cytoplasm and therefore an *n*-side location of the fusion site can be deduced. As shown in Table 3, PhoA activities for fusions 2, 3, 4 and 5 were 2.5 to 67-fold higher than the LacZ activities and a periplasmic location was assigned for the corresponding positions in *Arabidopsis* LTO1. Note that it is likely that the stability of each sandwich fusion accounts for the difference in PhoA activities. Fusion 1 displayed a high LacZ activity but a low PhoA activity, an indication that the fusion point is located in the cytoplasm. Based on the *n*- and *p*-side topological analogy between the compartments of the bacteria (cytoplasm/periplasm) and those of the thylakoid (stroma/lumen), we deduced that the N- and C- termini of LTO1 face the stroma and the lumen, respectively, while domains containing redox motifs and conserved cysteines are exposed to the lumen (Figure 14).

LTO1 partially complements for loss of DsbAB in bacteria

To provide further support for the proposed topology and function, we chose a heterologous complementation assay. In this assay, an *E. coli dsbAB* mutant was used to test the ability of LTO1 to restore disulfide bond formation in the periplasmic space. For this experiment, we chose an arabinose-inducible promoter to drive the expression of full-length *Arabidopsis* LTO1 cDNA and monitored bacterial motility, PhoA activity and

growth on MacConkey agar, which are dependent upon DsbAB. When FlgI, a flagellar motor protein in the periplasmic space is not disulfide bonded, the bacteria are non-motile (Dailey and Berg, 1993). This loss of motility can be readily visualized on low concentration agar. As shown in Figure 15A and Figure 15B, LTO1 partially restores the motility phenotype of a *dsbAB* mutant, demonstrating that the plant protein can promote disulfide bond formation. This restoration is arabinose dependent, confirming that LTO1 is indeed responsible for the observed restored motility. The activity of periplasmic PhoA, which requires two intramolecular disulfide bonds (Sone et al., 1997), was also partially restored upon expression of the plant protein (Figure 15C). In addition, while *E. coli* strains lacking DsbA and/or DsbB grow poorly on MacConkey agar, the *dsbAB* mutant expressing LTO1 grows well on MacConkey agar supplemented with the inducer arabinose (Table 4 and Figure 15D).

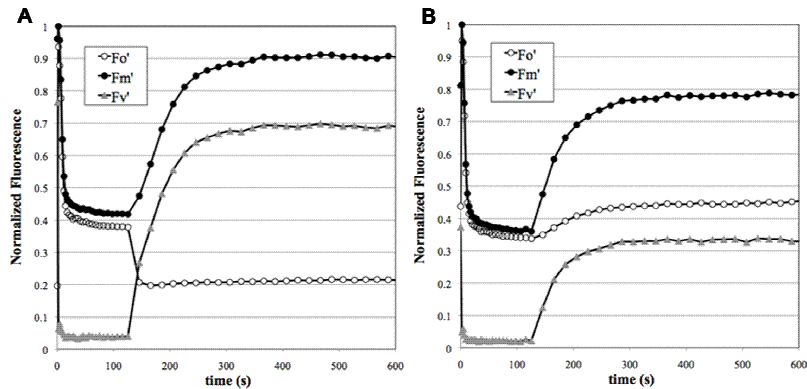


Figure 17 - The photosynthetic defect in the *lto1* mutant is due to a limitation in the electron flow from photosystem II. Fluorescence induction of representative leaves from wild-type (A) and *lto1* (B) plants. Fluorescence was measured using a 10- μ s pulse of 430-nm light and appropriate filters to transmit red light. Actinic illumination provided by 520-nm LEDs ($1.4 \text{ mmol photons m}^{-2} \text{ s}^{-1}$) commenced immediately after taking F_0 and F_M values at time 0. At each time point, fluorescence immediately before (F_0' , open circles) and after (F_M' , filled circles) a 80-ms saturating pulse was measured

during a brief window in which the actinic light was off (see Methods for details). After 2 minutes, the actinic light was extinguished and the recovery of fluorescence was followed in the same manner. The variable fluorescence at each point ($F_V' = F_M' - F_0'$) is also shown as gray triangles. All fluorescence values were normalized to F_M , and thus what is shown is actually F_M'/F_M (filled circles), F_0'/F_M (open circles), and F_V'/F_M (gray triangles).

We conclude that LTO1 partially compensates for the loss of bacterial DsbAB and displays sulfhydryl oxidizing activity. Our findings solidify the proposed lumenal location of the redox motifs and conserved cysteines (Figure 14) and suggest that the relevant targets of action of LTO1 are also lumen localized.

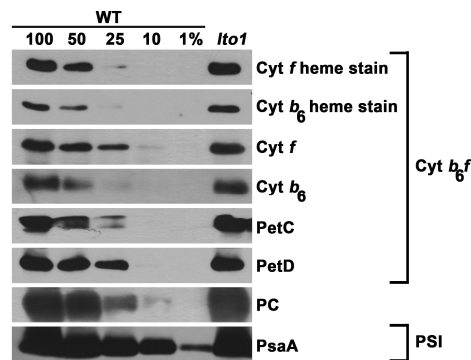


Figure 18 - Accumulation of cytochrome *b₆f* and photosystem I is not affected by loss of LTO1. Wild-type (WT) and *lto1* homozygous plants were analyzed for the accumulation of cytochrome *b₆f* subunits (cytochrome *b₆*, cytochrome *f*, PetC, PetD), plastocyanin (PC) and photosystem I subunit PsaA via immunoblotting. Heme staining was also performed to analyze the accumulation of holoforms of cytochrome *b₆* and *f*. Total protein samples corresponding to 16 μ g of chlorophyll were separated on a 12% SDS-acrylamide gel. For an estimation of the protein abundance in the *lto1* mutant, dilutions of the wild-type sample were loaded on the gel. Gels were transferred to membranes before heme staining by chemiluminescence or immunodetection.

Knock-down of *Arabidopsis* LTO1 impairs plant growth

To address the question of LTO1 function at the thylakoid membrane, we chose a reverse genetics approach and identified a T-DNA insertion in the promoter region of

Arabidopsis LTO1 (Figure 16A). Through PCR analysis and sequencing, we confirmed that the inserted T-DNA is located 45 bp from the predicted initiation codon of the *LTO1* ORF. Reverse transcript (RT) PCR analysis showed that the *LTO1* transcript accumulation is strongly reduced in the homozygous insertion line, suggesting that insertion of the T-DNA altered the transcriptional activity of *LTO1* (Figure 16B). This promoter region is also shared by *SENI*, which was shown to be involved in senescence (Schenk et al., 2005). However, we show that the transcription of *SENI* is not affected by the T-DNA insertion (Figure 16B). Homozygous *lto1* mutants display a severe growth phenotype compared to the wild-type *Columbia* ecotype when grown on soil. The phenotype is not as drastic when grown on sucrose-supplemented agar, indicating that the slow growth may be due to a defect in photosynthesis.

Loss of LTO1 produces a photosynthetic defect:

To test the hypothesis that the reduced growth seen in the mutant is a result of a photosynthetic defect, we conducted several spectroscopic tests on fresh leaves of *lto1* plants. Illumination with far-red light preferentially excites photosystem I (PSI) over photosystem II (PSII), resulting in net oxidation of the plastoquinone (PQ) pool, cytochrome *f*, plastocyanin (PC), and P₇₀₀ of PSI (Joliot and Joliot, 2005). The status of P₇₀₀ was monitored by 10- μ s flashes from a 705-nm LED. We found that the leaves of *lto1* plants exhibited P₇₀₀ oxidation by far-red light and re-reduction immediately upon termination of illumination (Supplemental Figure 2 online), indicating that they possessed functioning PSI. The absolute level of the P₇₀₀ photobleaching signal in *lto1* leaves was smaller than in wild-type leaves, but this was likely due to the fact that *lto1* leaves tended to be thinner than wild-type leaves. We concluded that the function of PSI

is not affected by the mutation. We did, however, notice that the net oxidation of P_{700} proceeded more quickly in the *lto1* leaves. Moreover, they lacked a kinetic inflection point early in the time course (see Supplemental Figure 2A online), which is likely due to an influx of electrons into the electron transfer chain from a light-dependent source. The source is most likely PSII, as the re-reduction of P_{700}^+ occurred with a higher rate in the *lto1* mutant in the dark (Supplemental Figure 2B and Supplemental Table 1 online). This would seem to rule out any defect in PC or cytochrome *b₆f* levels. The higher rate of P_{700}^+ re-reduction upon termination of illumination might be taken as an indication that thylakoids of *lto1* plants are engaged in cyclic electron transfer to a much higher extent than in wild-type plants.

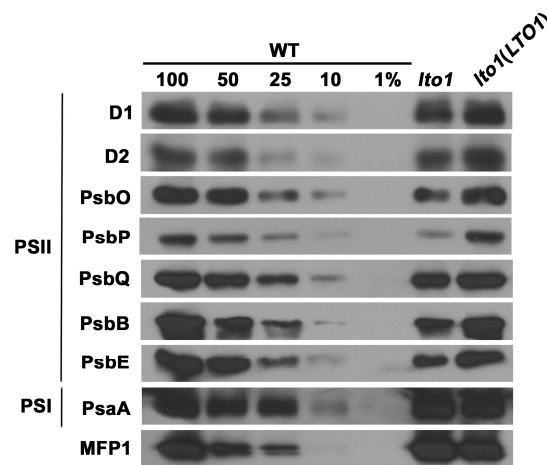


Figure 19 - Accumulation of photosystem II subunits is impacted by loss of LTO1. The accumulation of PSII subunits (D1, D2, PsbO, PsbP, PsbQ, PsbB, PsbE) in the *lto1* mutant, the *lto1* mutant complemented by the *LTO1-C-MYC* cDNA (under the control of the 35S promoter) and wild-type (WT) plants was analyzed via immunoblot analyses. PSI subunit PsaA and MFP1 (MAR-binding filament-like protein 1), a thylakoid-associated nucleoid-binding protein were used as control (Jeong et al., 2003). Thylakoid proteins corresponding to 7 μ g of chlorophyll were separated on a 12% SDS-acrylamide gel. For an estimation of the protein abundance in the *lto1* mutant, dilutions of the wild-type sample were loaded on the gel. Gels were transferred to membranes before immunodetection with antisera against PSII subunits, PsaA and MFP1.

We also examined directly the changes in the redox state of cytochrome *b₆f* cofactors induced by far-red light. We found that both the oxidation of cytochrome *f* and the reduction of cytochrome *b* occurred to a greater extent in the *lto1* plants during illumination, indicating a limitation in electron flow to the cytochrome *b₆f* complex in the light (Supplemental Figure 3 online). The kinetics of decay in the dark were roughly the same. In summary, there appears to be a limitation in light-driven electron flow to cytochrome *b₆f*, which would imply a defect in PSII function.

We tested this hypothesis by fluorescence induction analysis (Figure 17 and Table 5). The rise in fluorescence emission from chlorophyll (Chl) from the initial state in dark-adapted plants (F_0) to the maximal level (F_M) provoked by a 80-ms saturating pulse, otherwise known as the variable fluorescence (F_V), is a function of the quantum efficiency of PSII (Rohacek and Bartak, 1999). The F_V/F_M ratio is taken as a measure of the maximal quantum yield of PSII. In wild-type leaves, F_V/F_M was 0.8, which is a typical value for healthy plants, and the variation was about 1-2% of this value. In contrast, the F_V/F_M ratio in *lto1* leaves was about 0.5, with higher variability (~20%; Table 3). This indicates a rather severe defect in PSII. Upon continuous illumination, F_V dropped precipitously, due to a large decrease in F_M' (maximal fluorescence level in the light) in both wild-type and *lto1* leaves. However, we found that the level of Chl fluorescence before the saturating pulse (F_0') was actually lower than F_0 in *lto1* plants, which is unusual (see Discussion). Non-photochemical quenching in the *lto1* leaves exhibited enormous variation, and was not consistently higher or lower than wild-type leaves at the same light intensity (Table 3). While the *lto1* leaves seemed to suffer from

higher photoinhibition (loss of PSII activity due to illumination at high light fluxes) than wild-type leaves, the difference was not great (Table 3).



Figure 20 - Complementation of the *lto1* photosynthetic defect by LTO1 cDNA. Phenotypes of the wild type (WT), two independent *lto1* lines expressing the *LTO1-C-MYC* cDNA under the control of the 35S promoter (A and B) and *lto1* homozygous plants after 3 weeks of growth on soil.

Finally, we examined the function of ATP synthase, using the decay of the carotene bandshift signal at 520 nm as a spectroscopic marker for the transmembrane electric field of the thylakoid membrane (Sacksteder and Kramer, 2000). The rate of decay is a measure of how fast the proton motive force is expended, which is primarily due to ATP synthase activity. Although we saw slight differences between the wild-type and mutant leaves, in terms of the multi-phasic decay of the carotenoid bandshift signal, the overall decay was similar (Supplemental Figure 4 online). Thus, we see no evidence for major defects in the function of ATP synthase. In conclusion, our spectroscopic analysis of *lto1* leaves pinpoints PSII as the site of the photosynthetic defect caused by the *lto1* mutation. We saw no problems with the function of the other three major thylakoid membrane complexes: PSI, cytochrome *b₆f*, or ATP synthase.

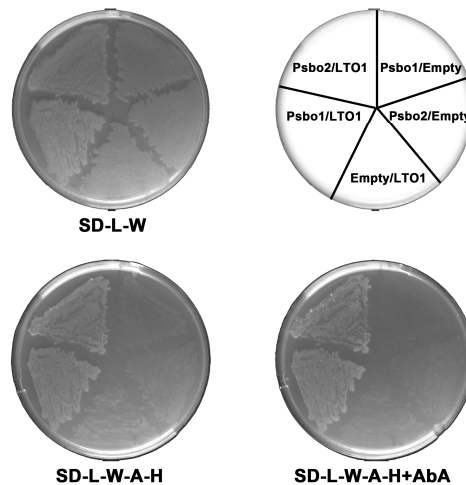


Figure 21 - PsbO1 and PsbO2 interact with the thioredoxin-like domain of LTO1 in a yeast two-hybrid assay. The soluble domain of the wild-type (WCSHC) or mutant (WCSHS) thioredoxin-like domain of LTO1 constitutes the bait and is expressed as a fusion with the GAL4 DNA binding domain from the *TRP1*-based pGBKT7 vector. *Arabidopsis* PsbO1 or PsbO2 constitute the prey and are expressed as a fusion with the GAL4 activation domain from the *LEU2*-based pGADT7 vector. The yeast Y2HGold reporter strain was co-transformed with various combinations of two-hybrid plasmids as indicated on the upper right side of the figure (“Empty” refers to the pGBKT7 or pGADT7 vectors). The yeast transformants were tested for adenine/histidine prototrophies and resistance to aureobasidin A, which depend on reconstitution of an active GAL4. One representative transformant for each combination was plated on solid medium lacking leucine and tryptophan (SD-L-W), incubated for 3 days at 28°C, and replicated on medium lacking leucine, tryptophan, adenine and histidine (SD-L-W-A-H) or lacking leucine, tryptophan, adenine, and histidine with aureobasidin A (SD-L-W-A-H+AbA) and incubated at 28°C for 5 days. GAL4-dependent adenine and histidine prototrophies and resistance to aureobasidin A indicate interaction between PsbO2 and wild-type LTO1, and also between PsbO1 and mutant LTO1.

Loss of LTO1 impacts PSII accumulation:

To further detail the impact on photosynthesis due to loss of LTO1, we carried out immunoblot analyses using antibodies against the subunits of PSI, PSII, and the cytochrome *b₆f* complex. We found that loss of LTO1 has no impact on the accumulation of the cytochrome *b₆f* subunits, including the cytochromes *b₆* and *f* that contain a heme

co-factor (Figure 18). The steady-state level of plastocyanin (PC), the electron carrier between the cytochrome *b₆f* and PSI, was unaffected by the *lto1* mutation (Figure 17). We also excluded a defect in PSI based on the fact that the abundance of PsaA, a core subunit whose accumulation is diagnostic of PSI assembly, is unchanged (Figure 18). In contrast, we noted a depletion of the PSII subunits, including D1, D2, PsbB (CP47) and PsbE (cytochrome *b₅₅₉*), which are the core proteins of the reaction center (Figure 19). Interestingly, there is also a severe reduction in the levels of PsbO, PsbP and PsbQ, three extrinsic proteins bound to the PSII core subunits on the lumenal side of the thylakoid membrane (Bricker and Frankel, 2011; Bricker et al., 2011; Popelkova and Yocum, 2011). Together, these three proteins define a functional module called the oxygen-evolving complex (OEC), which mediates the light-dependent oxidation of water.

A construct expressing the *LTO1* cDNA engineered with a C-terminus C-myc tag complements both the photoautotrophic growth and PSII defects when introduced in the *lto1* mutant (Figure 19, Figure 20 and Table 6). This demonstrates that the molecular lesion in *LTO1* is responsible for the PSII-deficient phenotype. Using an anti-C-myc antibody to probe thylakoid membrane extracts, we were able to detect a 40-kDa band corresponding to LTO1 in the lines complemented with the cDNA expressing construct (Supplemental Figure 6 online).

The thioredoxin-like domain of LTO1 interacts with PsbO1 and PsbO2

The finding that LTO1 exhibits sulfhydryl oxidizing activity and is required for PSII accumulation suggests that the formation of one or more disulfide bonds is needed for the biogenesis of this photosynthetic complex. Based on our heterologous complementation experiments, it is likely this step occurs on the lumenal side of the

thylakoid membrane. Interestingly, PsbO, a luminal subunit of the OEC, carries a single disulfide bond that is critical for PSII assembly and activity (Burnap et al., 1994; Betts et al., 1996; Wyman and Yocum, 2005). To test the hypothesis that PsbO is a relevant target of LTO1, we decided to see if the thioredoxin-like soluble domain of LTO1 (LTO1_{sol}), postulated to carry the sulfhydryl oxidizing activity, could interact with PsbO in a yeast two-hybrid assay. LTO1_{sol} was used as bait and PsbO1 and PsbO2, the two isoforms of *Arabidopsis* PsbO (Peltier et al., 2002; Schubert et al., 2002), were used as prey in a GAL4-based two-hybrid system. In one study, the second cysteine in the WCXXC motif was shown to be critical in detecting the interaction between thioredoxins and their targets using a yeast two-hybrid assay (Vignols et al., 2005). However, we found that both wild-type (WCSHC) and mutant (WCSHS) forms of LTO1_{sol} could interact with either PsbO1 or PsbO2, based on the recovery of GAL4-dependent adenine/histidine prototrophies and aureobasidin A-resistance in the yeast reporter strain (Figure 21). As expected, none of these polypeptides alone elicit such a response (Figure 21). This established both PsbO1 and PsbO2 as relevant targets of LTO1 action *in vivo*.

The soluble domain of LTO1 can catalyze disulfide bond formation in PsbO

To test the possibility that the single cysteine pair present in PsbO1 and PsbO2 could be oxidized by LTO1, we purified recombinant forms of LTO1_{sol} and PsbOs and performed *in vitro* redox assays. We attempted to purify PsbO1 as a recombinant protein, but the resulting polypeptide was proteolytically processed when expressed in bacteria. Recombinant PsbO2, on the other hand, was purified in its oxidized form and the disulfide bond present in the molecule could be chemically reduced in a dose-dependent fashion by the action of dithiothreitol (DTT) (Figure 22A). To test the ability of oxidized

LTO1_{sol} to introduce a disulfide bond in PsbO2, we incubated air-oxidized LTO1_{sol} with reduced PsbO2. This resulted in the oxidation of PsbO2 (Figure 22B, lane 3). Concomitant with the oxidation of PsbO, oxidized LTO1_{sol} was converted to its reduced form (Figure 22B, lane 3), an expected finding if LTO1_{sol} catalyzes disulfide bond formation. Quantification of the oxidized and reduced species indicates that one molecule of reduced PsbO2 was acted upon by one molecule of oxidized LTO1. It should be noted that, even though DTT-treatment fully reduced PsbO2, a small fraction of reduced PsbO2 can become re-oxidized, presumably because of traces of oxygen present in solution (Figure 22B, lane 2). Based on our redox assays, we conclude that the thioredoxin-like domain of LTO1 can catalyze disulfide bond formation in the PsbO2 target.

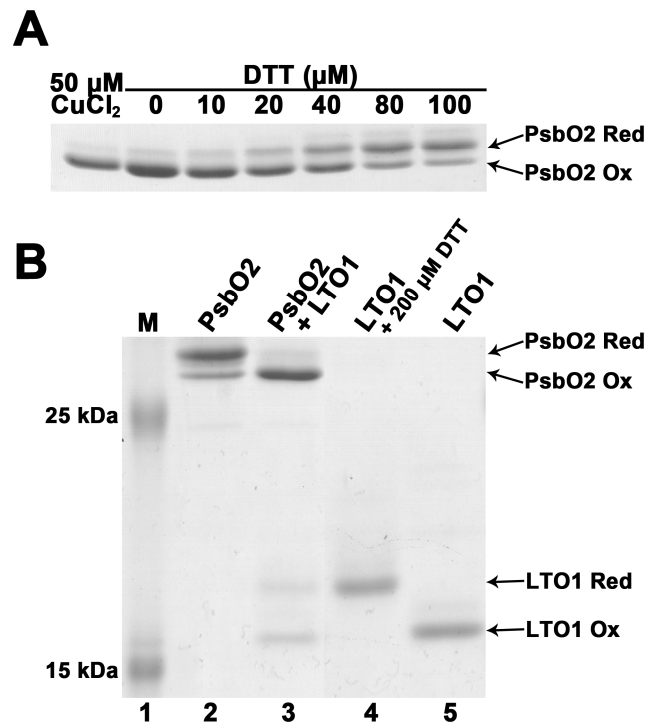


Figure 22 - The thioredoxin-like domain of LTO1 catalyzes disulfide bond formation in PsbO2. Recombinant proteins (PsbO2 and the thioredoxin-like domain of

LTO1) were treated with 4-acetamido-4'-maleimidylstilbene-2,2'-disulfonic acid (AMS), separated by non-reducing SDS-PAGE (15%) and visualized by Coomassie Brilliant Blue R-250 staining. The positions of reduced (*PsbO2 Red*) and oxidized (*PsbO2 Ox*) forms of PsbO2 and reduced (*LTO1 Red*) and oxidized (*LTO1 Ox*) forms of LTO1 are indicated by arrows. AMS is an alkylating reagent and AMS treatment of exposed thiols in PsbO2 and LTO1 results in an increased molecular mass of the alkylated molecules. Only reduced PsbO2 or LTO1 reacts with AMS. *A, DTT-dependent reduction of the disulfide in PsbO2.* Lane (1), recombinant PsbO2 was fully oxidized by incubation with 50 μM CuCl_2 . Lanes (2 to 7), air-oxidized PsbO2 was reduced by 1 h incubation with increasing concentrations of DTT. *B, LTO1-dependent oxidation of PsbO2 sulfhydryls.* Prestained protein ladder (Fermentas) was used in lane (1). Lane (2), reduced PsbO2 after removal of DTT ; lane (3), reduced PsbO2 (10 μM) mixed with oxidized LTO1 thioredoxin-like domain (16 μM) ; lane (4), DTT-reduced LTO1 thioredoxin-like domain, and lane (5), air-oxidized LTO1. Quantification using ImageJ software indicates that 72% of reduced PsbO2 (7.2 μM) becomes oxidized, whereas 44% of oxidized LTO1 (7.04 μM) is converted to its reduced form.

Discussion

The plastid VKOR-like protein defines a trans-thylakoid thio-oxidation pathway

In this paper, we have explored the function of LTO1, a plastid VKOR-like protein in *A. thaliana*. In plastids, VKOR-like proteins are present at the thylakoid membrane and carry a C-terminal, thioredoxin-like domain typical of that found in oxidoreductases belonging to the protein disulfide isomerase (PDI) family (Ellgaard and Ruddock, 2005). By analogy to VKOR in the ER, a plastid VKOR-like protein is presumed to participate in a transmembrane thio-oxidation pathway. One key question in terms of deducing the function of a plastid VKOR-like protein is to define its topological arrangement within the thylakoid membrane, particularly with respect to the domains predicted to catalyze redox chemistry. Using bacterial topological reporters, a luminal localization was assigned for the two cysteine pairs present in the VKOR-like domain and

the C-terminal thioredoxin-like domain of LTO1 (Figure 14). This result is in accord with the topological model deduced for a mycobacterial VKOR-like protein and also the crystal structure of a cyanobacterial VKOR-like protein. Both of these methods place the functional domains in the periplasm, which is analogous to the plastid lumen (Dutton et al., 2008; Li et al., 2010; Wang et al., 2011).

In proteobacteria, DsbA introduces disulfide bonds in cysteine containing targets while DsbB recycles DsbA to its oxidized form with transfer of electrons to a quinone (Depuydt et al., 2011; Kadokura and Beckwith, 2011). A role in disulfide bond formation for LTO1 is inferred from the fact that the plant protein is able to substitute for the function of DsbAB in bacteria (Figure 15). Further support for the involvement of LTO1 in sulfhydryl oxidation in the thylakoid lumen comes from our evidence that lumen resident PsbO can be oxidized by the thioredoxin-like domain of the protein in our *in vitro* assay (Figure 22). Previous studies with mycobacterial and cyanobacterial VKOR-like proteins have demonstrated that the thioredoxin-like domain carries DsbA-like activity while the VKOR-like central domain is functionally equivalent to DsbB (Singh et al., 2008; Dutton et al., 2010; Wang et al., 2011). *In vitro* assays show that the *Arabidopsis* LTO1 thioredoxin-like domain can transfer electrons to its VKOR-like central domain (Furt et al., 2010). This supports the view that the plastid protein operates in a manner similar to bacterial VKOR-like proteins in regard to thiol-disulfide chemistry.

As seen with bacterial VKOR-like proteins, it is expected that the sulfhydryl oxidizing activity of LTO1 is linked to the reduction of a quinone in the thylakoid membrane (Li et al., 2010). *In vitro* enzymatic assays indicate that the *Arabidopsis* VKOR-like protein is active in reducing phyloquinone but not plastoquinone, two

quinones found in plastids (Furt et al., 2010). The role of phylloquinone as a structural co-factor tightly bound to PSI is well documented (Brettel, 1997). However, it is unclear if phylloquinone participates in redox processes in addition to the known electron transfer reactions through PSI (Gross et al., 2006; Lohmann et al., 2006).

The redox activity of LTO1 is required for the assembly of PSII

Detailed phenotypic analysis of the *Arabidopsis lto1* mutant revealed that the function of the plastid VKOR-like protein is required for accumulation of PSII, a photosynthetic complex involved in the light-dependent reactions of photosynthesis (Figure 16 to Figure 20). Moreover, analysis of the decay of variable fluorescence after a 1-ms flash in the presence of the Q_B site inhibitor, DCMU [3-(3,4-dichlorophenyl)-1,1-dimethylurea] was consistent with the idea that there was a higher amount of PSII reaction centers with damaged OECs in the *lto1* mutant (Supplemental Figure 5 online). We reasoned that catalysis of a disulfide bond in a luminal target is a required step for the biogenesis of PSII. Interestingly, PsbO, a luminal subunit of PSII required for stable assembly of the OEC was shown to carry a single intramolecular disulfide that is strictly conserved in cyanobacteria and photosynthetic eukaryotes. *In vitro* studies established that this disulfide bond is critical to maintain the tertiary structure of PsbO (Tanaka et al., 1989; Betts et al., 1996; Wyman and Yocum, 2005). In chloroplast luminal extracts, reduction of the disulfide in PsbO1 and PsbO2 targets the proteins for degradation. This indicates that the oxidation state of the cysteines is a key determinant for the subunit stability *in vivo* (Hall et al., 2010). Further underscoring the importance of this disulfide, a mutation of one of the conserved cysteines in cyanobacterial PsbO results in complete loss of the subunit and yields a PSII defect (Burnap et al., 1994). In *Arabidopsis*, loss of

PsbO1 and PsbO2 impacts the stability of both extrinsic components of the OEC and core components of the reaction center (Yi et al., 2005). The resulting phenotype is similar to the one displayed by the *lto1* mutant lines (Figure 18). Considering that PsbO is a relevant target of LTO1 activity (Figure 22) and that the redox state of the sulfhydryls appears to be determinant for the stability of this subunit (Burnap et al., 1994; Hall et al., 2010), it is conceivable that the PSII assembly deficiency in the *lto1* mutant is caused by a sole defect in the oxidation of PsbO sulfhydryls. However, there are proteins required for PSII biogenesis that also have a disulfide bond, such as FKBP20-2, a lumen resident molecule (Lima et al., 2006). Therefore, we cannot rule out the possibility that additional factors might also contribute to the PSII deficient phenotype in the *lto1* mutant.

It is interesting that the fluorescence induction phenotype of the *lto1* mutant strongly resembles that of *Arabidopsis* mutants with low amounts of functional PsbO protein. The quantum yield of PSII fluorescence is decreased significantly in mutants of *PSBO1* (Murakami et al., 2002) and in RNAi mutants largely lacking both PsbO1 and PsbO2 (Yi et al., 2005). However, the PSII maximal quantum yield in the *lto1* mutant and in the *psbO* mutants is not as low as in mutants completely lacking PSII, where it effectively becomes zero (Bennoun et al., 1986). Moreover, in the *psbO-1* mutant, Murakami et al. found that the fluorescence level transiently dropped below the F_0 level during illumination, similar to what we saw in the *lto1* mutant (Murakami et al., 2002) (Figure 17). This phenomenon is not limited to *psbO* mutants, as it was also seen recently with mutants in the cytochrome b_{559} subunit of PSII (Bondarava et al.). One possibility is that the PQ pool is partially reduced in the dark in the *lto1* mutant, and in other mutants with low PSII activity, which would result in an increased F_0 level. Upon illumination,

PSI activity overwhelms PSII activity (due to the PSII deficiency) and the PQ pool becomes more oxidized, resulting in a fluorescence level lower than the dark level. We suggest that in such mutants, the cyclic electron flow pathway has been activated. This would allow the mutants to use PSI and cytochrome *b₆f* to pump protons and thereby synthesize ATP, in the absence of significant levels of linear electron flow due to the deficiency in PSII. This would explain both the elevated F_0 level and the fact that P_{700}^+ is re-reduced much faster in the *lto1* mutants compared to wild type (Supplemental Figure 2 online), an expected finding if cyclic electron transfer is elevated (Finazzi and Forti, 2004; Iwai et al., 2010; Peeva et al., 2010).

Are there other relevant targets of LTO1 sulfhydryl oxidizing activity?

The *lto1* mutant characterized during this study is a knock-down and additional defects could be revealed in conditions of complete loss of LTO1 function (Figure 16). Conceivably, LTO1 regulates the redox state of additional cysteine containing proteins residing in the thylakoid lumen. An indication that further targets exist comes from the observation that a cyanobacterial VKOR-like null mutant displays a pleiotropic growth defect incompatible with a sole defect in PSII (Singh et al., 2008). However, it is not known if this phenotype can be attributed to impaired disulfide bond formation in targets residing in the thylakoid lumen and/or in the periplasm. Other possible targets of LTO1 are proteins containing lumen-facing cysteines, which are active in the oxidized form. Only a few luminal proteins with known thiol-dependent enzymatic activities have been identified. Examples of such are violaxanthin de-epoxidase, an enzyme involved in dissipating excess light (Yamamoto and Kamite, 1972; Sokolove and Marsho, 1976), STT7/STN7, a kinase involved in adaptation to changes in light intensity (Depege et al.,

2003; Lemeille et al., 2009), and FKBP13, a prolyl isomerase postulated to act as a foldase for the Rieske protein (Gupta et al., 2002; Gopalan et al., 2004). It has now become apparent that thiol-disulfide chemistry is a catalyzed process not only restricted to bacterial energy-transducing membranes but operating also on the luminal side of the thylakoid membrane. Further genetic and biochemical dissection is needed to elaborate the thiol-metabolizing pathways and understand how they regulate the biogenesis of the thylakoid compartment.

Methods

Bacterial strains and growth media

Strains HK295 ($F^- \Delta ara-714 galU galK \Delta(lac)X74 rpsL thi$) (Kadokura and Beckwith, 2002) and HK329 (HK295 $\Delta dsbA \Delta dsbB$) (Eser et al., 2009) were a kind gift from Jonathan Beckwith. Luria-Bertani (LB) broth, LB agar and MacConkey agar were prepared as described previously (Silhavy et al., 1984). When indicated, ampicillin (50 $\mu\text{g/ml}$) and L-arabinose were used.

Heterologous complementation of the *dsbAB* mutant

The *LTO1* ORF was cloned, using the In-FusionTM system (ClonTech), into the arabinose inducible vector pBAD24 (Guzman et al., 1995) at *NcoI* and *SphI* sites to create plasmid pLTO200. Primers used for In-FusionTM cloning and sequencing of the resulting plasmids are listed in Table of primers (Supplemental methods online). The pBAD24 and pLTO200 plasmids were introduced into the $\Delta dsbAB$ HK329 strain and transformants assessed for complementation of motility and alkaline phosphatase (PhoA) deficient phenotypes. For motility tests, 10 μL of an overnight culture grown in M9

medium was inoculated into the center of an M9 medium plate (0.25% agar), with or without 0.002% arabinose. Plates were incubated overnight at 37°C and complementation of the motility phenotype was quantified by measuring the diameter of the swarm in centimeters using a metric ruler. Ten plates were measured for both the control pBAD24 and pLTO200 in both plus and minus arabinose conditions. The PhoA activities were measured as described in (Manoil, 1991) using overnight cultures in M9 medium, with or without arabinose.

Efficiency of plating assay

Strains HK295 (pBAD24), HK329 (pBAD24), and HK329 (pLTO200) were grown at 37°C overnight in LB broth supplemented with ampicillin. Cultures were serially diluted 1:10 in LB broth and about 2 µL of these dilutions were spotted onto LB agar and MacConkey agar either lacking or containing L-arabinose (0.2 %). Plates were incubated overnight at 37°C. EOP (efficiency of plating) values were calculated with respect to the growth of the wild-type strain HK295 (pBAD24) on LB agar.

Topological analysis of LTO1 via PhoA/LacZ α sandwich fusions

Four PhoA/LacZ α sandwich fusion constructs (pLTO212-pLTO215) were generated using In-FusionTM recombination with three PCR products as described in (Zhu et al., 2007). PCR products were generated using the *LTO1* cDNA or the complete PhoA/LacZ α fusion cassette in pMA650 as templates (Alexeyev and Winkler, 1999). The PCR products were then cloned into the isopropyl 1-thio- β -D-galactopyranoside (IPTG) inducible expression vector pMA657 (Alexeyev and Winkler, 1999) cut by *Bam*HI and *Xba*I. The pLTO211 plasmid was also generated by using In-FusionTM recombination at

SpeI in pLTO210, which was constructed by In-Fusion™ recombination of the *LTO1* ORF into pMA657. PhoA activity measurements were performed as in (Manoil, 1991). On the same cultures, LacZ activity measurements were performed as described in (Brickman and Beckwith, 1975). The leaky nature of the *lac* promoter allowed measurements to be performed without IPTG induction.

Yeast Two-hybrid Experiments

The soluble domain of LTO1 (Gln₂₄₇ to Gln₃₇₆) was used as bait, and the corresponding sequence was cloned *via* the In-Fusion™ technique (Clontech) as a PCR fragment at the *NdeI/SalI* sites of the pGBKT7 vector. The sequence corresponding to the soluble domain of wild-type LTO1 was PCR-amplified using LTO1-BD-F (5'-GATCTCAGAGGAGGACCTGCAACAACCAATCCCTTCACGC-3') and LTO1-BD-R (5'-TGCGGCCGCTGCAGGTCGACGCTGAAGTTGATT

GGTCTC-3') as primers and the *Arabidopsis LTO1* cDNA from the *Arabidopsis* Biological Resource Center (ABRC, The Ohio State University, OH, USA) (#U25043) as template. Plasmids expressing the mutant form of LTO1 (WCSHS) were constructed via the QuickChange II site-directed mutagenesis kit (Stratagene). *Arabidopsis* PsbO1 and PsbO2 (Ser₃₀ to Glu₃₃₂) or (Ser₂₉ to Glu₃₃₁) respectively, were used as prey, and the corresponding sequences were cloned *via* In-Fusion™ as a PCR fragment at the *NdeI/XhoI* of the pGADT7 vector. The sequence corresponding to PsbO1 was PCR-amplified using PsbO1-AD-F (5'-CGACGTACCAGATTACGCTCAATCGACTCAAGCCGTCGGC-3') and PsbO1-AD-R (5'-CGATTCATCTGCAGCTCGAGCCTCAAGTTGACCATAACCACAC-3') and the sequence corresponding to PsbO2 was PCR-amplified using PsbO2-AD-F (5'-

BL21(DE3) strain (Novagen) carrying pET24b- PsbO2 or pET24b-LTO1opt was grown from a 20-mL LB broth overnight starter culture. To induce the recombinant proteins, IPTG was added to a final concentration of 0.5 mM at $A_{600} = 0.4$ and the cultures were further grown for 3 h at 37°C. Cells were then harvested by centrifugation at 4,000 X g for 20 min at 4°C, and the pellet was stored at -20°C. Batch purification of the His₆-tagged proteins was performed under denaturing conditions (6 M urea) using nickel-nitrilotriacetic acid resin (Qiagen). Recombinant PsbO2 and LTO1 were dialyzed in a refolding buffer (25 mM Tris, pH 7.5) and stored at -80 °C.

PsbO2 in 25 mM Tris-HCl (pH 7.5) was reduced by 200 μM DTT during 1 h on ice. DTT was eliminated by buffer exchange using the Amicon Centriprep system (Ultracel-10 membrane, Millipore). Reduced PsbO2 (10 μM) in 25 mM Tris-HCl (pH 7.5) was incubated for 60 min at 25°C in the absence or presence of oxidized soluble LTO1 (16 μM) in 25 mM Tris-HCl (pH 7.5). After incubation, proteins were precipitated with trichloroacetic acid (final 5%), washed with ice-cold acetone, and then dissolved in buffer containing 50 mM Tris-HCl (pH 6.8), 2% SDS, 10 mM 4-acetamido-4'-maleimidylstilbene-2,2'-disulfonic acid (AMS). After a 90-min incubation, reduced (AMS derivative) and oxidized forms of PsbO2 and LTO1 were separated by 15% non-reducing SDS-PAGE and visualized by Coomassie staining

Growth of *A. thaliana*

The *Col-0* ecotype of *A. thaliana* was used as the wild type (WT). The T-DNA lines SALK_151963C (*lto1*) were provided as confirmed homozygotes by ABRC. Seeds were surface-sterilized and sown on Murashige and Skoog plates (with or without 2% sucrose) or on soil, and stratified at 4°C for 48 h in the dark before germination. Plants

were grown in controlled-environment chambers at a room humidity of 50% and provided daily with 16 h of light ($80\text{-}120 \mu\text{E m}^{-2} \text{s}^{-1}$) and 8 h of dark at 22°C .

Molecular characterization of the *lto1* mutant lines

The SALK_151963C (*lto1*) line was analyzed for the presence and orientation of the T-DNA via PCR using genomic DNA as a template and the following primer pairs: S-Exon1D (5'-ATGGAAACCACTGCTTTTAAC-3') and Exon2R (5'-TCAGATGAAGAACATTTAATC-3'); RB1 (5'-AGTGTTTGACAGGATATATTG-3') and Exon2R (5'-TCAGATGAAGAACATTTAATC-3'); RB1 (5'-AGTGTTTGACAGGATATATTG-3') and Stop (5'-TTACTGAAGTTGATTGGTCTC-3'); LB1 (5'-GCGTGGACCGCTTGCTGCAACT-3') and S-Exon1D (5'-ATGGAAACCACTGCTTTTAAC-3').

RNA extraction and RT-PCR

The leaves of 21-day-old *lto1* and wild-type plants propagated on soil were used for total RNA isolation (Iratni et al., 1997). One microgram of DNase I-treated RNA was reverse transcribed using 200 units of Superscript II reverse transcriptase (Invitrogen) according to the manufacturer's protocol. The reaction was performed in the presence of 1 μL of 100 μM Oligo(dT)₁₈ in a total volume of 15 μL at 42°C for 50 min. Aliquots (1 μL) were used as template for the PCR reaction with *LTO1*-specific primers Exon1D (5'-ATGATGGCGAGGTTTGTCTG-3') and Stop (5'-TTACTGAAGTTGATTGGTCTC-3'), *SENI*-specific primers S-Exon1D (5'-ATGGAAACCACTGCTTTTAAC-3') and S-Stop R (5'-TCACTCTTCTACCGGCAGCTC-3'), and *TUB2*-specific primers TUB2-F (5'-CTCAAGAGGTTCTCAGCAGTA-3') and TUB2-R (5'-TCACCTTCTTCATCCGCAGTT-3'). PCR amplification products were separated by

electrophoresis in agarose gel and ethidium bromide stained. The gel was imaged using an imaging system.

Plasmids for Plant Transformation

For the complementation experiments, the *LTO1* full-length cDNA (#U25043) was obtained from ABRC. The *LTO1* coding sequence (excluding the stop codon) was amplified by PCR with platinum *Pfx* DNA polymerase (Invitrogen) using the primers pENT/LTO1-F (5'-CACCATGATGGCGAGGTTTGTTC-3') and pENTR/LTO1-R (5'-CTGAAGTTGATTGGTCTCATTTGCC-3'). The amplified product was cloned using Gateway Technology into the pENTR/D-TOPO vector (Invitrogen), and then transferred into the pGWB20 destination vector (Dr. T. Nakagawa, Shimane University, Matsue, Japan) previously linearized by *Xho*I. The resulting plasmid (p35S-*LTO1-C-MYC*) was transferred to *Agrobacterium tumefaciens* GV3101 by electroporation. The *lto1* plants were transformed using the floral dip method (Clough and Bent, 1998) and selection of the T1 generation of transgenics was performed on Murashige and Skoog plates with kanamycin (30 $\mu\text{g}\cdot\text{mL}^{-1}$) and hygromycin B (30 $\mu\text{g}\cdot\text{mL}^{-1}$). Seedlings were transplanted onto soil two weeks after germination and grown in controlled-environment chambers.

Protein preparation and analysis

Total plant protein extracts were prepared following the method described in (Hurkman and Tanaka, 1986) and protein concentrations were determined by using the Bio-Rad DC Protein Kit (with BSA as a standard). Total protein was extracted with a SDS containing solubilization buffer, and chlorophyll concentration was then determined. When necessary, Coomassie-stained gels were used to assess equal loading. For

immunoblot analyses, the proteins were separated by SDS-PAGE, blotted onto Immobilon-P membranes (Millipore), and immunodecorated with antibodies. Commercially available antibodies against plastocyanin, PsaA, D1, D2, PsbD, PsbO, PsbP, PsbQ (Agrisera), and C-myc (Sigma) were used. The anti-PetC and anti-PetD antibodies were provided by Dr. Barkan (U. of Oregon). Antisera against cytochrome *f*, cytochrome *b₆*, cytochrome *b₅₅₉*, and MFP1 were gifts from Dr. Merchant (UCLA), Dr. deVitry (CNRS), Dr. Meiherrhoff (Heinrich-Heine-Universität), and Dr. Meier (Ohio State University), respectively.

Fusion	Position	LacZ	PhoA	Topology
1	74	73 (± 22)	4 (± 3)	<i>n</i> -side
2	113	19 (± 4)	78 (± 7)	<i>p</i> -side
3	191	16 (± 7)	40 (± 5)	<i>p</i> -side
4	195	14 (± 8)	80 (± 5)	<i>p</i> -side
5	573	19 (± 6)	1269 (± 28)	<i>p</i> -side

Table 3 - Topological analysis of *Arabidopsis* LTO1 from PhoA and LacZ fusion analysis. Measurements of alkaline phosphatase (PhoA) and β -galactosidase (LacZ) activities of sandwich fusions at the indicated positions within LTO1. Measurements were taken on at least two separate bacterial clones and correspond to an average of three representative measurements. The \pm S.D. is indicated for those measurements. Fusion numbers correspond to those indicated in **Figure 14**. Values are expressed in arbitrary units for LacZ and Miller units for PhoA. The *p*-side corresponds to the bacterial periplasm and the lumen of the chloroplast, while the *n*-side corresponds to the bacterial cytoplasm and the stroma of the chloroplast.

Fluorescence induction

A freshly cut leaf was placed in the leaf cuvette of a JTS-10 LED spectrometer (Bio-Logic, France). Fluorescence emission was measured by using a 10- μ s pulse of light

from a 520-nm LED as the excitation source, and a 670-nm high-pass filter was placed in front of the sample detector. A BG39 filter was placed in front of the reference detector to measure the excitation pulse, allowing proper normalization of fluorescence emission. Actinic light and saturating pulses were provided by a 520-nm LED array. Before each run, leaves were allowed to dark adapt for 30-60 s followed by a 2-s treatment with far-red light (743 nm peak with full width at half maximum of 30 nm; photon flux = 25 mmol m⁻² s⁻¹) to drive complete oxidation of the PQ pool. At each time point, fluorescence was measured (F_0 or F_0'), followed immediately by an 80-ms saturating pulse to fully oxidize the PQ pool, and then fluorescence was measured 100 μ s after the pulse was over (F_M or F_M'). The first pair of points should thus provide F_0 and F_M . The actinic light was turned on 100 ms later, fluorescence measurements were taken 2 s after that, and then 24 more pairs of measurements were taken in an exponentially-spaced fashion for 2 minutes total. The actinic light was turned on 100 ms later, fluorescence measurements were taken 2 s after that, and then 24 more pairs of measurements were taken in an exponentially-spaced fashion for 2 minutes total. The actinic light was then extinguished, and 24 more time points were taken every 20 s. Note that the actinic light was briefly turned off while fluorescence measurements were made: at each time point, the actinic light was turned off, the F_0' measurement was taken 100 μ s later, the 80-ms saturating pulse was given 20 μ s later, and then 100 μ s later the F_M' measurement was taken, 20 μ s after which the actinic light was turned back on. Thus, all fluorescence measurements were taken in the absence of any light beside the excitation source, avoiding complications or the necessity of subtraction of additional signals induced by the actinic or saturating lights. We found that F_M' after 2 s of actinic light was slightly

higher (~4%) than F_M in the wild type case, indicating that the 80-ms pulse is not completely saturating. The difference was greater in the case of the *lto1* mutant, consistent with the idea that it has a smaller antenna size. Thus, for the purposes of normalization of the data shown in Figure 17, we used the F_M' value measured at 2 s, which was the highest fluorescence value measured in all cases.

Strain	Medium	$F_V/F_M (\pm SD), n = 5$
Wild type	MS	0.828 ± 0.007
<i>lto1</i>	MS	0.581 ± 0.068
<i>lto1 + LTO1</i>	MS	0.831 ± 0.005
Wild type	MS + Suc	0.815 ± 0.008
<i>lto1</i>	MS + Suc	0.522 ± 0.113
<i>lto1 + LTO1</i>	MS + Suc	0.828 ± 0.003

Table 4 - Efficiency of plating on MacConkey agar of dsbAB strains expressing *Arabidopsis* LTO1. ^a EOP (efficiency of plating) values were calculated with respect to the growth of the wild-type strain HK295 (pBAD24) on LB agar containing ampicillin. Amp = ampicillin, Mac = MacConkey, Ara = arabinose

Accession numbers

Sequence data from this article can be found in the EMBL/GenBank data libraries under accession numbers ACN43307 and ACN43308 for *Chlamydomonas reinhardtii* *LTO1* cDNAs and accession numbers AAM65737 for *Arabidopsis LTO1* cDNA.

Acknowledgments

This work is supported by a Muscular Dystrophy Association (4727) grant, a National Science Foundation grant (MCB-0920062) to P.H., a M. Russell technology grant to S.C. and by a grant (DE-FG02-98ER20314MOD012) to K.R. from the Division

of Chemical Sciences, Geosciences, and Biosciences, Office of Basic Energy Sciences of the U.S. Department of Energy . We thank Dr. T.M. Bricker for the gift of antibodies, Dr. Lamb for critical reading of the manuscript and Rebecca Davis for performing the experiments shown in Figure 15D. We are also grateful the *Arabidopsis* Biological Resource Center at Ohio State for the *Arabidopsis LTO1* cDNA.

	Wild Type	<i>lto1</i>
Actinic Light Intensity	Average \pm SD, $n = 6$	Average \pm SD, $n = 8$
170 $\mu\text{E m}^{-2} \text{s}^{-1}$		
F_V/F_M	0.81 \pm 0.01	0.49 \pm 0.11
NPQ	1.17 \pm 0.08	0.90 \pm 0.79
1400 $\mu\text{E m}^{-2} \text{s}^{-1}$		
F_V/F_M	0.80 \pm 0.01	0.48 \pm 0.11
NPQ	1.370 \pm 0.06	1.82 \pm 1.15
Photoinhibition (%)	6.0 \pm 1.3	9.9 \pm 1.9

Table 5 - Quantum efficiency, non-photochemical quenching and photoinhibition in wild-type and *lto1* lines. Fluorescence parameters F_V/F_M (maximum quantum yield of PSII), NPQ (nonphotochemical quenching) and photoinhibitions were calculated based on fluorescence measurements like those shown in **Figure 17** using formulae described in (Rohacek and Bartak, 1999). $F_V/F_M = (F_M - F_0)/F_M$, where F_0 is the initial fluorescence emission after dark adaptation and immediately before a saturating pulse, F_M is the maximal fluorescence emission immediately after the saturating pulse, and the variable fluorescence parameter, $F_V = F_M - F_0$. $\text{NPQ} = (F_M - F_M')/F_M'$, where F_M' is the maximal fluorescence emission after adaptation to the actinic light (after 2 minutes). $\text{Photoinhibition} = 1 - (F_V''/F_M'')/(F_V/F_M)$, where F_V'' and F_M'' are the maximal and variable fluorescence, respectively, after 2 minutes exposure to 1400 $\mu\text{E m}^{-2} \text{s}^{-1}$ actinic light followed by 8 minutes of dark recovery (i.e., irreversible loss of quantum efficiency).

Table 4. Quantum Efficiency of Wild-Type, *lto1*, and *LTO1*-Complemented *lto1* Lines

Strain	Medium	$F_V/F_M (\pm SD), n = 5$
Wild type	MS	0.828 ± 0.007
<i>lto1</i>	MS	0.581 ± 0.068
<i>lto1 + LTO1</i>	MS	0.831 ± 0.005
Wild type	MS + Suc	0.815 ± 0.008
<i>lto1</i>	MS + Suc	0.522 ± 0.113
<i>lto1 + LTO1</i>	MS + Suc	0.828 ± 0.003

Table 6 - Quantum efficiency of wild-type, *lto1* and *LTO1*-complemented *lto1* lines. Maximum quantum yield of PSII (F_V/F_M) was measured as described in Table 3 and Methods. Each type of plant was grown from seeds on MS or MS + 2% sucrose medium under moderate light ($\sim 80 \mu\text{mol PAR photons m}^{-2} \text{s}^{-1}$). Leaves from five separate plants were removed and immediately assayed.

Chapter 4: The ARG9 gene encodes the plastid resident N-acetyl ornithine aminotransferase in the green alga

Chlamydomonas reinhardtii

¹Claire Remacle, ²Sara Cline, ¹Layla Boutaffala[#], ²Stéphane Gabilly,
^{1,2}Véronique Larosa, ²M. Rosario Barbieri, ¹Nadine Coosemans,
²Patrice P. Hamel*

Eukaryotic Cell September 2009 vol. 8 no. 9 1460-1463

¹ Genetics of Microorganisms Laboratory, Department of Life Sciences, Université de Liège, B-4000, Liège, Belgium

²Department of Plant Cellular and Molecular Biology and Department of Molecular and Cellular Biochemistry, The Ohio State University, 43210, Columbus, OH, USA

[#] Present address: Université de Liège GIGA-R / Virologie – Immunologie, B-4000, Liège, Belgium

* To whom correspondence should be addressed:

Patrice Hamel: The Ohio State University, 500 Aronoff Laboratory, 318 W. 12th Ave., Columbus, OH 43210. Phone: (614)-292-3817; Fax: (614)-292-6345 ; E-mail: hamel.16@osu.edu.

AUTHOR CONTRIBUTIONS: P.H., and C.R. designed the experiments, analyzed the data, and wrote the article. S.C. performed the genetic and phenotypic analysis of chloroplast transformants. All other authors contributed equally to additional experiments.

Abstract:

Here we report the characterization of the *Chlamydomonas reinhardtii* ARG9 gene

which encodes the plastid resident N-acetyl ornithine aminotransferase involved in arginine synthesis. Integration of an engineered *ARG9* cassette in the plastid chromosome of the nuclear *arg9* mutant restores arginine prototrophy. This suggests that *ARG9* could be used as a new selectable marker for plastid transformation.

Identification of the *ARG9* mutation

In the green alga *Chlamydomonas reinhardtii*, the *arg9-1* and *arg9-2* mutations result in arginine auxotrophy because of a deficiency in N-acetyl-ornithine aminotransferase activity (NAOAT) (Loppes and Heindricks, 1986). Out of the two *arg9* mutants originally isolated (Loppes and Heindricks, 1986), only the *arg9-2* strain was found to be an arginine auxotroph while the *arg9-1* mutation has reverted to wild type. We reasoned that the *arg9-2* mutation mapped to the structural gene for NAOAT and identified a candidate *ARG9* gene ([XP_001698091](#)) based on the similarity of the predicted gene product to *Saccharomyces cerevisiae* NAOAT, Arg8p. Three full length cDNAs were identified and sequenced (accession number [EU711276](#)). Both the *ARG9* genomic DNA and full-length cDNAs restored arginine prototrophy when introduced in the *arg9-2* mutant (not shown). Sequencing the *ARG9* genomic locus in the *arg9-2* strain identified a G to A transition at codon 317 resulting in a glycine to arginine mutation at a strictly conserved residue in NAOATs.

Results

Functional Confirmation of *ARG9*

Next, we tested if *Chlamydomonas ARG9* could functionally replace the Arg8 protein in yeast by expressing the *ARG9* cDNA in an *arg8*-null mutant that is deficient in

NAOAT. Figure 23 shows that expression of the *ARG9* cDNA from the plasmid-born *PGK1* promoter is able to partially restore arginine prototrophy. Since the yeast *arg8* mutant can be complemented by the *Chlamydomonas* ARG9 protein, it is likely that the algal protein expressed in yeast is targeted to the mitochondria where NAOAT typically functions in fungi (Slocum, 2005). Indeed, the N-terminal extension of the candidate ARG9 protein exhibits features typical of a plastid or mitochondria targeting sequence, such as the propensity to form an amphiphilic α -helix (Neupert and Herrmann, 2007).

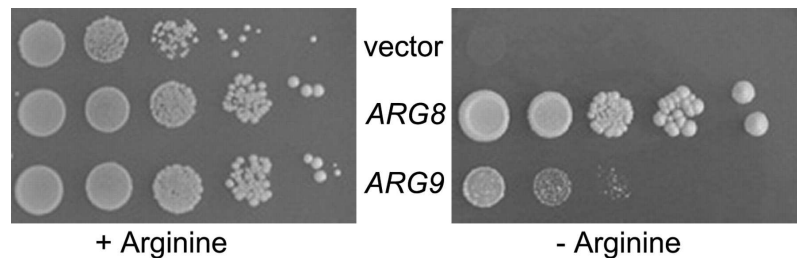


Figure 23 - Heterologous functional complementation of the *S. cerevisiae* *arg8* mutant by the *C. reinhardtii* ARG9 cDNA encoding NAOAT. The yeast *arg8* mutant (NB880) was transformed by yeast expression vector pFL61 (vector), pFL61/*ARG8* expressing the yeast *ARG8* gene (*ARG8*) and pFL61/*ARG9* expressing the *Chlamydomonas* *ARG9* cDNA (*ARG9*). Dilution series (10X) of each transformant were plated on synthetic complete medium with or without arginine and incubated at 28°C for 7 days or 14 days, respectively.

Localization of ARG9

The sublocalization of the ARG9 protein was examined by immunoblot analysis using an antibody raised against Arg8p, the *S. cerevisiae* NAOAT that is resident in the mitochondrial matrix. The anti-Arg8p antibody cross-reacted with species in mitochondrial and plastid fractions of *Chlamydomonas* cells (Figure 24). We identified the 48 kDa species in the plastid fraction as the ARG9 protein based on the predicted size

of the mature protein. This species was also present in the *arg9-2* strain suggesting that the *arg9-2* mutant accumulates a non functional ARG9 protein. The cross-reacting species detected in the mitochondrial fraction are of higher electrophoretic mobility and could correspond to non-specific bands or splicing variants of the *ARG9* transcript that specify a mitochondrial protein or dual targeted ARG9 protein. Complementation experiments described below indicate that the primary site of action of ARG9 is the plastid. Based on our analyses, we concluded that NAOAT is located in the plastid in *Chlamydomonas* but cannot exclude the possibility that it also operates in the mitochondrion. The operation of plastid localized enzymes involved in arginine biosynthesis in *Chlamydomonas* is also supported by studies suggesting that argininosuccinate lyase (ASL) could also be resident in the chloroplast (Auchincloss et al., 1999)

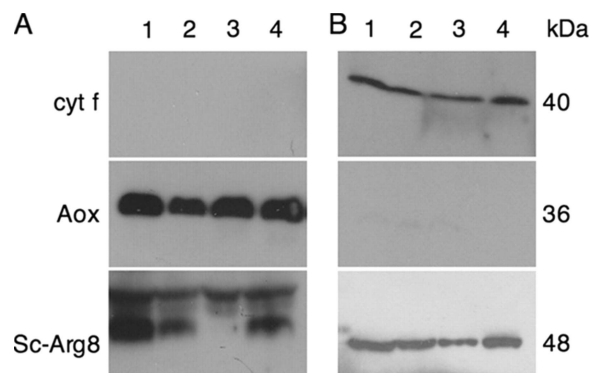


Figure 24 - ARG9 localizes to the plastid in *Chlamydomonas*. Proteins from mitochondria (A) and chloroplast (B) enriched fractions were separated by SDS-PAGE and immobilized on a nylon membrane. The membrane was immunodecorated using antibodies against Arg8p, Aox or cytochrome *f*. The purity of each fraction was verified by using an antibody against a known protein resident in the mitochondria (Aox) or in the chloroplast (Cyt *f*). 1 to 3: *arg9-2* transformants complemented by the genomic *ARG9* and 4: *arg9-2* mutant.

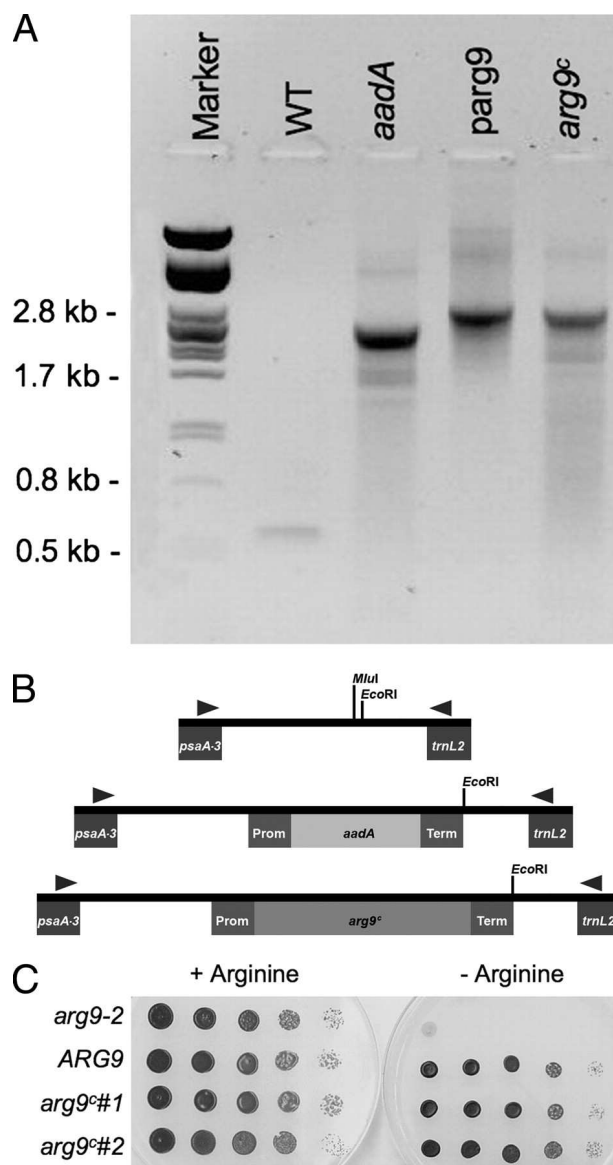


Figure 25 - Plastid transformation of the *arg9-2* strain with the *arg9c* cassette restores arginine prototrophy. A. Molecular analysis of the plastid transformants was performed by PCR using diagnostic primers (F and R) lying outside the region of homology in the transforming DNA (see B). PCR amplification products were separated by electrophoresis in agarose gel and ethidium bromide stained. The gel was imaged using an imaging system (Kodak Image Station 2000R). *Pst*I-digested λ phage DNA was used as marker for size. DNA extractions from strain CC125 (WT), an *arg9-2* *Spec*^R transformant (*aadA*), an *arg9-2* Arg⁺ transformant (*arg9^c*) or plasmid *pmp-arg9^c* (*parg9*) were used as template in the PCR reaction. The *pmp-arg9^c* plasmid contains the *arg9^c* cassette and 5 kb of chloroplast DNA flanking the region of homology between the *aadA* and *arg9^c* cassette. B. Illustration of expected PCR products using the diagnostic primers

F (left arrow) and R (right arrow) and plastid DNA as templates from wild type strain (WT), Spec^R transformant (*aadA*) and Arg⁺ transformant (*arg9^c*). The neutral site lies between the *psaA-3* and *trnL2* genes on the chloroplast genome. The *Mlu*I and *Eco*RI sites used for cloning of the *aadA* cassette are indicated. The *Mlu*I site is lost in the cloning of the *aadA* cassette. The expected size for the PCR products are 600 bp (WT), 2533 bp (*aadA*) and 2971 bp (*arg9^c*). C. Growth of untransformed *arg9* mutant (*arg9-2*), *arg9-2* transformed by pARG9g containing a 7 kb genomic DNA fragment with the *ARG9* gene (*ARG9*) and two independent *arg9-2* plastid transformants expressing the *arg9^c* cassette (*arg9^c* #1 and 2) on TAP and arginine supplemented TAP medium. 4×10^6 cells for each strain were serially diluted (10 times for each dilution), plated and incubated for 4 days.

Restoration of Nuclear Mutant via Chloroplast Transformation

We reasoned that the *ARG9* gene relocated to the plastid chromosome of an *arg9-2* strain should be able to restore arginine prototrophy if the ARG9 protein is successfully expressed and active in the organelle. For this experiment, we chose the *ARG9* cDNA from *Arabidopsis thaliana*, whose nuclear genome has a codon bias (44% GC) closer to the plastid genome than the nuclear genome of *Chlamydomonas*. Moreover, the frequency of codons in the *Chlamydomonas* plastid genes made it likely that the *Arabidopsis* cDNA would be translated by the set of plastid tRNAs. Using an existing spectinomycin resistance cassette (*aadA*) for plastid transformation we designed an *arg9^c* (*c* for chloroplast) cassette for expression of the *Arabidopsis* NAOAT in the chloroplast of *Chlamydomonas* (Goldschmidt-Clermont, 1991). As a proof of concept, we first targeted the *aadA* cassette to an integration site on the plastid chromosome that is neutral with respect to chloroplast function (Hamel et al., 2003). A spectinomycin-resistant transformant (Spec^R) was generated by biolistic transformation of the *mt⁺ arg9-2* mutant (Hamel et al., 2003). The presence of the *aadA* gene at the expected location in the plastid chromosome was detected by diagnostic PCR (Figure 25AB). Next, we replaced the *aadA* cassette with the *arg9^c* cassette, which expresses the *A. thaliana* ARG9 protein

from the same promoter and terminator as the *aadA* cassette (plasmid KS/*arg9^c*) (Figure 25B). Based on our alignments of NAOATs, we reasoned that the first 48 residues of ARG9 might include the plastid targeting sequence and were therefore not necessary if ARG9 is synthesized on plastid ribosomes. Replacement of the *aadA* marker by the *arg9^c* cassette is expected to occur by homologous recombination between the *atpA* promoter and *rbcL* terminator sequences that are common to both the *aadA* and *arg9^c* cassettes (Figure 25B). The *mt⁺ arg9-2 Spec^R* strain was bombarded with the pKS/*arg9^c* plasmid and transformants were selected on medium lacking arginine. A few transformants were able to grow on the selective medium (Arg⁺) suggesting that ARG9 was successfully expressed from the plastid genome. Molecular analysis of two independent Arg⁺ transformants showed that they were heteroplasmic for the presence of the *aadA* and *arg9^c* cassettes and expectedly were also Spec^R (not shown). In a former study, we have shown that the segregation of plastid markers is facilitated if heteroplasmic transformants are converted to gametes, presumably because gametes undergo a reduction of the copy number of their chloroplast genomes (Hamel et al., 2003). To achieve homoplasmy for the *arg9^c* marker, we induced gametogenesis of two *arg9-2 Spec^R Arg⁺* plastid transformants and retrieved vegetative clones by plating the gametes on medium without arginine. Two independent clones were further analyzed and found to contain the *arg9^c* cassette using diagnostic primers lying outside the regions of homology between the *aadA* and *arg9^c* cassettes (Figure 25AB). Expectedly, the clones are still arginine prototrophs but have lost the spectinomycin resistance (not shown), indicating that they have become homoplasmic for the *arg9^c* cassette. This suggests that the *arg9^c* cassette was able to replace the *aadA* cassette in the plastid chromosome and could be

successfully expressed to complement the *arg9-2* mutation. Interestingly, we found that the level of growth on medium without arginine of the plastid transformants expressing *arg9^c* was comparable to that of nuclear transformants complemented with the *ARG9* genomic DNA (Figure 25C).

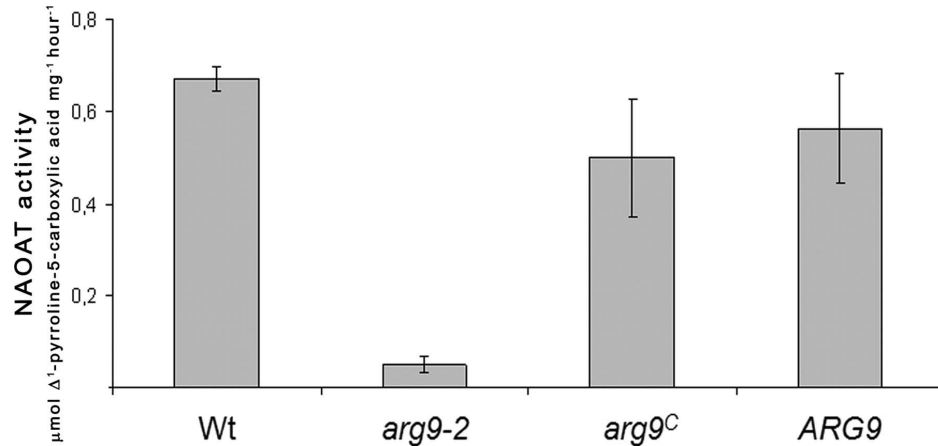


Figure 26 - Restoration of NAOAT activity in nuclear and plastid transformants. Soluble extracts of strains *cw15 mt-* (Wt), *cw- arg9-2* transformed with pARG9g (*ARG9*) and *arg9-2* transformed with the *arg9^c* cassette (*arg9^c*). Only one representative of plastid or nuclear transformant is shown. For each strain, at least three biological replicates were included in the experiments. Error bars indicate SD. The activity is expressed in μmol of Δ¹-pyrroline-5-carboxylic acid.mg⁻¹ protein⁻¹. hour⁻¹

To provide an additional proof of the successful relocation of the *arg9^c* gene to the plastid chromosome, we tested for non-mendelian segregation of the arginine prototrophy phenotype in the plastid transformants. In genetic crosses of *C. reinhardtii*, nuclear markers segregate according to Mendelian genetics, but chloroplast genes are inherited uniparentally from the *mt+* parent (Harris, 1989). Hence, it is expected that the Arg⁺ trait can only be transmitted to the progeny if the plastid transformant is of *mt+* sexual type. We crossed an Arg⁺ plastid transformant (*mt+ arg9-2 arg9^c*) to a *mt⁻ arg9-2* mutant and

performed bulk segregation of the progeny. As expected, all the 40 spores examined in the progeny were arginine prototrophs because they inherited the *arg9^c* cassette from the *mt+* parent. An Arg⁺ (*mt- arg9-2 arg9^c*) spore from this progeny was selected and diagnostic PCR confirmed the presence of the *arg9^c* cassette in the chloroplast genome (not shown). This spore was then used to do the reciprocal cross by the *mt+ arg9-2* mutant. We examined 42 spores and all of them were arginine auxotrophs as expected because the plastid trait cannot be transmitted by the *mt-* parent.

In order to show functional complementation of the *arg9^c*, we prepared cellular extracts and measured NAOAT activity in both plastid transformants and nuclear transformants complemented by the *Chlamydomonas ARG9* genomic DNA. The *arg9-2* mutation results in very little detectable NAOAT activity while the enzymatic activity was significantly restored in both nuclear and plastid transformants (Figure 26). We concluded that integration of the *A. thaliana ARG9* cDNA into the plastid chromosome of *C. reinhardtii* resulted in the successful expression of an enzymatically active NAOAT. Our results indicate that the *arg9^c* cassette could be developed as a marker for chloroplast transformation in *Chlamydomonas*. The manipulation of the chloroplast genome of microalgae for the commercial production of recombinant molecules is a recent and promising advance in the biotech industry (Purton, 2007). For obvious reasons, the use of arginine as selection for plastid transformation will be of significant value considering that all markers employed so far are derived from bacterial antibiotic resistance genes (Purton, 2007).

Proof of Concept

The *arg9-2* mutation is a non-reverting mutation ($<10^{-10}$). We took advantage of

this property and tested the effectiveness of the *ARG9* gene as a marker for insertional mutagenesis in the nucleus. In *Chlamydomonas*, integration of transforming DNA into the nuclear genome occurs via non homologous recombination events that are presumed to happen at random loci (Galvan et al., 2007). Thus, nuclear markers such as the *ARG7* gene that encodes argininosuccinate lyase (ASL) are routinely used as tool to generate insertional mutants (Galvan et al., 2007). About 3,000 arginine prototrophic transformants were generated using the *arg9-2* mutant as a recipient strain and the *ARG9* gene as a transforming DNA. Since we are interested in a separate project in isolating mutants deficient for mitochondrial function, we screened for candidate mutants on the basis of their slow growth phenotype in the dark, a phenotypic trait of complex I-minus mutants (Remacle et al., 2008). Out of 3,000 insertional transformants, two arginine prototrophs displayed a slow growth phenotype in the dark. Co-segregation of the slow growth phenotype with the Arg⁺ trait was observed suggesting that insertion of the *ARG9* gene interrupts a gene controlling respiration. However, neither mutant was deficient for complex I activity as determined by enzymatic measurement or in-gel staining (data not shown). We concluded that the slow growth phenotype is probably due to a defect in other respiratory enzymes but this was not further investigated. In conclusion, our results show that *ARG9* could also be used efficiently as an insertional marker to generate nuclear mutants of interest.

Acknowledgments

V.L. is supported by FRIA (Fonds pour la Recherche Industrielle et Appliquée). Research projects in the authors' (P.H. and C.R.) laboratories are funded by a United Mitochondrial Disease Foundation research grant, grants 2.4538.05, 2.4601.08 and

1.5.255.08 from Fonds de la Recherche Scientifique (FRS-FNRS) and R.CFRA.0931 (C.R). C.R. was supported by a sabbatical grant from FRS-FNRS during her stay at Ohio State University (Summers 2006 and 2007). We are also grateful to Drs. J. Schragger and A. Grossman (Stanford) for providing the *Chlamydomonas ARG9* cDNAs and the *Arabidopsis* Biological Resource Center for the *Arabidopsis ARG9* cDNA.

Conclusion

In conclusion, we have demonstrated here: (1) the expansion of a uniquely plastidic cytochrome *c* assembly System via the identification of CCS2, the first OPR gene to be identified by screening for a post-translational assembly process; (2) the presence of a thiol oxidant that interacts with PsbO within the oxidizing compartment of the chloroplast lumen and; (3) the malleability of the chloroplast genome via complementation of a nuclear mutant by transformation of the chloroplast.

The identification of an OPR protein involved cytochrome *c* assembly opens up a host of questions and possibilities for chloroplast bioengineering. If CCS2, like its fellow OPR family members, is found to regulate the expression of *CcsA*, it will be the first instance of the regulation of an assembly factor encoded by the chloroplast genome. This will be intriguing, as these assembly factors are traditionally believed to be largely unregulated and expressed at a constitutive basal level. If this is the case, it broaches the question: why would there be such tight regulation (noting the cytochrome *c* minus phenotype in (Figure 8 & Figure 9) on such an assembly factor. Furthermore, use of such a tightly regulated system could provide an excellent method for toxic gene expression in the chloroplast.

If CCS2 is not involved in the regulation of *CcsA*, its presence in

Chlamydomonas opens up a wholly new need in plastid biogenesis of cytochromes *cs* that has hitherto been unsuspected.

In the case of a luminal thiol-oxidase, there are many implications for such a protein. Presence of a thiol oxidant within the lumen was previously believed to be unnecessary, because of the predominance of oxidizing protons with this compartment. However, with the discovery of LTO1, we are left with many questions about the thiol-disulfide pathways within the chloroplast. For instance, is there a reducing pathway necessary for PsbO assembly like that seen in bacteria, or do eukaryotes handle the problem of free-disulfides differently than their prokaryotic counterparts? Furthermore, the presence of such a pathway opens up the doors for production of disulfide-bridge containing proteins within the lumen of plants and algae.

In work not presented here, the molecular lesion in another *ccs* allele, *ccs6*, was identified. This lesion removes three genes from the nucleus of *Chlamydomonas*. One of these genes has an ortholog in *Arabidopsis* that is co-regulated with CCS4. This introduces the intriguing possibility of a completely novel redox pathway inside the chloroplast.

Finally, in considering chloroplast genome bioengineering, we are left marvelling at the plasticity of these organelles. The ability to complement a chloroplast targeted protein by transformation of the chloroplast itself is a powerful tool that our lab already harnessed to our own benefit. This is particularly relevant in *Chlamydomonas*, as we are currently unable to perform transformations via homologous recombination within the nucleus. However, we are able to manipulate the chloroplast genome in this manner. The ability to complement nuclear mutants in this way gives us a powerful tool in dissecting

chloroplast pathways.

References

- Ahuja, U., Kjelgaard, P., Schulz, B.L., Thony-Meyer, L., and Hederstedt, L.** (2009). Haem-delivery proteins in cytochrome c maturation System II. *Mol Microbiol* **73**, 1058-1071.
- Aldridge, C., Cain, P., and Robinson, C.** (2009). Protein transport in organelles: Protein transport into and across the thylakoid membrane. *Febs J* **276**, 1177-1186.
- Alexeyev, M.F., and Winkler, H.H.** (1999). Membrane topology of the *Rickettsia prowazekii* ATP/ADP translocase revealed by novel dual pho-lac reporters. *J. Mol. Biol.* **285**, 1503-1513.
- Allen, M.D., del Campo, J.A., Kropat, J., and Merchant, S.S.** (2007). FEA1, FEA2, and FRE1, encoding two homologous secreted proteins and a candidate ferrireductase, are expressed coordinately with FOX1 and FTR1 in iron-deficient *Chlamydomonas reinhardtii*. *Eukaryot Cell* **6**, 1841-1852.
- Anbudurai, P.R., Mor, T.S., Ohad, I., Shestakov, S.V., and Pakrasi, H.B.** (1994). The *ctpA* gene encodes the C-terminal processing protease for the D1 protein of the photosystem II reaction center complex. *Proc Natl Acad Sci U S A* **91**, 8082-8086.
- Andersson, B., Aro, E.-M., Aro, E.-M., and Andersson, B.** (2004). Photodamage and D1 Protein Turnover in Photosystem II Regulation of Photosynthesis (Springer Netherlands), pp. 377-393.
- Armbruster, U., Zuhlke, J., Rengstl, B., Kreller, R., Makarenko, E., Ruhle, T., Schunemann, D., Jahns, P., Weisshaar, B., Nickelsen, J., and Leister, D.** (2012). The Arabidopsis thylakoid protein PAM68 is required for efficient D1 biogenesis and photosystem II assembly. *Plant Cell* **22**, 3439-3460.
- Aro, E.M., McCaffery, S., and Anderson, J.M.** (1993a). Photoinhibition and D1 Protein Degradation in Peas Acclimated to Different Growth Irradiances. *Plant Physiol* **103**, 835-843.
- Aro, E.M., Virgin, I., and Andersson, B.** (1993b). Photoinhibition of Photosystem II. Inactivation, protein damage and turnover. *Biochim Biophys Acta* **1143**, 113-134.
- Auchincloss, A.H., Loroach, A.I., and Rochaix, J.D.** (1999). The argininosuccinate lyase gene of *Chlamydomonas reinhardtii*: cloning of the cDNA and its characterization as a selectable shuttle marker. *Mol Gen Genet* **261**, 21-30.

- Auchincloss, A.H., Zerges, W., Perron, K., Girard-Bascou, J., and Rochaix, J.D.** (2002). Characterization of Tbc2, a nucleus-encoded factor specifically required for translation of the chloroplast *psbC* mRNA in *Chlamydomonas reinhardtii*. *J Cell Biol* **157**, 953-962.
- Bailey, T.L., and Elkan, C.** (1994). Fitting a mixture model by expectation maximization to discover motifs in biopolymers. *Proc Int Conf Intell Syst Mol Biol* **2**, 28-36.
- Balczun, C., Bunse, A., Hahn, D., Bennoun, P., Nickelsen, J., and Kuck, U.** (2005). Two adjacent nuclear genes are required for functional complementation of a chloroplast trans-splicing mutant from *Chlamydomonas reinhardtii*. *Plant J* **43**, 636-648.
- Bally, J., Paget, E., Droux, M., Job, C., Job, D., and Dubald, M.** (2008). Both the stroma and thylakoid lumen of tobacco chloroplasts are competent for the formation of disulphide bonds in recombinant proteins. *Plant Biotechnol. J.* **6**, 46-61.
- Balsera, M., Arellano, J.B., Revuelta, J.L., de las Rivas, J., and Hermoso, J.A.** (2005). The 1.49 Å resolution crystal structure of PsbQ from photosystem II of *Spinacia oleracea* reveals a PPII structure in the N-terminal region. *J Mol Biol* **350**, 1051-1060.
- Barber, J.** (2008). Crystal structure of the oxygen-evolving complex of photosystem II. *Inorg Chem* **47**, 1700-1710.
- Barbieri, M.R., Larosa, V., Nouet, C., Subrahmanian, N., Remacle, C., and Hamel, P.P.** (2011). A forward genetic screen identifies mutants deficient for mitochondrial complex I assembly in *Chlamydomonas reinhardtii*. *Genetics* **188**, 349-358.
- Becker, K., Cormann, K.U., and Nowaczyk, M.M.** (2011). Assembly of the water-oxidizing complex in photosystem II. *J Photochem Photobiol B* **104**, 204-211.
- Beckett, C.S., Loughman, J.A., Karberg, K.A., Donato, G.M., Goldman, W.E., and Kranz, R.G.** (2000). Four genes are required for the system II cytochrome *c* biogenesis pathway in *Bordetella pertussis*, a unique bacterial model. *Mol Microbiol* **38**, 465-481.
- Bellafiore, S., Ferris, P., Naver, H., Gohre, V., and Rochaix, J.D.** (2002). Loss of Albino3 leads to the specific depletion of the light-harvesting system. *Plant Cell* **14**, 2303-2314.
- Bennoun, P., Spierer-Herz, M., Erickson, J., Girard-Bascou, J., Pierre, Y., Delosme, M., and Rochaix, J.D.** (1986). Characterization of photosystem II mutants of *Chlamydomonas reinhardtii* lacking the *psbA* gene. *Plant Mol. Biol.* **6**, 151-160.
- Benz, M., Bals, T., Gugel, I.L., Piotrowski, M., Kuhn, A., Schunemann, D., Soll, J., and Ankele, E.** (2009). Alb4 of Arabidopsis promotes assembly and stabilization of a non chlorophyll-binding photosynthetic complex, the CF1CF0-ATP synthase. *Mol Plant* **2**, 1410-1424.
- Bernard, D.G., Gabilly, S.T., Dujardin, G., Merchant, S., and Hamel, P.P.** (2003).

- Overlapping Specificities of the Mitochondrial Cytochrome *c* and *c*₁ Heme Lyases. *Journal of Biological Chemistry* **278**, 49732-49742.
- Bernard, D.G., Quevillon-Cheruel, S., Merchant, S., Guiard, B., and Hamel, P.P.** (2005). Cyc2p, a membrane-bound flavoprotein involved in the maturation of mitochondrial *c*-type cytochromes. *J. Biol. Chem.* **280**, 39852-39859.
- Betts, S.D., Ross, J.R., Hall, K.U., Pichersky, E., and Yocum, C.F.** (1996). Functional reconstitution of photosystem II with recombinant manganese-stabilizing proteins containing mutations that remove the disulfide bridge. *Biochim. Biophys. Acta* **1274**, 135-142.
- Boehm, M., Romero, E., Reisinger, V., Yu, J., Komenda, J., Eichacker, L.A., Dekker, J.P., and Nixon, P.J.** (2011). Investigating the early stages of photosystem II assembly in *Synechocystis sp. PCC 6803*: isolation of CP47 and CP43 complexes. *J Biol Chem* **286**, 14812-14819.
- Boekema, E.J., Hankamer, B., Bald, D., Kruip, J., Nield, J., Boonstra, A.F., Barber, J., and Rogner, M.** (1995). Supramolecular structure of the photosystem II complex from green plants and cyanobacteria. *Proc Natl Acad Sci U S A* **92**, 175-179.
- Bondarava, N., Gross, C.M., Mubarakshina, M., Golecki, J.R., Johnson, G.N., and Krieger-Liszkay, A.** (2010). Putative function of cytochrome *b*₅₅₉ as a plastoquinol oxidase. *Physiol. Plant.* **138**, 463-473.
- Bonnard, G., Corvest, V., Meyer, E.H., and Hamel, P.P.** (2010). Redox processes controlling the biogenesis of *c*-type cytochromes. *Antioxid Redox Signal* **13**, 1385-1401.
- Bonnefoy, N., Chalvet, F., Hamel, P., Slonimski, P.P., and Dujardin, G.** (1994). OXA1, a *Saccharomyces cerevisiae* nuclear gene whose sequence is conserved from prokaryotes to eukaryotes controls cytochrome oxidase biogenesis. *J Mol Biol* **239**, 201-212.
- Boulouis, A., Raynaud, C., Bujaldon, S., Aznar, A., Wollman, F.A., and Choquet, Y.** (2011). The nucleus-encoded trans-acting factor MCA1 plays a critical role in the regulation of cytochrome *f* synthesis in *Chlamydomonas* chloroplasts. *Plant Cell* **23**, 333-349.
- Brettel, K.** (1997). Electron transfer and arrangement of the redox cofactors in photosystem I. *Biochim. Biophys. Acta* **1318**, 322-373.
- Bricker, T.M., and Frankel, L.K.** (2011). Auxiliary functions of the PsbO, PsbP and PsbQ proteins of higher plant Photosystem II: a critical analysis. *J Photochem Photobiol B* **104**, 165-178.
- Bricker, T.M., Roose, J.L., Fagerlund, R.D., Frankel, L.K., and Eaton-Rye, J.J.** (2011). The extrinsic proteins of Photosystem II. *Biochim Biophys Acta* **1817**, 121-142.
- Brickman, E., and Beckwith, J.** (1975). Analysis of the regulation of *Escherichia coli* alkaline phosphatase synthesis using deletions and *phi80* transducing phages. *J.*

- Mol. Biol. **96**, 307-316.
- Burnap, R.L.** (2004). D1 protein processing and Mn cluster assembly in light of the emerging Photosystem II structure. *Physical Chemistry Chemical Physics* **6**, 4803-4809.
- Burnap, R.L., Qian, M., Shen, J.R., Inoue, Y., and Sherman, L.A.** (1994). Role of disulfide linkage and putative intermolecular binding residues in the stability and binding of the extrinsic manganese-stabilizing protein to the photosystem II reaction center. *Biochemistry* **33**, 13712-13718.
- Cai, W., Ma, J., Chi, W., Zou, M., Guo, J., Lu, C., and Zhang, L.** (2012). Cooperation of LPA3 and LPA2 is essential for photosystem II assembly in *Arabidopsis*. *Plant Physiol* **154**, 109-120.
- Calderone, V., Trabucco, M., Vujicic, A., Battistutta, R., Giacometti, G.M., Andreucci, F., Barbato, R., and Zanotti, G.** (2003). Crystal structure of the PsbQ protein of photosystem II from higher plants. *EMBO Rep* **4**, 900-905.
- Carrell, C.J., Zhang, H., Cramer, W.A., and Smith, J.L.** (1997). Biological identity and diversity in photosynthesis and respiration: structure of the lumen-side domain of the chloroplast Rieske protein. *Structure* **5**, 1613-1625.
- Cha, H.J., Dalal, N.G., Pham, M.Q., Kramer, S.F., Vakharia, V.N., and Bentley, W.E.** (2002). Monitoring foreign protein expression under baculovirus p10 and polh promoters in insect larvae. *Biotechniques* **32**, 986, 988, 990 passim.
- Chen, H., Zhang, D., Guo, J., Wu, H., Jin, M., Lu, Q., Lu, C., and Zhang, L.** (2006). A Psb27 homologue in *Arabidopsis thaliana* is required for efficient repair of photodamaged photosystem II. *Plant Mol Biol* **61**, 567-575.
- Chen, M., Samuelson, J.C., Jiang, F., Muller, M., Kuhn, A., and Dalbey, R.E.** (2002). Direct interaction of YidC with the Sec-independent Pf3 coat protein during its membrane protein insertion. *J Biol Chem* **277**, 7670-7675.
- Choquet, Y., Zito, F., Wostrikoff, K., and Wollman, F.A.** (2003). Cytochrome *f* translation in *Chlamydomonas* chloroplast is autoregulated by its carboxyl-terminal domain. *Plant Cell* **15**, 1443-1454.
- Choquet, Y., Stern, D.B., Wostrikoff, K., Kuras, R., Girard-Bascou, J., and Wollman, F.A.** (1998). Translation of cytochrome *f* is autoregulated through the 5' untranslated region of *petA* mRNA in *Chlamydomonas* chloroplasts. *Proceedings of the National Academy of Sciences* **95**, 4380-4385.
- Clough, S.J., and Bent, A.F.** (1998). Floral dip: a simplified method for *Agrobacterium*-mediated transformation of *Arabidopsis thaliana*. *Plant J.* **16**, 735-743.
- Cormann, K.U., Bangert, J.A., Ikeuchi, M., Rogner, M., Stoll, R., and Nowaczyk, M.M.** (2009). Structure of Psb27 in solution: implications for transient binding to photosystem II during biogenesis and repair. *Biochemistry* **48**, 8768-8770.
- Corvest, V., Murrey, D.A., Bernard, D.G., Knaff, D.B., Guiard, B., and Hamel, P.P.** (2010). *c*-type cytochrome assembly in *Saccharomyces cerevisiae*: a key residue for apocytochrome *c*₁/lyase interaction. *Genetics* **186**, 561-571.

- Crooks, G.E., Hon, G., Chandonia, J.M., and Brenner, S.E.** (2004). WebLogo: a sequence logo generator. *Genome Res* **14**, 1188-1190.
- D'Andrea, L.D., and Regan, L.** (2003). TPR proteins: the versatile helix. *Trends Biochem Sci* **28**, 655-662.
- Dailey, F.E., and Berg, H.C.** (1993). Mutants in disulfide bond formation that disrupt flagellar assembly in *Escherichia coli*. *Proc. Natl. Acad. Sci. U S A* **90**, 1043-1047.
- Dalbey, R.E., and Robinson, C.** (1999). Protein translocation into and across the bacterial plasma membrane and the plant thylakoid membrane. *Trends Biochem Sci* **24**, 17-22.
- Depege, N., Bellafiore, S., and Rochaix, J.D.** (2003). Role of chloroplast protein kinase Stt7 in LHCII phosphorylation and state transition in *Chlamydomonas*. *Science* **299**, 1572-1575.
- Depuydt, M., Messens, J., and Collet, J.-F.** (2011). How Proteins Form Disulfide Bonds. *Antioxid. Redox Signal.* **15**, 49-66.
- Deshmukh, M., Brasseur, G., and Daldal, F.** (2000). Novel *Rhodobacter capsulatus* genes required for the biogenesis of various *c*-type cytochromes. *Mol Microbiol* **35**, 123-138.
- Dewez, D., Park, S., Garcia-Cerdan, J.G., Lindberg, P., and Melis, A.** (2009). Mechanism of REP27 protein action in the D1 protein turnover and photosystem II repair from photodamage. *Plant Physiol* **151**, 88-99.
- Drager, R.G., Girard-Bascou, J., Choquet, Y., Kindle, K.L., and Stern, D.B.** (1998). In vivo evidence for 5'→3' exonuclease degradation of an unstable chloroplast mRNA. *Plant J* **13**, 85-96.
- Dreyfuss, B.W., Hamel, P.P., Nakamoto, S.S., and Merchant, S.** (2003). Functional analysis of a divergent system II protein, Ccs1, involved in *c*-type cytochrome biogenesis. *J Biol Chem* **278**, 2604-2613.
- Dreyfuss, B.W., Merchant, S.** (1998). (The Netherlands: Kluwer Academic Publishers).
- Dutton, R.J., Boyd, D., Berkmen, M., and Beckwith, J.** (2008). Bacterial species exhibit diversity in their mechanisms and capacity for protein disulfide bond formation. *Proc. Natl. Acad. Sci. U S A* **105**, 11933-11938.
- Dutton, R.J., Wayman, A., Wei, J.-R., Rubin, E.J., Beckwith, J., and Boyd, D.** (2010). Inhibition of bacterial disulfide bond formation by the anticoagulant warfarin. *Proc. Natl. Acad. Sci. U S A* **107**, 297-301.
- Eberhard, S., Loiselay, C., Drapier, D., Bujaldon, S., Girard-Bascou, J., Kurat, R., Choquet, Y., and Wollman, F.A.** (2011). Dual functions of the nucleus-encoded factor TDA1 in trapping and translation activation of *atpA* transcripts in *Chlamydomonas reinhardtii* chloroplasts. *Plant J* **67**, 1055-1066.
- Ellgaard, L., and Ruddock, L.W.** (2005). The human protein disulphide isomerase family: substrate interactions and functional properties. *EMBO Rep* **6**, 28-32.
- Emanuelsson, O., Nielsen, H., and von Heijne, G.** (1999). ChloroP, a neural network-

- based method for predicting chloroplast transit peptides and their cleavage sites. *Protein Sci* **8**, 978-984.
- Eser, M., Masip, L., Kadokura, H., Georgiou, G., and Beckwith, J.** (2009). Disulfide bond formation by exported glutaredoxin indicates glutathione's presence in the *E. coli* periplasm. *Proc Natl Acad Sci U S A* **106**, 1572-1577.
- Feissner, R.E., Richard-Fogal, C.L., Frawley, E.R., Loughman, J.A., Earley, K.W., and Kranz, R.G.** (2006). Recombinant cytochromes *c* biogenesis systems I and II and analysis of haem delivery pathways in *Escherichia coli*. *Mol Microbiol* **60**, 563-577.
- Ferguson, S.J., Stevens, J.M., Allen, J.W., and Robertson, I.B.** (2008). Cytochrome *c* assembly: a tale of ever increasing variation and mystery? *Biochim Biophys Acta* **1777**, 980-984.
- Finazzi, G., and Forti, G.** (2004). Metabolic Flexibility of the Green Alga *Chlamydomonas reinhardtii* as Revealed by the Link between State Transitions and Cyclic Electron Flow. *Photosynth. Res.* **82**, 327-338.
- Francs-Small, C.C., Kroeger, T., Zmudjak, M., Ostersetzer-Biran, O., Rahimi, N., Small, I., and Barkan, A.** (2011). A PORR domain protein required for *rpl2* and *ccmF(C)* intron splicing and for the biogenesis of *c*-type cytochromes in *Arabidopsis* mitochondria. *Plant J* **69**, 996-1005.
- Frawley, E.R., and Kranz, R.G.** (2009). CcsBA is a cytochrome *c* synthetase that also functions in heme transport. *Proc Natl Acad Sci U S A* **106**, 10201-10206.
- Furt, F., Oostende, C., Widhalm, J.R., Dale, M.A., Wertz, J., and Basset, G.J.** (2010). A bimodular oxidoreductase mediates the specific reduction of phylloquinone (vitamin K) in chloroplasts. *Plant J.* **64**, 38-46.
- Gabilly, S.T., Kropat, J., Karamoko, M., Page, M.D., Nakamoto, S.S., Merchant, S.S., and Hamel, P.P.** (2011). A novel component of the disulfide-reducing pathway required for cytochrome *c* assembly in plastids. *Genetics* **187**, 793-802.
- Gabilly, S.T., Dreyfuss, B.W., Karamoko, M., Corvest, V., Kropat, J., Page, M.D., Merchant, S.S., and Hamel, P.P.** (2010). CCS5, a thioredoxin-like protein involved in the assembly of plastid *c*-type cytochromes. *J Biol Chem* **285**, 29738-29749.
- Galvan, A., Gonzalez-Ballester, D., and Fernandez, E.** (2007). Insertional mutagenesis as a tool to study genes/functions in *Chlamydomonas*. *Adv Exp Med Biol* **616**, 77-89.
- Gerdes, L., Bals, T., Klostermann, E., Karl, M., Philippar, K., Hunken, M., Soll, J., and Schunemann, D.** (2006). A second thylakoid membrane-localized Alb3/OxaI/YidC homologue is involved in proper chloroplast biogenesis in *Arabidopsis thaliana*. *J Biol Chem* **281**, 16632-16642.
- Giege, P., Grienenberger, J.M., and Bonnard, G.** (2008). Cytochrome *c* biogenesis in mitochondria. *Mitochondrion* **8**, 61-73.
- Gohre, V., Ossenbuhl, F., Crevecoeur, M., Eichacker, L.A., and Rochaix, J.D.** (2006).

- One of two Alb3 proteins is essential for the assembly of the photosystems and for cell survival in *Chlamydomonas*. *Plant Cell* **18**, 1454-1466.
- Goldschmidt-Clermont, M.** (1991). Transgenic expression of aminoglycoside adenine transferase in the chloroplast: a selectable marker of site-directed transformation of *Chlamydomonas*. *Nucleic Acids Res* **19**, 4083-4089.
- Goodstadt, L., and Ponting, C.P.** (2004). Vitamin K epoxide reductase: homology, active site and catalytic mechanism. *TIBS* **29**, 289-292.
- Gopalan, G., He, Z., Balmer, Y., Romano, P., Gupta, R., Héroux, A., Buchanan, B.B., Swaminathan, K., and Luan, S.** (2004). Structural analysis uncovers a role for redox in regulating FKBP13, an immunophilin of the chloroplast thylakoid lumen. *Proc. Natl. Acad. Sci. U S A* **101**, 13945-13950.
- Grasse, N., Mamedov, F., Becker, K., Styring, S., Rogner, M., and Nowaczyk, M.M.** (2011). Role of novel dimeric Photosystem II (PSII)-Psb27 protein complex in PSII repair. *J Biol Chem* **286**, 29548-29555.
- Gross, J., Cho, W.K., Lezhneva, L., Falk, J., Krupinska, K., Shinozaki, K., Seki, M., Herrmann, R.G., and Meurer, J.** (2006). A plant locus essential for phyloquinone (vitamin K1) biosynthesis originated from a fusion of four eubacterial genes. *J. Biol. Chem.* **281**, 17189-17196.
- Grossman, A.R., Karpowicz, S.J., Heinnickel, M., Dewez, D., Hamel, B., Dent, R., Niyogi, K.K., Johnson, X., Alric, J., Wollman, F.A., Li, H., and Merchant, S.S.** (2011). Phylogenomic analysis of the *Chlamydomonas* genome unmasks proteins potentially involved in photosynthetic function and regulation. *Photosynth. Res.* **106**, 3-17.
- Gupta, R., Mould, R.M., He, Z., and Luan, S.** (2002). A chloroplast FKBP interacts with and affects the accumulation of Rieske subunit of cytochrome *b₆f* complex. *Proc. Natl. Acad. Sci. U S A* **99**, 15806-15811.
- Guzman, L.M., Belin, D., Carson, M.J., and Beckwith, J.** (1995). Tight regulation, modulation, and high-level expression by vectors containing the arabinose PBAD promoter. *J. Bacteriol.* **177**, 4121-4130.
- Hall, M., Mata-Cabana, A., Akerlund, H.E., Florencio, F.J., Schroder, W.P., Lindahl, M., and Kieselbach, T.** (2010). Thioredoxin targets of the plant chloroplast lumen and their implications for plastid function. *Proteomics* **10**, 987-1001.
- Hamel, P., Corvest, V., Giege, P., and Bonnard, G.** (2009). Biochemical requirements for the maturation of mitochondrial *c*-type cytochromes. *Biochim Biophys Acta* **1793**, 125-138.
- Hamel, P.P., Dreyfuss, B.W., Xie, Z., Gabilly, S.T., and Merchant, S.** (2003). Essential histidine and tryptophan residues in CcsA, a system II polytopic cytochrome *c* biogenesis protein. *J Biol Chem* **278**, 2593-2603.
- Harris, E.H.** (1989). *The Chlamydomonas Sourcebook: A comprehensive guide to biology and laboratory use.* (San Diego, CA: Academic Press).
- Hell, K., Neupert, W., and Stuart, R.A.** (2001). Oxa1p acts as a general membrane

- insertion machinery for proteins encoded by mitochondrial DNA. *Embo J* **20**, 1281-1288.
- Heras, B., Shouldice, S.R., Totsika, M., Scanlon, M.J., Schembri, M.A., and Martin, J.L.** (2009). DSB proteins and bacterial pathogenicity. *Nat. Rev. Micro.* **7**, 215-225.
- Herrmann, J.M., Kauff, F., and Neuhaus, H.E.** (2009). Thiol oxidation in bacteria, mitochondria and chloroplasts: Common principles but three unrelated machineries? *Biochim. Biophys. Acta* **1793**, 71-77.
- Horton, P., Park, K.J., Obayashi, T., Fujita, N., Harada, H., Adams-Collier, C.J., and Nakai, K.** (2007). WoLF PSORT: protein localization predictor. *Nucleic Acids Res* **35**, W585-587.
- Howe, G., and Merchant, S.** (1992). The biosynthesis of membrane and soluble plastidic *c*-type cytochromes of *Chlamydomonas reinhardtii* is dependent on multiple common gene products. *Embo J* **11**, 2789-2801.
- Howe, G., and Merchant, S.** (1993). Maturation of thylakoid lumen proteins proceeds post-translationally through an intermediate in vivo. *Proc Natl Acad Sci U S A* **90**, 1862-1866.
- Howe, G., and Merchant, S.** (1994). Role of heme in the biosynthesis of cytochrome *c*₆. *J Biol Chem* **269**, 5824-5832.
- Hurkman, W.J., and Tanaka, C.K.** (1986). Solubilization of plant membrane proteins for analysis by two-dimensional gel electrophoresis. *Plant Physiol.* **81**, 802-806.
- Hynds, P.J., Plucken, H., Westhoff, P., and Robinson, C.** (2000). Different lumen-targeting pathways for nuclear-encoded versus cyanobacterial/plastid-encoded Hcf136 proteins. *FEBS Lett* **467**, 97-100.
- Ifuku, K., Ido, K., and Sato, F.** (2011). Molecular functions of PsbP and PsbQ proteins in the photosystem II supercomplex. *J Photochem Photobiol B* **104**, 158-164.
- Ifuku, K., Nakatsu, T., Kato, H., and Sato, F.** (2004). Crystal structure of the PsbP protein of photosystem II from *Nicotiana tabacum*. *EMBO Rep* **5**, 362-367.
- Ifuku, K., Yamamoto, Y., Ono, T.A., Ishihara, S., and Sato, F.** (2005). PsbP protein, but not PsbQ protein, is essential for the regulation and stabilization of photosystem II in higher plants. *Plant Physiol* **139**, 1175-1184.
- Inaba, K.** (2009). Disulfide bond formation system in *Escherichia coli*. *J Biochem* **146**, 591-597.
- Inagaki, N., Yamamoto, Y., Mori, H., and Satoh, K.** (1996). Carboxyl-terminal processing protease for the D1 precursor protein: cloning and sequencing of the spinach cDNA. *Plant Mol Biol* **30**, 39-50.
- Inoue, K., Dreyfuss, B.W., Kindle, K.L., Stern, D.B., Merchant, S., and Sodeinde, O.A.** (1997). Ccs1, a nuclear gene required for the post-translational assembly of chloroplast *c*-type cytochromes. *J Biol Chem* **272**, 31747-31754.
- Iratni, R., Diederich, L., Harrak, H., Bligny, M., and Lerbs-Mache, S.** (1997). Organ-specific transcription of the *rrn* operon in spinach plastids. *J. Biol. Chem.* **272**,

13676-13682.

- Ishihara, S., Takabayashi, A., Ido, K., Endo, T., Ifuku, K., and Sato, F.** (2007). Distinct functions for the two PsbP-like proteins PPL1 and PPL2 in the chloroplast thylakoid lumen of *Arabidopsis*. *Plant Physiol* **145**, 668-679.
- Ishikawa, Y., Schröder, W.P., and Funk, C.** (2005). Functional analysis of the PsbP-like protein (sll1418) in *Synechocystis sp. PCC 6803*. *Photosynthesis Research* **84**, 257-262.
- Ito, K., and Inaba, K.** (2008). The disulfide bond formation (Dsb) system. *Curr Opin Struct Biol* **18**, 450-458.
- Iwai, M., Takizawa, K., Tokutsu, R., Okamuro, A., Takahashi, Y., and Minagawa, J.** (2010). Isolation of the elusive supercomplex that drives cyclic electron flow in photosynthesis. *Nature* **464**, 1210-1213.
- Jeong, S.Y., Rose, A., and Meier, I.** (2003). MFP1 is a thylakoid-associated, nucleoid-binding protein with a coiled-coil structure. *Nucleic Acids Res.* **31**, 5175-5185.
- Jiang, F., Yi, L., Moore, M., Chen, M., Rohl, T., Van Wijk, K.J., De Gier, J.W., Henry, R., and Dalbey, R.E.** (2002). Chloroplast YidC homolog Albino3 can functionally complement the bacterial YidC depletion strain and promote membrane insertion of both bacterial and chloroplast thylakoid proteins. *J Biol Chem* **277**, 19281-19288.
- Joliot, P., and Joliot, A.** (2005). Quantification of cyclic and linear flows in plants. *Proc. Natl. Acad. Sci. U S A* **102**, 4913-4918.
- Kadokura, H., and Beckwith, J.** (2002). Four cysteines of the membrane protein DsbB act in concert to oxidize its substrate DsbA. *EMBO J* **21**, 2354-2363.
- Kadokura, H., and Beckwith, J.** (2010). Mechanisms of oxidative protein folding in the bacterial cell envelope. *Antioxid Redox Signal* **13**, 1231-1246.
- Kadokura, H., and Beckwith, J.** (2011). Mechanisms of Oxidative Protein Folding in the Bacterial Cell Envelope. *Antioxid. Redox Signal.* **13**, 1231-1246.
- Kato, Y., and Sakamoto, W.** (2009). Protein Quality Control in Chloroplasts: A Current Model of D1 Protein Degradation in the Photosystem II Repair Cycle. *Journal of Biochemistry* **146**, 463-469.
- Kato, Y., Sakamoto, W., and Kwang, W.J.** (2010). Chapter 4 - New Insights into the Types and Function of Proteases in Plastids. In *International Review of Cell and Molecular Biology* (Academic Press), pp. 185-218.
- Kato, Y., Miura, E., Ido, K., Ifuku, K., and Sakamoto, W.** (2009). The variegated mutants lacking chloroplastic FtsHs are defective in D1 degradation and accumulate reactive oxygen species. *Plant Physiol* **151**, 1790-1801.
- Katzen, F., and Beckwith, J.** (2002). Disulfide bond formation in periplasm of *Escherichia coli*. *Methods Enzymol* **348**, 54-66.
- Katzen, F., Deshmukh, M., Daldal, F., and Beckwith, J.** (2002). Evolutionary domain fusion expanded the substrate specificity of the transmembrane electron transporter DsbD. *Embo J* **21**, 3960-3969.

- Kern, M., Scheithauer, J., Kranz, R.G., and Simon, J.** (2010a). Essential histidine pairs indicate conserved haem binding in epsilonproteobacterial cytochrome *c* haem lyases. *Microbiology* **156**, 3773-3781.
- Kern, M., Eisel, F., Scheithauer, J., Kranz, R.G., and Simon, J.** (2010b). Substrate specificity of three cytochrome *c* haem lyase isoenzymes from *Wolinella succinogenes*: unconventional haem c binding motifs are not sufficient for haem c attachment by Nrfl and CcsA1. *Mol Microbiol* **75**, 122-137.
- Klinkert, B., Ossenbuhl, F., Sikorski, M., Berry, S., Eichacker, L., and Nickelsen, J.** (2004). Prata, a periplasmic tetratricopeptide repeat protein involved in biogenesis of photosystem II in *Synechocystis sp. PCC 6803*. *J Biol Chem* **279**, 44639-44644.
- Klostermann, E., Droste Gen Helling, I., Carde, J.P., and Schunemann, D.** (2002). The thylakoid membrane protein ALB3 associates with the cpSecY-translocase in *Arabidopsis thaliana*. *Biochem J* **368**, 777-781.
- Komenda, J., Sobotka, R., and Nixon, P.J.** (2012). Assembling and maintaining the Photosystem II complex in chloroplasts and cyanobacteria. *Curr Opin Plant Biol.*
- Komenda, J., Nickelsen, J., Tichy, M., Prasil, O., Eichacker, L.A., and Nixon, P.J.** (2008). The cyanobacterial homologue of HCF136/YCF48 is a component of an early photosystem II assembly complex and is important for both the efficient assembly and repair of photosystem II in *Synechocystis sp. PCC 6803*. *J Biol Chem* **283**, 22390-22399.
- Kranz, R., Lill, R., Goldman, B., Bonnard, G., and Merchant, S.** (1998). Molecular mechanisms of cytochrome *c* biogenesis: three distinct systems. *Mol Microbiol* **29**, 383-396.
- Kranz, R.G., Richard-Fogal, C., Taylor, J.S., and Frawley, E.R.** (2009). Cytochrome *c* biogenesis: mechanisms for covalent modifications and trafficking of heme and for heme-iron redox control. *Microbiol Mol Biol Rev* **73**, 510-528, Table of Contents.
- Kroll, D., Meierhoff, K., Bechtold, N., Kinoshita, M., Westphal, S., Vothknecht, U.C., Soll, J., and Westhoff, P.** (2001). VIPP1, a nuclear gene of *Arabidopsis thaliana* essential for thylakoid membrane formation. *Proc Natl Acad Sci U S A* **98**, 4238-4242.
- Kuras, R., Saint-Marcoux, D., Wollman, F.A., and de Vitry, C.** (2007). A specific *c*-type cytochrome maturation system is required for oxygenic photosynthesis. *Proc Natl Acad Sci U S A* **104**, 9906-9910.
- Kuras, R., de Vitry, C., Choquet, Y., Girard-Bascou, J., Culler, D., Buschlen, S., Merchant, S., and Wollman, F.A.** (1997). Molecular genetic identification of a pathway for heme binding to cytochrome *b₆*. *J Biol Chem* **272**, 32427-32435.
- Le Brun, N.E., Bengtsson, J., and Hederstedt, L.** (2000). Genes required for cytochrome *c* synthesis in *Bacillus subtilis*. *Mol Microbiol* **36**, 638-650.
- Lemeille, S., Willig, A., Depège-Fargeix, N., Delessert, C., Bassi, R., and Rochaix, J.-**

- D.** (2009). Analysis of the Chloroplast Protein Kinase Stt7 during State Transitions. *PLoS Biol* **7**, e1000045.
- Lennartz, K., Bossmann, S., Westhoff, P., Bechtold, N., and Meierhoff, K.** (2006). HCF153, a novel nuclear-encoded factor necessary during a post-translational step in biogenesis of the cytochrome *b₆f* complex. *Plant J* **45**, 101-112.
- Lennartz, K., Plücker, H., Seidler, A., Westhoff, P., Bechtold, N., and Meierhoff, K.** (2001). *HCF164* encodes a thioredoxin-like protein involved in the biogenesis of the cytochrome *b₆f* complex in Arabidopsis. *Plant Cell* **13**, 2539-2351.
- Leyva-Guerrero, E., Narayanan, N.N., Ihemere, U., and Sayre, R.T.** (2012). Iron and protein biofortification of cassava: lessons learned. *Curr Opin Biotechnol* **23**, 257-264.
- Li, Q., Hu, H.Y., Wang, W.Q., and Xu, G.J.** (2001). Structural and redox properties of the leaderless DsbE (CcmG) protein: both active-site cysteines of the reduced form are involved in its function in the *Escherichia coli* periplasm. *Biol Chem* **382**, 1679-1686.
- Li, W., Schulman, S., Dutton, R.J., Boyd, D., Beckwith, J., and Rapoport, T.A.** (2010). Structure of a bacterial homologue of vitamin K epoxide reductase. *Nature* **463**, 507-512.
- Lima, A., Lima, S., Wong, J.H., Phillips, R.S., Buchanan, B.B., and Luan, S.** (2006). A redox-active FKBP-type immunophilin functions in accumulation of the photosystem II supercomplex in *Arabidopsis thaliana*. *Proc. Natl. Acad. Sci. U S A* **103**, 12631-12636.
- Liu, H., Roose, J.L., Cameron, J.C., and Pakrasi, H.B.** (2011a). A genetically tagged Psb27 protein allows purification of two consecutive photosystem II (PSII) assembly intermediates in *Synechocystis 6803*, a cyanobacterium. *J Biol Chem* **286**, 24865-24871.
- Liu, H., Huang, R.Y., Chen, J., Gross, M.L., and Pakrasi, H.B.** (2011b). Psb27, a transiently associated protein, binds to the chlorophyll binding protein CP43 in photosystem II assembly intermediates. *Proc Natl Acad Sci U S A* **108**, 18536-18541.
- Lo, S.M., and Theg, S.M.** (2012). Role of Vesicle-Inducing Protein in Plastids1 in cpTat Transport at the Thylakoid. *Plant J*.
- Lohmann, A., Schottler, M.A., Brehelin, C., Kessler, F., Bock, R., Cahoon, E.B., and Dormann, P.** (2006). Deficiency in phyloquinone (vitamin K1) methylation affects prenyl quinone distribution, photosystem I abundance, and anthocyanin accumulation in the *Arabidopsis AtmenG* mutant. *J. Biol. Chem.* **281**, 40461-40472.
- Loiselay, C., Gumpel, N.J., Girard-Bascou, J., Watson, A.T., Purton, S., Wollman, F.A., and Choquet, Y.** (2008). Molecular identification and function of cis- and trans-acting determinants for *petA* transcript stability in *Chlamydomonas reinhardtii* chloroplasts. *Mol Cell Biol* **28**, 5529-5542.

- Loppes, R., and Heindricks, R.** (1986). New arginine-requiring mutants in *Chlamydomonas reinhardtii*. Archives of Microbiology **143**, 348-352.
- Lurin, C., Andres, C., Aubourg, S., Bellaoui, M., Bitton, F., Bruyere, C., Caboche, M., Debast, C., Gualberto, J., Hoffmann, B., Lecharny, A., Le Ret, M., Martin-Magniette, M.L., Mireau, H., Peeters, N., Renou, J.P., Szurek, B., Tacconnat, L., and Small, I.** (2004). Genome-wide analysis of *Arabidopsis* pentatricopeptide repeat proteins reveals their essential role in organelle biogenesis. Plant Cell **16**, 2089-2103.
- Lyska, D., Paradies, S., Meierhoff, K., and Westhoff, P.** (2007). HCF208, a homolog of *Chlamydomonas* CCB2, is required for accumulation of native cytochrome *b₆* in *Arabidopsis thaliana*. Plant Cell Physiol **48**, 1737-1746.
- Ma, J., Peng, L., Guo, J., Lu, Q., Lu, C., and Zhang, L.** (2007). LPA2 is required for efficient assembly of photosystem II in *Arabidopsis thaliana*. Plant Cell **19**, 1980-1993.
- Mabbitt, P.D., Rautureau, G.J., Day, C.L., Wilbanks, S.M., Eaton-Rye, J.J., and Hinds, M.G.** (2009). Solution structure of Psb27 from cyanobacterial photosystem II. Biochemistry **48**, 8771-8773.
- Mamedov, F., Nowaczyk, M.M., Thapper, A., Rogner, M., and Styring, S.** (2007). Functional characterization of monomeric photosystem II core preparations from *Thermosynechococcus elongatus* with or without the Psb27 protein. Biochemistry **46**, 5542-5551.
- Manoil, C.** (1991). Analysis of membrane protein topology using alkaline phosphatase and β -galactosidase gene fusions. Methods Cell Biol. **34**, 61-75.
- Martin, W., Rujan, T., Richly, E., Hansen, A., Cornelsen, S., Lins, T., Leister, D., Stoebe, B., Hasegawa, M., and Penny, D.** (2002). Evolutionary analysis of *Arabidopsis*, cyanobacterial, and chloroplast genomes reveals plastid phylogeny and thousands of cyanobacterial genes in the nucleus. Proc Natl Acad Sci U S A **99**, 12246-12251.
- Merchant, S.S., Prochnik, S.E., Vallon, O., Harris, E.H., Karpowicz, S.J., Witman, G.B., Terry, A., Salamov, A., Fritz-Laylin, L.K., Marechal-Drouard, L., Marshall, W.F., Qu, L.H., Nelson, D.R., Sanderfoot, A.A., Spalding, M.H., Kapitonov, V.V., Ren, Q., Ferris, P., Lindquist, E., Shapiro, H., Lucas, S.M., Grimwood, J., Schmutz, J., Cardol, P., Cerutti, H., Chanfreau, G., Chen, C.L., Cognat, V., Croft, M.T., Dent, R., Dutcher, S., Fernandez, E., Fukuzawa, H., Gonzalez-Ballester, D., Gonzalez-Halphen, D., Hallmann, A., Hanikenne, M., Hippler, M., Inwood, W., Jabbari, K., Kalanon, M., Kuras, R., Lefebvre, P.A., Lemaire, S.D., Lobanov, A.V., Lohr, M., Manuell, A., Meier, I., Mets, L., Mittag, M., Mittelmeier, T., Moroney, J.V., Moseley, J., Napoli, C., Nedelcu, A.M., Niyogi, K., Novoselov, S.V., Paulsen, I.T., Pazour, G., Purton, S., Ral, J.P., Riano-Pachon, D.M., Riekhof, W., Rymarquis, L., Schroda, M., Stern, D., Umen, J., Willows, R., Wilson, N., Zimmer, S.L.,**

- Allmer, J., Balk, J., Bisova, K., Chen, C.J., Elias, M., Gendler, K., Hauser, C., Lamb, M.R., Ledford, H., Long, J.C., Minagawa, J., Page, M.D., Pan, J., Pootakham, W., Roje, S., Rose, A., Stahlberg, E., Terauchi, A.M., Yang, P., Ball, S., Bowler, C., Dieckmann, C.L., Gladyshev, V.N., Green, P., Jorgensen, R., Mayfield, S., Mueller-Roeber, B., Rajamani, S., Sayre, R.T., Brokstein, P., Dubchak, I., Goodstein, D., Hornick, L., Huang, Y.W., Jhaveri, J., Luo, Y., Martinez, D., Ngau, W.C., Otilar, B., Poliakov, A., Porter, A., Szajkowski, L., Werner, G., Zhou, K., Grigoriev, I.V., Rokhsar, D.S., and Grossman, A.R. (2007). The *Chlamydomonas* genome reveals the evolution of key animal and plant functions. *Science* **318**, 245-250.
- Merendino, L., Perron, K., Rahire, M., Howald, I., Rochaix, J.D., and Goldschmidt-Clermont, M.** (2006). A novel multifunctional factor involved in *trans*-splicing of chloroplast introns in *Chlamydomonas*. *Nucleic Acids Res* **34**, 262-274.
- Meurer, J., Plucken, H., Kowallik, K.V., and Westhoff, P.** (1998). A nuclear-encoded protein of prokaryotic origin is essential for the stability of photosystem II in *Arabidopsis thaliana*. *Embo J* **17**, 5286-5297.
- Meyer, E.H., Giege, P., Gelhaye, E., Rayapuram, N., Ahuja, U., Thony-Meyer, L., Grienenberger, J.M., and Bonnard, G.** (2005). AtCCMH, an essential component of the *c*-type cytochrome maturation pathway in *Arabidopsis* mitochondria, interacts with apocytochrome *c*. *Proc. Natl. Acad. Sci. U S A* **102**, 16113-16118.
- Michoux, F., Takasaka, K., Boehm, M., Komenda, J., Nixon, P.J., and Murray, J.W.** (2012). Crystal structure of the Psb27 assembly factor at 1.6 Å: implications for binding to Photosystem II. *Photosynth Res* **110**, 169-175.
- Missiakas, D., Georgopoulos, C., and Raina, S.** (1994). The *Escherichia coli* dsbC (*xprA*) gene encodes a periplasmic protein involved in disulfide bond formation. *Embo J* **13**, 2013-2020.
- Moore, M., Harrison, M.S., Peterson, E.C., and Henry, R.** (2000). Chloroplast Oxa1p homolog albino3 is required for post-translational integration of the light harvesting chlorophyll-binding protein into thylakoid membranes. *J Biol Chem* **275**, 1529-1532.
- Mori, H., Summer, E.J., Ma, X., and Cline, K.** (1999). Component specificity for the thylakoidal Sec and Delta pH-dependent protein transport pathways. *J Cell Biol* **146**, 45-56.
- Motohashi, K., and Hisabori, T.** (2006). HCF164 Receives Reducing Equivalents from Stromal Thioredoxin across the Thylakoid Membrane and Mediates Reduction of Target Proteins in the Thylakoid Lumen. *J. Biol. Chem.* **281**, 35039-35047.
- Motohashi, K., and Hisabori, T.** (2010). CcdA is a thylakoid membrane protein required for the transfer of reducing equivalents from stroma to thylakoid lumen in the higher plant chloroplast. *Antioxid. Redox Signal.* **13**, 1169-1176.
- Mulo, P., Sirpio, S., Suorsa, M., and Aro, E.M.** (2008). Auxiliary proteins involved in

- the assembly and sustenance of photosystem II. *Photosynth Res* **98**, 489-501.
- Murakami, R., Ifuku, K., Takabayashi, A., Shikanai, T., Endo, T., and Sato, F.** (2002). Characterization of an *Arabidopsis thaliana* mutant with impaired psbO, one of two genes encoding extrinsic 33-kDa proteins in photosystem II. *FEBS Lett.* **523**, 138-142.
- Neupert, W., and Herrmann, J.M.** (2007). Translocation of proteins into mitochondria. *Annu Rev Biochem* **76**, 723-749.
- Nickelsen, J.** (1999). Transcripts containing the 5' untranslated regions of the plastid genes *psbA* and *psbB* from higher plants are unstable in *Chlamydomonas reinhardtii* chloroplasts. *Mol Gen Genet* **262**, 768-771.
- Nield, J., and Barber, J.** (2006). Refinement of the structural model for the Photosystem II supercomplex of higher plants. *Biochim Biophys Acta* **1757**, 353-361.
- Nilsson, R., and van Wijk, K.J.** (2002). Transient interaction of cpSRP54 with elongating nascent chains of the chloroplast-encoded D1 protein; 'cpSRP54 caught in the act'. *FEBS Lett* **524**, 127-133.
- Nixon, P.J., Michoux, F., Yu, J., Boehm, M., and Komenda, J.** (2010). Recent advances in understanding the assembly and repair of photosystem II. *Ann Bot* **106**, 1-16.
- Nordhues, A., Schottler, M.A., Unger, A.K., Geimer, S., Schonfelder, S., Schmollinger, S., Rutgers, M., Finazzi, G., Soppa, B., Sommer, F., Muhlhaus, T., Roach, T., Krieger-Liszkay, A., Lokstein, H., Crespo, J.L., and Schroda, M.** (2012). Evidence for a role of VIPP1 in the structural organization of the photosynthetic apparatus in *Chlamydomonas*. *Plant Cell* **24**, 637-659.
- Nowaczyk, M.M., Hebel, R., Schlotter, E., Meyer, H.E., Warscheid, B., and Rogner, M.** (2006). Psb27, a cyanobacterial lipoprotein, is involved in the repair cycle of photosystem II. *Plant Cell* **18**, 3121-3131.
- Ossenbuhl, F., Gohre, V., Meurer, J., Krieger-Liszkay, A., Rochaix, J.D., and Eichacker, L.A.** (2004). Efficient assembly of photosystem II in *Chlamydomonas reinhardtii* requires Alb3.1p, a homolog of *Arabidopsis* ALBINO3. *Plant Cell* **16**, 1790-1800.
- Page, M.D., and Ferguson, S.J.** (1997). *Paracoccus denitrificans* CcmG is a periplasmic protein-disulphide oxidoreductase required for *c*- and aa3-type cytochrome biogenesis; evidence for a reductase role in vivo. *Mol Microbiol* **24**, 977-990.
- Page, M.L.D., Hamel, P.P., Gabilly, S.T., Zegzouti, H., Perea, J.V., Alonso, J.M., Ecker, J.R., Theg, S.M., Christensen, S.K., and Merchant, S.** (2004). A Homolog of Prokaryotic Thiol Disulfide Transporter CcdA Is Required for the Assembly of the Cytochrome *b₆f* Complex in *Arabidopsis* Chloroplasts. *J. Biol. Chem.* **279**, 32474-32482.
- Park, S., Khamai, P., Garcia-Cerdan, J.G., and Melis, A.** (2007). REP27, a tetratricopeptide repeat nuclear-encoded and chloroplast-localized protein, functions in D1/32-kD reaction center protein turnover and photosystem II repair

- from photodamage. *Plant Physiol* **143**, 1547-1560.
- Pasch, J.C., Nickelsen, J., and Schunemann, D.** (2005). The yeast split-ubiquitin system to study chloroplast membrane protein interactions. *Appl Microbiol Biotechnol* **69**, 440-447.
- Peeva, V.N., Toth, S.Z., Cornic, G., and Ducruet, J.M.** (2010). Thermoluminescence and P700 redox kinetics as complementary tools to investigate the cyclic/chlororespiratory electron pathways in stress conditions in barley leaves. *Physiol. Plant*.
- Peltier, J.-B.t., Emanuelsson, O., Kalume, D.r.E., Ytterberg, J., Friso, G., Rudella, A., Liberles, D.A., Söderberg, L., Roepstorff, P., von Heijne, G., and van Wijk, K.J.** (2002). Central Functions of the Lumenal and Peripheral Thylakoid Proteome of *Arabidopsis* Determined by Experimentation and Genome-Wide Prediction. *Plant Cell* **14**, 211-236.
- Peng, L., Ma, J., Chi, W., Guo, J., Zhu, S., Lu, Q., Lu, C., and Zhang, L.** (2006). LOW PSII ACCUMULATION1 is involved in efficient assembly of photosystem II in *Arabidopsis thaliana*. *Plant Cell* **18**, 955-969.
- Pisa, R., Stein, T., Eichler, R., Gross, R., and Simon, J.** (2002). The *nrfI* gene is essential for the attachment of the active site haem group of *Wolinella succinogenes* cytochrome *c* nitrite reductase. *Mol Microbiol* **43**, 763-770.
- Plucken, H., Muller, B., Grohmann, D., Westhoff, P., and Eichacker, L.A.** (2002). The HCF136 protein is essential for assembly of the photosystem II reaction center in *Arabidopsis thaliana*. *FEBS Lett* **532**, 85-90.
- Popelkova, H., and Yocum, C.F.** (2011). PsbO, the manganese-stabilizing protein: Analysis of the structure-function relations that provide insights into its role in photosystem II. *J. Photochem. Photobiol. B* **104**, 179-190.
- Promnares, K., Komenda, J., Bumba, L., Nebesarova, J., Vacha, F., and Tichy, M.** (2006). Cyanobacterial small chlorophyll-binding protein ScpD (HliB) is located on the periphery of photosystem II in the vicinity of PsbH and CP47 subunits. *J Biol Chem* **281**, 32705-32713.
- Purton, S.** (2007). Tools and techniques for chloroplast transformation of *Chlamydomonas*. *Adv Exp Med Biol* **616**, 34-45.
- Purton, S., and Rochaix, J.D.** (1994). Complementation of a *Chlamydomonas reinhardtii* mutant using a genomic cosmid library. *Plant Mol Biol* **24**, 533-537.
- Quinn, J.M., and Merchant, S.** (1998). Copper-responsive gene expression during adaptation to copper deficiency. *Methods Enzymol* **297**, 263-279.
- Rayapuram, N., Hagenmuller, J., Grienberger, J.M., Bonnard, G., and Giege, P.** (2008). The three mitochondrial encoded CcmF proteins form a complex that interacts with CCMH and *c*-type apocytochromes in *Arabidopsis*. *J Biol Chem* **283**, 25200-25208.
- Raynaud, C., Loiselay, C., Wostrikoff, K., Kuras, R., Girard-Bascou, J., Wollman, F.A., and Choquet, Y.** (2007). Evidence for regulatory function of nucleus-

- encoded factors on mRNA stabilization and translation in the chloroplast. *Proc Natl Acad Sci U S A* **104**, 9093-9098.
- Reid, E., Cole, J., and Eaves, D.J.** (2001). The *Escherichia coli* CcmG protein fulfils a specific role in cytochrome *c* assembly. *Biochem J* **355**, 51-58.
- Remacle, C., Barbieri, M.R., Cardol, P., and Hamel, P.P.** (2008). Eukaryotic complex I: functional diversity and experimental systems to unravel the assembly process. *Mol Genet Genomics* **280**, 93-110.
- Remacle, C., Hamel, Patrice, Larosa, Véronique, Subrahmanian, Nitya, Cardol, Pierre.** (2012). A structural perspective on complex I. In *Complexes I in the green lineage.*, L. Sazanov, ed (
- Richard-Fogal, C.L., Frawley, E.R., Bonner, E.R., Zhu, H., San Francisco, B., and Kranz, R.G.** (2009). A conserved haem redox and trafficking pathway for cofactor attachment. *Embo J* **28**, 2349-2359.
- Riemer, J., Fischer, M., and Herrmann, J.M.** (2011). Oxidation-driven protein import into mitochondria: Insights and blind spots. *Biochim. Biophys. Acta* **1808**, 981-989.
- Rishavy, M.A., Usabalieva, A., Hallgren, K.W., and Berkner, K.L.** (2011). Novel Insight into the Mechanism of the Vitamin K Oxidoreductase (VKOR). *J. Biol. Chem.* **286**, 7267-7278.
- Robinson, C., and Mant, A.** (1997). Targeting of proteins into and across the thylakoid membrane. *Trends in Plant Science* **2**, 431-437.
- Rochaix, J.D.** (2012). Assembly of the photosynthetic apparatus. *Plant Physiol* **155**, 1493-1500.
- Rohacek, K., and Bartak, M.** (1999). Technique of the modulated chlorophyll fluorescence: basic concepts, useful parameters, and some applications. *Photosynthetica* **37**, 339-363.
- Roose, J.L., and Pakrasi, H.B.** (2004). Evidence that D1 processing is required for manganese binding and extrinsic protein assembly into photosystem II. *J Biol Chem* **279**, 45417-45422.
- Roose, J.L., and Pakrasi, H.B.** (2008). The Psb27 protein facilitates manganese cluster assembly in photosystem II. *J Biol Chem* **283**, 4044-4050.
- Roy, A., Kucukural, A., and Zhang, Y.** (2010). I-TASSER: a unified platform for automated protein structure and function prediction. *Nat Protoc* **5**, 725-738.
- Sacksteder, C.A., and Kramer, D.M.** (2000). Dark-interval relaxation kinetics (DIRK) of absorbance changes as a quantitative probe of steady-state electron transfer. *Photosynth. Res.* **66**, 145-158.
- Sakamoto, W.** (2006). Protein Degradation Machineries in Plastids. *Annual Review of Plant Biology* **57**, 599-621.
- Samuelson, J.C., Jiang, F., Yi, L., Chen, M., de Gier, J.W., Kuhn, A., and Dalbey, R.E.** (2001). Function of YidC for the insertion of M13 procoat protein in *Escherichia coli*: translocation of mutants that show differences in their

- membrane potential dependence and Sec requirement. *J Biol Chem* **276**, 34847-34852.
- Samuelson, J.C., Chen, M., Jiang, F., Moller, I., Wiedmann, M., Kuhn, A., Phillips, G.J., and Dalbey, R.E.** (2000). YidC mediates membrane protein insertion in bacteria. *Nature* **406**, 637-641.
- Sanders, C., Turkarslan, S., Lee, D.-W., and Daldal, F.** (2010). Cytochrome *c* biogenesis: the Ccm system. *TIM* **18**, 266-274.
- Sato, N.** (2010). Phylogenomic and structural modeling analyses of the PsbP superfamily reveal multiple small segment additions in the evolution of photosystem II-associated PsbP protein in green plants. *Mol Phylogenet Evol* **56**, 176-186.
- Schenk, P.M., Kazan, K., Rusu, A.G., Manners, J.M., and Maclean, D.J.** (2005). The *SEN1* gene of *Arabidopsis* is regulated by signals that link plant defence responses and senescence. *Plant Physiol. Biochem.* **43**, 997-1005.
- Schiott, T., Throne-Holst, M., and Hederstedt, L.** (1997a). *Bacillus subtilis* CcdA-defective mutants are blocked in a late step of cytochrome *c* biogenesis. *J Bacteriol* **179**, 4523-4529.
- Schiott, T., von Wachenfeldt, C., and Hederstedt, L.** (1997b). Identification and characterization of the *ccdA* gene, required for cytochrome *c* synthesis in *Bacillus subtilis*. *J Bacteriol* **179**, 1962-1973.
- Schmitz-Linneweber, C., and Small, I.** (2008). Pentatricopeptide repeat proteins: a socket set for organelle gene expression. *Trends Plant Sci* **13**, 663-670.
- Schottkowski, M., Gkalypoudis, S., Tzekova, N., Stelljes, C., Schunemann, D., Ankele, E., and Nickelsen, J.** (2009). Interaction of the periplasmic PrtA factor and the PsbA (D1) protein during biogenesis of photosystem II in *Synechocystis sp. PCC 6803*. *J Biol Chem* **284**, 1813-1819.
- Schubert, M., Petersson, U.A., Haas, B.J., Funk, C., Schröder, W.P., and Kieselbach, T.** (2002). Proteome Map of the Chloroplast Lumen of *Arabidopsis thaliana*. *J. Biol. Chem.* **277**, 8354-8365.
- Schulman, S., Wang, B., Li, W., and Rapoport, T.A.** (2011). Vitamin K epoxide reductase prefers ER membrane-anchored thioredoxin-like redox partners. *Proc. Natl. Acad. Sci. U S A* **107**, 15027-15032.
- Seidler, A.** (1996). The extrinsic polypeptides of Photosystem II. *Biochim Biophys Acta* **1277**, 35-60.
- Settles, A.M., and Martienssen, R.** (1998). Old and new pathways of protein export in chloroplasts and bacteria. *Trends Cell Biol* **8**, 494-501.
- Shevchik, V.E., Condemine, G., and Robert-Baudouy, J.** (1994). Characterization of DsbC, a periplasmic protein of *Erwinia chrysanthemi* and *Escherichia coli* with disulfide isomerase activity. *Embo J* **13**, 2007-2012.
- Shi, L.X., Hall, M., Funk, C., and Schroder, W.P.** (2012). Photosystem II, a growing complex: updates on newly discovered components and low molecular mass proteins. *Biochim Biophys Acta* **1817**, 13-25.

- Sideris, D.P., and Tokatlidis, K.** (2011). Oxidative Protein Folding in the Mitochondrial Intermembrane Space. *Antioxid. Redox Signal.* **13**, 1189-1204.
- Silhavy, T.J., Berman, M. L., and Enquist, L.W.** (1984). Experiments with gene fusions. (Plainview, N.Y.: Cold Spring Harbor Laboratory Press).
- Singh, A.K., Bhattacharyya-Pakrasi, M., and Pakrasi, H.B.** (2008). Identification of an Atypical Membrane Protein Involved in the Formation of Protein Disulfide Bonds in Oxygenic Photosynthetic Organisms. *J. Biol. Chem.* **283**, 15762-15770.
- Slocum, R.D.** (2005). Genes, enzymes and regulation of arginine biosynthesis in plants. *Plant Physiol Biochem* **43**, 729-745.
- Sokolove, P.M., and Marsho, T.V.** (1976). Ascorbate-independent carotenoid de-epoxidation in intact spinach chloroplasts. *Biochim. Biophys. Acta* **430**, 321-326.
- Sone, M., Kishigami, S., Yoshihisa, T., and Ito, K.** (1997). Roles of disulfide bonds in bacterial alkaline phosphatase. *J. Biol. Chem.* **272**, 6174-6178.
- Stengel, A., Gugel, I.L., Hilger, D., Rengstl, B., Jung, H., and Nickelsen, J.** (2012). Initial steps of photosystem II de novo assembly and preloading with manganese take place in biogenesis centers in *Synechocystis*. *Plant Cell* **24**, 660-675.
- Summerfield, T.C., Winter, R.T., and Eaton-Rye, J.J.** (2005a). Investigation of a requirement for the PsbP-like protein in *Synechocystis sp. PCC 6803*. *Photosynthesis Research* **84**, 263-268.
- Summerfield, T.C., Shand, J.A., Bentley, F.K., and Eaton-Rye, J.J.** (2005b). PsbQ (Sll1638) in *Synechocystis sp. PCC 6803* is required for photosystem II activity in specific mutants and in nutrient-limiting conditions. *Biochemistry* **44**, 805-815.
- Sun, G., Sharkova, E., Chesnut, R., Birkey, S., Duggan, M.F., Sorokin, A., Pujic, P., Ehrlich, S.D., and Hulett, F.M.** (1996). Regulators of aerobic and anaerobic respiration in *Bacillus subtilis*. *J Bacteriol* **178**, 1374-1385.
- Sundberg, E., Slagter, J.G., Fridborg, I., Cleary, S.P., Robinson, C., and Coupland, G.** (1997). ALBINO3, an Arabidopsis nuclear gene essential for chloroplast differentiation, encodes a chloroplast protein that shows homology to proteins present in bacterial membranes and yeast mitochondria. *Plant Cell* **9**, 717-730.
- Sveshnikov, D., Funk, C., and Schröder, W.** (2007). The PsbP-like protein (sll1418) of *Synechocystis sp. PCC 6803* stabilises the donor side of Photosystem II. *Photosynthesis Research* **93**, 101-109.
- Takahashi, S., and Badger, M.R.** (2010). Photoprotection in plants: a new light on photosystem II damage. *Trends Plant Sci* **16**, 53-60.
- Tanaka, S., Kawata, Y., Wada, K., and Hamaguchi, K.** (1989). Extrinsic 33-kilodalton protein of spinach oxygen-evolving complexes: kinetic studies of folding and disulfide reduction. *Biochemistry* **28**, 7188-7193.
- Tasaki, E., and Sugita, M.** (2010). The moss *Physcomitrella patens*, a model plant for the study of RNA editing in plant organelles. *Plant Signal Behav* **5**, 727-729.
- Thony-Meyer, L.** (1997). Biogenesis of respiratory cytochromes in bacteria. *Microbiol Mol Biol Rev* **61**, 337-376.

- Thornton, L.E., Ohkawa, H., Roose, J.L., Kashino, Y., Keren, N., and Pakrasi, H.B.** (2004). Homologs of Plant PsbP and PsbQ Proteins Are Necessary for Regulation of Photosystem II Activity in the Cyanobacterium *Synechocystis 6803*. *The Plant Cell Online* **16**, 2164-2175.
- Tie, J.K., and Stafford, D.W.** (2008). Structure and function of vitamin K epoxide reductase. *Vitam. Horm.* **78**, 103-130.
- Vaistij, F.E., Goldschmidt-Clermont, M., Wostrikoff, K., and Rochaix, J.D.** (2000). Stability determinants in the chloroplast psbB/T/H mRNAs of *Chlamydomonas reinhardtii*. *Plant J* **21**, 469-482.
- Vazquez-Acevedo, M., Cardol, P., Cano-Estrada, A., Lapaille, M., Remacle, C., and Gonzalez-Halphen, D.** (2006). The mitochondrial ATP synthase of chlorophycean algae contains eight subunits of unknown origin involved in the formation of an atypical stator-stalk and in the dimerization of the complex. *J Bioenerg Biomembr* **38**, 271-282.
- Vignols, F., Brehelin, C., Surdin-Kerjan, Y., Thomas, D., and Meyer, Y.** (2005). A yeast two-hybrid knockout strain to explore thioredoxin-interacting proteins *in vivo*. *Proc. Natl. Acad. Sci. U S A* **102**, 16729-16734.
- Villalobos, A., Ness, J., Gustafsson, C., Minshull, J., and Govindarajan, S.** (2006). Gene Designer: a synthetic biology tool for constructing artificial DNA segments. *BMC Bioinformatics* **7**, 285.
- Vothknecht, U.C., Otters, S., Hennig, R., and Schneider, D.** (2011). Vipp1: a very important protein in plastids?! *J Exp Bot* **63**, 1699-1712.
- Wang, X., Dutton, R.J., Beckwith, J., and Boyd, D.** (2011). Membrane Topology and Mutational Analysis of *Mycobacterium tuberculosis* VKOR, a Protein Involved in Disulfide Bond Formation and a Homologue of Human Vitamin K Epoxide Reductase. *Antioxid. Redox Signal.* **14**, 1413-1420.
- Wei, L., Guo, J., Ouyang, M., Sun, X., Ma, J., Chi, W., Lu, C., and Zhang, L.** (2010). LPA19, a Psb27 homolog in *Arabidopsis thaliana*, facilitates D1 protein precursor processing during PSII biogenesis. *J Biol Chem* **285**, 21391-21398.
- Woolhead, C.A., Thompson, S.J., Moore, M., Tissier, C., Mant, A., Rodger, A., Henry, R., and Robinson, C.** (2001). Distinct Albino3-dependent and -independent pathways for thylakoid membrane protein insertion. *J Biol Chem* **276**, 40841-40846.
- Wostrikoff, K., Choquet, Y., Wollman, F.A., and Girard-Bascou, J.** (2001). TCA1, a single nuclear-encoded translational activator specific for *petA* mRNA in *Chlamydomonas reinhardtii* chloroplast. *Genetics* **159**, 119-132.
- Wyman, A.J., and Yocum, C.F.** (2005). Structure and activity of the photosystem II manganese-stabilizing protein: role of the conserved disulfide bond. *Photosynth. Res.* **85**, 359-372.
- Xie, Z., and Merchant, S.** (1996). The plastid-encoded *ccsA* gene is required for heme attachment to chloroplast *c*-type cytochromes. *J Biol Chem* **271**, 4632-4639.

- Xie, Z., Culler, D., Dreyfuss, B.W., Kuras, R., Wollman, F.A., Girard-Bascou, J., and Merchant, S.** (1998). Genetic analysis of chloroplast *c*-type cytochrome assembly in *Chlamydomonas reinhardtii*: One chloroplast locus and at least four nuclear loci are required for heme attachment. *Genetics* **148**, 681-692.
- Yamamoto, H.Y., and Kamite, L.** (1972). The effects of dithiothreitol on violaxanthin de-epoxidation and absorbance changes in the 500-nm region. *Biochim. Biophys. Acta* **267**, 538-543.
- Yi, X., Hargett, S.R., Frankel, L.K., and Bricker, T.M.** (2009). The PsbP protein, but not the PsbQ protein, is required for normal thylakoid architecture in *Arabidopsis thaliana*. *FEBS Letters* **583**, 2142-2147.
- Yi, X., McChargue, M., Laborde, S., Frankel, L.K., and Bricker, T.M.** (2005). The manganese-stabilizing protein is required for photosystem II assembly/stability and photoautotrophy in higher plants. *J. Biol. Chem.* **280**, 16170-16174.
- Yi, X., Hargett, S.R., Liu, H., Frankel, L.K., and Bricker, T.M.** (2007). The PsbP protein is required for photosystem II complex assembly/stability and photoautotrophy in *Arabidopsis thaliana*. *J Biol Chem* **282**, 24833-24841.
- Yin, S., Sun, X., and Zhang, L.** (2008). An *Arabidopsis* ctpA homologue is involved in the repair of photosystem II under high light. *Chinese Science Bulletin* **53**, 1021-1026.
- Zhang, D., Zhou, G., Liu, B., Kong, Y., Chen, N., Qiu, Q., Yin, H., An, J., Zhang, F., and Chen, F.** (2011). HCF243 encodes a chloroplast-localized protein involved in the D1 protein stability of the *Arabidopsis* photosystem II complex. *Plant Physiol* **157**, 608-619.
- Zhang, L., Paakkanen, V., Suorsa, M., and Aro, E.M.** (2001). A SecY homologue is involved in chloroplast-encoded D1 protein biogenesis. *J Biol Chem* **276**, 37809-37814.
- Zhang, Y.** (2008). I-TASSER server for protein 3D structure prediction. *BMC Bioinformatics* **9**, 40.
- Zhu, B., Cai, G., Hall, E.O., and Freeman, G.J.** (2007). In-fusion assembly: seamless engineering of multidomain fusion proteins, modular vectors, and mutations. *Biotechniques* **43**, 354-359.
- Zybailov, B., Rutschow, H., Friso, G., Rudella, A., Emanuelsson, O., Sun, Q., and van Wijk, K.J.** (2008). Sorting signals, N-terminal modifications and abundance of the chloroplast proteome. *PLoS ONE* **3**, e1994.